J. Braz. Chem. Soc., Vol. 18, No. 3, 463-512, 2007.
Printed in Brazil - ©2007 Sociedade Brasileira de Química
0103 - 5053 $6.00+0.00

Review

Laser Induced Breakdown Spectroscopy

Celio Pasquini,* Juliana Cortez, Lucas M. C. Silva and Fabiano B. Gonzaga

Instituto de Química, Universidade Estadual de Campinas, CP 6154 13084-971 Campinas-SP, Brazil

Esta revisão descreve os aspectos fundamentais, a instrumentação, as aplicações e tendências futuras de uma técnica analítica que se encontra em seu estágio de consolidação e que está em vias de estabelecer o seu nicho entre as técnicas espectrofotométricas modernas. A técnica é denominada Espectroscopia de Emissão em Plasma Induzido por Laser (em inglês, Laser Induced Breakdown Spectroscopy, LIBS) e sua principal característica está no uso de pulsos de laser como fonte de energia para vaporizar a amostra e excitar a emissão de radiação eletromagnética, a partir de seus elementos e/ou fragmentos moleculares. A radiação emitida é analisada por meio de instrumentos ópticos de alta resolução e as suas intensidades são medidas, usualmente com detectores rápidos de estado sólido. Em conjunto, esses dispositivos permitem a geração e a medida de um espectro de emissão de faixa ampla do fenômeno induzido pelo pulso de laser. O espectro registrado contém informação qualitativa e quantitativa que pode ser correlacionada com a identidade da amostra ou empregada na determinação da quantidade de seus constituintes. Essa revisão é dividida em quatro partes. A primeira aborda aspectos históricos da técnica e os conceitos teóricos relevantes associados com LIBS; então, os aspectos práticos de diversas abordagens experimentais e instrumentais empregadas na implementação da técnica são revistos de forma crítica; as aplicações encontradas na literatura, incluindo aquelas que empregam quimiometria, são classificadas e exemplificadas por meio de trabalhos relevantes recentemente publicados. Finalmente, uma tentativa de estabelecer uma avaliação global e as perspectivas futuras para a técnica é apresentada.

This review describes the fundamentals, instrumentation, applications and future trends of an analytical technique that is in its early stages of consolidation and is establishing its definitive niches among modern spectrometric techniques. The technique has been named Laser Induced Breakdown Spectroscopy (LIBS) and its main characteristic stands in the use of short laser pulses as the energy source to vaporize samples and excite the emission of electromagnetic radiation from its elements and/or molecular fragments. The emitted radiation is analyzed by high resolution optics and the intensities are recorded, usually by fast triggered solid state detectors. Together, these devices allow producing and registering a wide ranging emission spectrum of the short-lived phenomenon induced by the laser pulse. The spectrum contains qualitative and quantitative information which can be correlated with sample identity or can be used to determine the amount of its constituents. This review is divided in four parts. First, the relevant historical and theoretical concepts associated with LIBS are presented; then the main practical aspects of the several experimental and instrumental approaches employed for implementation of the technique are critically described; the applications related in the literature, including those making use of chemometrics, are classified and exemplified with relevant and recently published work. Finally, an attempt to portray an overall evaluation and future perspectives of the technique are presented.

Keywords: Laser Induced Breakdown Spectroscopy, LIBS, atomic emission spectroscopy

1. Introduction

Analytical techniques based on emission of electromagnetic radiation produced after excitation of atoms, ions or molecules present in a sample have been around for quite a while. Usually, these techniques employ some type of energy source to promote the species present in the sample to higher energy levels from where they decay, emitting characteristic radiation that is collected, sent to a wavelength selector and detected. The sample can be a solid, liquid or gas. However, some of the emission techniques can not deal directly with the original

*e-mail: pasquini@iqm.unicamp.br

samples and some type of treatment must precede their presentation for analysis. Although the measurement step is rapid, precise and sensitive, sample treatment is often slow, cumbersome and prone to induce errors due to contamination and losses. Furthermore, the necessity of sample treatment limits the use of these techniques in the field, a requirement increasingly under investigation to match the interests of the Environmental Chemistry, Process Analytical Chemistry, Forensic Analysis, Archaeological Analysis and many others areas of science that present sound arguments to make a reality of the dream of take the instrument to the untouched sample and not the inverse.

Of course many efforts have been devoted to minimize or even eliminate the necessity of sample treatment. A good example is the use of electrical arcs or sparks for vaporization and excitation of conductive samples such as metallic alloys. With the limitation of applicability to conductive samples, the technique of the classic spectrography, carried out with modern instrumentation, is capable of producing impressive results and portable instruments have been developed to permit *in situ* analysis with high precision and accuracy, although with only moderate detectivities.

This review describes a modern analytical technique based on emission spectroscopy that employs a short pulse of high energy radiation generated by a laser focused on a sample, in order to attain representative vaporization and excitation. The technique is named Laser Induced Breakdown Spectroscopy (LIBS) and numerous reviews[1-11] and three recent text books[12-14] have already been published addressing both general and specific aspects, in the relatively short period after the technique had undergone a renewed interest in the beginnings of the eighties. On the other hand, the technique has recently experienced an exponential growth in interest, reflected by an increasing number of publications, and, apparently, its niche in the general field of Analytical Chemistry are ready to be defined. Therefore, the expectation of the present review on the fundamentals, instrumentation and applications of LIBS, including most recent achievements, is to help those who want to be introduced to the technique while providing up-to-date information on instrumentation, applications and its real potential for micro and remote essentially non-destructive and direct analysis.

1.1. LIBS technique outline

Simplicity is one of the main characteristics of a LIBS system. The necessary instrumentation can be summarized as depicted in Figure 1, as a short duration (*ca*. 5 ns or shorter) pulsed laser, a focusing lens, collecting optics for the emitted radiation, a wavelength analyzer and a detector, all computer controlled. The simplest way to produce the analytical information (spectral lines of emission generated by the analytes) using LIBS is to fire a single laser pulse on a solid sample. The impinged radiant energy of the pulse must be higher than the breakdown energy for the sample material. Thus, in the first instants, the atomic and molecular structure of the sample will be broken and heated, causing vaporization of a small fraction of the material (from hundreds of ng to a few μg). This vaporized material may contain free neutral atoms, ions, molecular fragments and free electrons. Further the incoming energy of the same laser pulse can sustain high temperature plasma (> 10,000 K) in which the vaporized species can be excited and return later to their less energetic levels by emitting electromagnetic radiation. These wavelengths can be selectively associated to the presence of the analytes and whose intensity is proportional to their content in the sample. Despite being generated by distinct phenomena, data analysis and interpretation are made much in the same way as in the old arc/spark excitation spectroscopy as well as in modern ICP OES instruments. Of course, the sample, in the case of LIBS, does not need to be conductive.

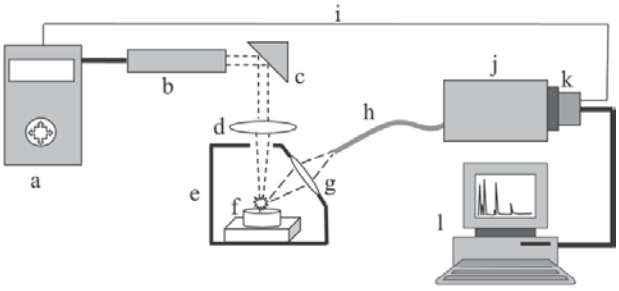

Figure 1. Schematic diagram of a simple LIBS system.(a) laser source and cooler; (b) pulsed laser head; (c) mirror; (d) focusing lens; (e) excitation chamber; (f) sample; (g) collecting optics; (h) optical fiber; (i) detector trigger signal; (j) wavelength selector; (k) detector array and (l) microcomputer.

1.2. Historical summary

The laser is the fundamental and distinctive part of the LIBS instrument. Therefore, this technique's history passes, initially, by the theory of stimulated emission of radiation proposed by Einstein early in 1917,[15] which later made the laser existence possible. The first insight on a laser operating in the visible spectrum range was due to Shawlow and Townes in 1958.[16] Maiman constructed the first ruby laser employing optical pumping in 1960[17] and

two years later Brech and Cross detected, for the first time, the spectrum of a plasma induced in a material vaporized by a ruby laser.[18] However, an auxiliary spark source was employed to produce the plasma and subsequent spectral emission. The first direct spectral analysis made by LIBS can be attributed to Runge *et al*. in 1964[19] and the first model for the laser breakdown of a gas was proposed only one year later by Zel'dovich and Raizer.[20]

The first commercial instruments were fabricated by Jarrell-Ash and Carl Zeiss in the beginning of the 70's. However it should be mentioned that these instruments employed the energy of the laser pulse only to ablate the sample while excitation was made by an electric arc.

The advent of more stable, fast and robust lasers, with better beam quality, high resolution/wide spectral range dispersion optics (such as the echelle based spectrographs), and sensitive gated image detectors based on arrays of intensified charge coupled devices (ICCD) provided strong impulses towards improving and applying LIBS since the beginning of the 80's.[21,22]

The last 26 years have witnessed the results of the efforts made by a number of companies and research laboratories towards the development of commercial instruments, of new applications and of theoretical models providing a profound insight into the fundamentals of LIBS and associated phenomena. In the last decade, for instance, the number of papers related to fundamentals and applications of LIBS reached about 600. The number of papers published on LIBS during the year of 2005 was about 350 and an exponential growth may be foreseen for this technique.[23]

1.3. The LIBS concept and related phenomena

1.3.1. Initiation of the induced plasma

Recently, it has been accepted that the acronym LIBS should be used to refer to the spectroscopic technique that employs a laser pulse as the only source of energy to simultaneously prepare the sample and produce an emission spectrum of analytical value. The name of the technique does not include a "plasma" term. The main reason for this omission is in the fact that the LIBS is not always characterized by plasma formation. A Debye number with values equal or higher than unity (in order to achieve a plasma condition) is not always observed in a LIBS experiment. Therefore the acronym LIPS where the "P" states for "plasma" is not recommended,[23] although it is still possible to find, in the specialized literature, papers employing this acronym for the same technique as LIBS.

The LIBS concept, which distinguishes the technique from others based on induced spectral emission, is that of using a laser pulse to ablate a minute quantity of the material to a condition that may then be excited by the energy supplied by the same pulse or by a subsequent pulse. This latter case involves the double-pulse technique, also described in this work. Of course, if the material is already in the gaseous phase, part of the energy does not need to be spent in sample vaporization. Many of the distinct characteristics of LIBS, such as its quasi-non-destructive and micro-analytical character, speed, in field and remote applications for both conductive and non-conductive samples, which can be liquids, solids and gases or even in aerosol forms, come from this concept.

The basic phenomena that need to be considered to understand and control a LIBS experiment for its evolvement into a useful analytical tool are: first, those related with the laser interaction directly with the sample; then, later, the laser interaction with the ablated material (electrons, molecules, atoms, ions and tiny particles) and the coupling of its remaining pulse energy are of primordial importance to reach a condition of reproducible and sensitive excitation and spectral emission.

The irradiance is a very important paramenter regarding the effects caused by the laser interaction with the sample and plasma evolution. The average irradiance of a stigmatic collimated pulsed laser beam at the focusing area (beam waist) is given by:

$$I_f = \pi E_L D^2 / 4\tau_L f^2 \lambda^2 (M^2)^2 \quad (1)$$

where I_f is the irradiance (usually expressed in W m^{-2}), E_L is the energy of the laser pulse, D is the diameter of iluminated aperture of the focusing lens (or the laser beam diameter), τ_L is the pulse duration, f is the lens focal length, λ is the laser wavelength, and M^2 is the the beam propagation ratio. For a beam ideally Gaussian, M^2 is equal to 1. Typical values for beams produced by Nd:YAG lasers are between 2 to 10. *Fluence* is the time integrated value in J m^{-2}.

Figure 2 shows, schematically, what happens at and near the point where a short duration laser pulse of sufficient energy strikes the surface of a solid sample. The sequence of events starts with the breakdown of the material, local heating occurs and a high pressure vapor is produced while a shock wave, propagating at supersonic speed, is created as the vapor expands. This initial interaction of the laser beam with a material is not a simple matter and depends on many characteristics of both the laser and the material. From this first moment on, the evolution of the plasma depends on a series of other factors related, for instance, to the irradiance of the laser (W m^{-2}), to the size of the vapor bubbles and the vapor

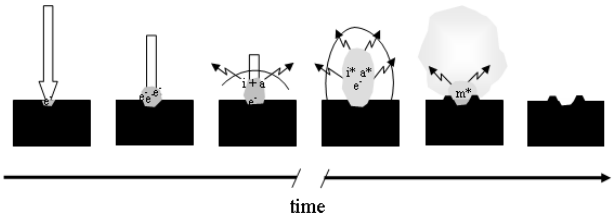

Figure 2. Sequence of events following the striking of a focused short laser pulse (*ca*. 5 ns) on the surface of a solid sample. The thick arrow represents the laser pulse and its length the pulse duration. e^-, free electrons; i, ionic species; a, atomic species; m, molecular species; *, excited species.

composition and to the composition and pressure of the atmosphere surrounding the sample, as well as, to the laser wavelength.

The breakdown of the target material, occurring at the initial moments after the laser pulse strikes the sample target (up to few ps), is reached when the density of free carriers (electrons) reaches about 10^{18} cm^{-3}. The existence of such a quantity of free electrons promotes a high optical absorption in the plasma, allowing it to be extended in direction of the beam which sustains it for the remainder of the laser pulse.[9,12]

Researchers committed to studying this stage of laser-sample interactions agree that the way the plasma is initiated differs for different media. If the target material is a gas, seed electrons will be generated by multiphoton absorption or cascade ionization. The tunnel effect can contribute when irradiances above 10^{12} W cm^{-2} are employed. Cascade ionization will start if, at least, one free electron is present in the path of the laser beam. This electron can be produced by the effect of cosmic ray ionization or by means of a breakdown induced in a gas impurity. This electron will gain energy by means of inverse *bremsstrahlung* (photon energy from the laser beam transferred to continuously increase the kinetic energy of the electrons).[24] The energetic electrons will induce, by collision, the ionization of other atoms whose electrons will continue to absorb energy from the laser, causing an exponential increase in the number of free electrons.

Multiphoton absorption causes ionization if the sum of the energy of the absorbed photons is greater than the ionization potential of an atom. Only short wavelength photons can supply such energy as the ionization potential for most gases are greater than 10 eV. Meanwhile, the probability of simultaneous absorption of photons decreases with the number of photons necessary to cause ionization. Therefore, this phenomenon can play a relevant role in the generation of free electrons only if the laser beam is of short wavelength or if the gas is at low density when the collision-based cascade ionization diminishes.

When the target sample is a liquid, the mechanism of breakdown is not as well known as in the gas case. The liquid is treated as an amorphous solid and its electron movement is quite complex.[25] However, the formation of an initial number of free electrons is described by the same type of interactions, based on cascade ionization or multiphoton absorption.

For solid samples their conductive (metallic) or non-conductive (isolator) nature is relevant to define the mechanism of initiation of the laser-induced plasma. For metallic samples, electrons of the conduction band absorb laser photons and the energy of excited electrons is dissipated by their collisions with the lattice of the material. This is a thermal conductivity phenomenon. Direct absorption of the laser energy by the ions in the lattice is prevented by the dielectric screening provided by the electrons.

In semiconductor and isolator solids the creation of electron-hole pairs by multiphoton absorption, instead of the electron heating that occurs in metals and their recombination, among other electron-lattice interactions, is considered one of the main mechanisms of energy dissipation acting during the initialization of the plasma in this type of material.[26]

1.3.2. Plasma evolution and termination

Although the initial phenomena involved in the establishment of the initial breakdown plasma differ as a function of the nature of the target sample, its further evolution apparently occurs in a similar way. The ablated material expands at supersonic velocities producing a shock wave which propagates from the surface towards the surrounding atmosphere. The laser plume continues to absorb energy from the laser during the duration of the pulse, the species are excited producing an emitting plasma that is visible to the naked eye. Then the plume starts to reduce its velocity of propagation due to collisions with the surrounding gas, and slows down to speeds close to that of sound. The plasma will then cool down by self absorption (quenching) and recombination between electrons and ions, generating neutral species and clusters after plasma extinction.

A typical time elapsed since the initiation of the process of plasma formation, shortly after the laser pulse reaches the sample surface, till its extinction, is from a few tenths of microseconds to a few milliseconds.

1.3.3. Ablation

Ablation is the sampling process of the LIBS analytical technique when applied to solid or liquid samples.[27] It limits the amount of constituents (analytes) that will be detached from the sample by the laser pulse and introduced into the

induced plasma, contributing to its formation and expansion by supplying the neutral and ionic species that, together with the free electrons, will sustain the plasma by means of laser absorption (multiphoton ionization or inverse *bremsstrahlung*). In fact, if a plasma is formed in a surrounding medium of gaseous species with high ionization potential (helium, for instance) the only way it can be sustained is by means of the presence of the ablated material.

Similar to any other analytical sampling process, the ablated portion of the sample should be representative of the original sample, independent of whether micro or bulk analyses are being considered. It means that this process can not induce fractionation of the sample constituents, altering their composition in the ablated material in relation to that in the original sample. Of course, adequate calibration can overcome this problem by correlating the composition of the ablated material with that of the sample by means of the use of reference standards which match the samples.

Ablation has been the subject of many studies, both theoretical and experimental, whose main objectives are to understand the relationship between the various instrumental parameters (pulse duration, laser wavelength and pulse irradiance and fluence), sample characteristics (thermal conductivity, thermal diffusivity, surface reflectivity, optical absorption coefficient, melting and boiling point), environmental atmospheric composition and the amount of ablated material.[28,29] Remarkable differences are observed when the pulse duration is reduced from nanoseconds to pico and femtoseconds.[28] For the shorter pulses the time scale approaches or is below the phonon relaxation time. It means that the energy of the laser pulse must be transferred to the material before it can reach the thermal equilibrium. The ablation process is more related to photo-physical rupture of bond than to the thermal melting, boiling and vaporization found with the nanosecond time scale. It is advocated that ablation produced by such short laser pulses can avoid or minimize fractionation and contribute to the reproducibility of the LIBS signal. Another interesting characteristic of the femtosecond pulses is that the induced plasma expands very quickly (at least at an order of magnitude faster than with the nanosecond scale) because it is not reheated by absorption of the laser beam. The emission line intensities, of course, also decay faster and over a negligible background (low *bremsstrahlung* emission) eliminating the necessity of using time resolved detectors.

1.3.4. Plasma shielding

Another relevant phenomenon occurring during plasma expansion is related to its capacity of impeding the remainder of the laser pulse energy from reaching the sample surface. The phenomena is called plasma shield and its immediate effect is to reduce or stop the ablation of the sample after plasma induction.[30] If the plasma shielding occurs too early, the mass ablated may not be enough to produce a measurable analytical signal. The main process leading to plasma shielding is absorption of the laser energy by the electrons (inverse *bremsstrahlung*) and multiphoton ionization (mainly for shorter laser wavelengths). For instance, if the atmosphere surrounding the sample is argon (a gas with a low ionization potential), the plasma shielding is stronger than if helium (high ionization potential) is employed. Emission signals about 16 times higher were observed for copper emission from a pure metallic sample when helium replaces argon as the atmosphere gas in a LIBS experiment.[31] The crater volume eroded in the sample is proportionally higher for the experiment made in a helium atmosphere. The presence of an easily ionizable gas assists by increasing the electron density of the plasma due to collisions between ablated atoms, electrons and ambient gas. The increased electron density intensifies the laser absorption, causing shielding.

The large reduction of interactions among neutral and ionized species and electrons when ultra-short (fs) pulses are employed explains the low plasma shielding observed for LIBS carried out with laser pulses in the range of hundreds of femtoseconds.[7, 9]

In principle the plasma shield can be taken as an undesirable phenomenon preventing LIBS from reaching better detectivity, by decreasing the ablated mass from a sample. However, it should be pointed out that when the absorption of the laser radiation occurs in the shielding process, it gives rise to a higher plasma temperature which can increase the emission intensity and dissociate any tiny particle that has been ablated.

The collective behavior of the optically dense plasma obtained at high power density defines a plasma resonant frequency, $\upsilon_{p,}$ given by

$$\upsilon_p = (4\pi n_e e^2 / m_e)^{½} = 8.9 \times 10^3 (n_e)^{½} \quad (2)$$

in which n_e is the electron density (cm^{-3}), in the plasma, *e*, is the electron charge, and m_e, is the electron mass. There could be a critical electron density for what the plasma frequency equals the laser frequency, υ_l, ($\upsilon_p = \upsilon_l$). At this point the laser radiation is strongly absorbed by the plasma. When $\upsilon_l < \upsilon_p$, the laser radiation is reflected by the plasma. Both phenomena reduce the mass ablated from the sample.

After the plasma has been initiated, the electron density can reach values as high as 10^{23} in few picoseconds.

Considering the critical electron density for the wavelength 1064 nm is about 10^{21} cm^{-3}, the remainder of a typical fundamental Nd:YAG laser pulse (5 ns, 1064 nm) will be reflected by the plasma surface as long as this density can be sustained.

1.4. Theoretical studies and calibration-free LIBS

Theoretical studies related to LIBS are carried out by means of models proposed to account for the effect of relevant factors associated with laser parameters, the sample and its environment.[29,32-37] Then, the results predicted by models can be evaluated against experimental data.[29,32]

There are two motivations to theoretically study plasma formation and its optical properties. One is to better understand the phenomenon of plasma formation and evolution and the generation of the analytical spectral emission signal. A good model should be able to predict accurately the spectral distribution of the emitted radiation. The other is related with the search for absolute analysis, the so-called "calibration-free LIBS".

The models continue to be improved and more and more effects are added to improve comparisons with the experimental results. For instance, in a recent paper[28] a model to describe the role of laser-induced melting and vaporization of metals during LIBS analysis considered: (*i*) laser-solid interaction, melting and evaporation of the metallic sample, which is described with a 1-D heat conduction equation; (*ii*) vapor plume expansion at an ambient pressure of 1 atm, calculated with fluid dynamics equations, such as continuity equations of vapor mass density, total mass density (vapor + atmospheric gas), momentum (Navier-Stokes) and energy; (*iii*) plasma formation in the expanding vapor plume, where (because of the collisional regime) the local thermal equilibrium (LTE) approximation was made, which allows the degree of ionization to be calculated with the Saha equation; (*iv*) laser-plasma interaction due to inverse *bremsstrahlung* and photo-ionization, which results in plasma shielding of the incoming radiation of the laser pulse. However, the authors recognized that other processes such as nanoparticles formation, splashing of the molten target and explosive boiling of the target, may play an important role in the way that the laser interacts with the sample and that the plasma evolves. Probably these and many other factors will be included in future papers addressing theoretical studies of LIBS in order to describe the induced plasma more accurately.

Models that include the capacity of predicting the temperature, electron density, dominant broadening mechanism (collision or stark), the temporal evolution of the plasma temperature, the spatial and temporal distributions of atom, ion, electron densities and the plasma spectrum in a pre-selected wavelength window are now being developed.[38,39] These models, which supply a theoretical way to link the observed spectral features to the plasma composition, make absolute analysis (calibration-free LIBS) a more and more realistic issue.

The plasma experimental parameters are usually estimated from spectroscopic data generated by the plasma itself, namely by the line intensities and their ratio which reflect the relative population of neutral or ionic excited species in the plasma. The more relevant parameters are the plasma temperature (T), and electron density (n_e).

The plasma temperature can be estimate from the Boltzmann and Saha equations. The first applies for the relative population of energy levels of one species, while the second applies for the neutral and its ionic forms distribution. The use of the Boltzmann distribution results in the following equation,

$$I'/I = (\lambda g'A'/ \lambda' gA) \exp[-(E'- E)/kT) \quad (3)$$

where I'and I are the line intensities (or integrated line intensities) for a given species, g and g' are the statistical weights of the levels, E and E' are the levels energy corresponding to the emission lines, *k* is the Boltzmann constant, A is the transition probability, and T is the plasma tenperature. Equation 2 can be employed to determine the temperature by the two line intensities method. However, the measurement of relative intensities is difficult to access with precision. Therefore, the temperature can be found more precisely if multiple measurement of lines intensities are made and a graph is produced as result of the equation below,

$$\ln(I\lambda/gA) = -E/kT - \ln(4\pi Z/hcN_o) \quad (4)$$

where I is the line intensity, λ, is the line wavelength, E is the energy of the upper state, Z is partition function usually taken as the statistical weight of the ground state, *h* is the Planck constant, c is the light speed, and N_o if the population of the ground state. The graph of the rigth term against E will result in a straight line whose slope is -1/*k*T.

The Saha equation also can be employed for the estimation of the plasma temperature. The equation is,

$$N(Z,0)n_e/N(Z-1,0) = 2g(Z,0)/g(Z-1,0)(mkT/2\pi'^2)^{3/2} \exp(\Delta E/kT) \quad (5)$$

where N(Z,0) is the population of the ground state of the ion stage Z, N(Z-1,0) is the population of the ground state of the

ion stage Z-1, m is the electron mass, ΔE is the ionization energy of stage Z relative to stage Z-1 and n_e is the electron density of the plasma. In order to make use of this equation n_e must be estimated from other experimental data.

The experimental estimation of the electron density of the plasma is made by means of measurements of some emission line widths. The effect of the electron density on the line width, knowing as Stark effect, allows relating these parameters by the equation,

$$w_{total} \approx [1 + 1.75\ P(1 - 0.75r)](n_e/10^{16})w \qquad (6)$$

where w_{total} is the line half-width at half maximum (HWHM), P is a parameter giving the ion contribution, r is the ratio of the mean distance between ions to the Debye radius and w is the HWHM Stark width caused by the electron density. The values for w can be found in the literature for P = 0 and $n_e = 10^{16}$ electrons cm^{-3}.

In the field of calibration-free LIBS, it is possible to find some papers employing the experimental results (line emission intensities, for instance) to directly infer the constituent concentrations of the ablated sample. For instance, it has been demonstrated that the analysis of 9 elements in an aluminum alloy can be carried out by employing the spectral line intensities detected from all constituents of the sample over a wide spectral wavelength range and plotting a family of Boltzmann curves.[40] An improved procedure was developed to account for line self absorption (a effect that induces non-linearity to the analytical curve) and applied to the analysis of steel, with even more success.[41]

Research in the field of calibration-free LIBS will certainly continue to grow and it represents a very interesting aspect of the technique with respect to overcoming one of its drawbacks related to severe matrix effects the characteristics of the sample can impose on the emission spectra.

One important factor to be considered in calibration-free analysis by LIBS is fractionation. If the relative composition of the analytes in the plasma is altered by the ablation process (something that is more than reasonable) then only theoretical models capable of including such effects will permit accurate calibration-free applications. However, this sort of drawback may be minimised, in the future, via instrumentation, by employing shorter pulse (fs) lasers that minimize fractionation.[42]

1.5. LIBS analytical signal

Figure 3 shows typical LIBS signals obtained by shooting pulses of 5.5 ns of a Nd:YAG laser of 120 mJ at an irradiance of about 16.7 x 10^{10} W cm^{-2} onto the surface of a sample of copper foil. The signals were obtained by integrating the emitted radiation for 1 μs after 10, 100, 1,000, 2,500 ns of the laser shooting.

The intense continuous background, due to the major *bremsstrahlung* emission mechanism, predominates at the first instants of the plasma life. Emission lines are broad mainly due the stark effect caused by the high density of free electrons. However, after a few hundreds of nanoseconds, characteristic atomic lines can be very clearly distinguished as the free electrons start to be captured by ions and neutral atoms and the highly excited species decay to lower energy levels. At the same time, line narrowing is observed as the major effects causing line broadening (collision and stark) become weaker. As the plasma expands and cools the relative intensities of the emission lines can change due to energy distribution among the plasma species. Finally after a while, the emission signal is representative only of the most persistent lines of the elements present in higher concentrations in the sample.

The ability to monitor the emitted radiation with time resolution of nanoseconds results in a useful way to select the most informative and reproducible sampling time window of the whole life time of the plasma. Some authors have named this technique Time-Resolved Laser Induced Breakdown Spectroscopy (TRELIBS).[43,44] Modern detectors, described in the next section, based on ICCD technology are capable of achieving such temporal resolution and are contributing to make LIBS into a more useful analytical tool. With common lasers such as Nd:YAG and with pulse durations in the range of few nanoseconds, TRELIBS has become the most popular way to improve the analytical performance of the laser induced plasma spectrometry.

The use of time-integrated spatially resolved LIBS (TSRELIBS) has also been employed to sample the plasma plume in a region where background radiation is not intense.[45] Despite this approach can simplify the LIBS instrumentation by preclude the use of expensive gated detectors, it has not achieved the same popularity of TRELIBS due the physical instrumental modifications (positioning of the collecting optics) that need to be implemented during signal optimization. On the other hand, the control of the delay time after shooting the laser pulse is, by far, simpler and already included in the software of the gated cameras.

Once optimized for a given sample type and for one or more analytes, the LIBS spectra present very good selectivity and line intensities, measured as peak height or area and provide quantitative analytical information.

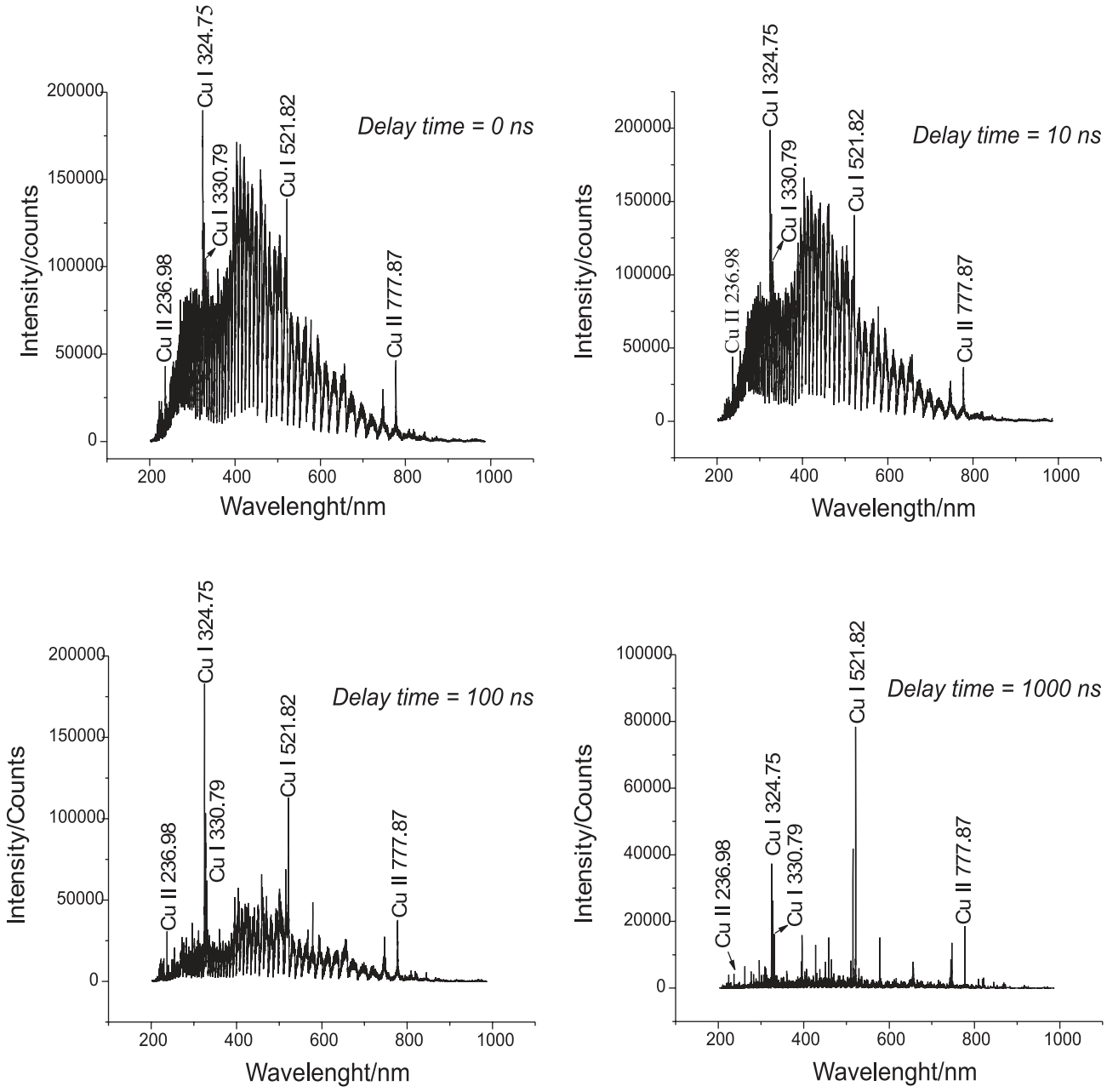

Figure 3. Set of spectra obtained for a time resolved LIBS experiment after six laser pulses fired on a fresh surface of a 1.0 mm thick copper foil. Each spectrum was obtained by integrating the emitted radiation for 1 μs after a variable delay time had elapsed after the laser pulse was applied. Laser: Nd:YAG, 120 mJ pulse^{-1}. Pulse duration: 5.0 ns. Irradiance estimated at the sample surface: 16.7×10^{10} W cm^{-2}. Wavelength selector: Echelle Andor 5000. Detector: ICCD camera, Andor Istar 2000.

Therefore, data treatment is very simple for most of the applications. The severe effects of the sample matrix can be overcome by employing matched standards, while the lack of reproducibility of the emission intensity associated with instrumental variations can be corrected by the use of an internal standard, where intensity ratios (analyte/internal standard) are used to construct the analytical curve instead of absolute peak heights.

2. Instrumentation

Song *et al.*[6] have recently published a review specifically about the instrumentation used in LIBS, though several other reviews[1-11] about LIBS applications also discuss the instrumentation related to this technique. In addition, reviews about general spectroscopic instrumentation, detectors for spectrometry, and lasers are

very useful for understanding the principles of operation of some devices used in LIBS instrumentation.[46-54] As a typical LIBS instrument is made up of well defined parts, including a laser source for sample ablation and excitation, an optical system for driving and collecting the laser and plasma radiations, a wavelength analyzer, and a detection system, the following sections will describe the instrumentation in this sequence, highlighting the technological advances of recent years. Two additional sections describe mobile instruments, due to the increasing interest in this area, and commercial instruments, which, after a premature commercialization in the 1960s and 1970s, have only recently become available again.

2.1. Lasers

A laser source is basically constituted of an active medium, where the laser radiation is generated (by energy decay of an excited species) and amplified by a process called light amplification by stimulated emission of radiation (giving origin to the acronym LASER), and an excitation source for this active medium. The active medium is placed between two dielectric coatings (mirrors), constituting the so-called laser cavity, where one of them is highly reflecting at the laser radiation wavelength (rear mirror) and the other one is partially reflecting (output mirror) so that the laser beam can be extracted. As a result, the generated radiation passes through the active medium several times, re-exciting it and, if the energy losses in this process are lower than the gain, the final emitted radiation is amplified. The active medium can be a gas, such as CO_2, N_2, a combination of He/Ne, or excimers (a halogen bonded to a noble gas); a liquid, such as an organic dye solution, giving origin to dye lasers; or even a solid, such as ruby (a Cr^{3+}-doped aluminum oxide crystal), Ti:saphire (a Ti^{3+}-doped aluminum oxide crystal), Nd:YAG (a Nd^{3+}-doped yttrium-aluminum garnet crystal), giving origin to solid state lasers. The active medium can be excited, for instance, by an electrical discharge, common for gas lasers, or the incidence of photons, more used in solid state lasers. The excitation by photons is made using lamps, called flashlamps (such as a xenon glow discharge lamp), and, more recently, another laser, such as a diode laser (a laser whose cavity is placed within a light emitting diode).[5,51-54]

As the LIBS technique involves the application of a laser pulse on a sample surface, the laser source must employ some mechanism to extract a pulse of radiation with a reproducible duration time, also called pulse duration, from the laser cavity. This can be made simply by pulsing the flashlamp, where the laser pulse will be produced as long as the energy amplification in the cavity is above its losses until the end of the flashlamp pulse, or, in a more complex way, by techniques such as mode-locking, much employed in ultra-short pulse lasers (discussed later), and Q-switching. Both can be active or passive. Q-switching is based on preventing radiation amplification from successive traveling in the active medium by increasing the energy losses and, suddenly, enabling emission by fast loss reduction.[51-55]

In active Q-switching, the variation of the energy losses is made by a combination of a polarizer and some device for polarization rotation inside the laser cavity, between the active medium and the rear mirror.[51] Therefore, after the initially generated radiation passes through the polarizer, becoming polarized, the switching between no polarization rotation and 90° rotation enables fast switching between activation and deactivation of the laser beam, allowing the production of laser pulses with a few nanoseconds of pulse duration, up to tens of hertz of pulse repetition rates, and up to hundreds of millijoules of pulse energy. The polarization rotation can be made by an electro-optical device (used in almost all papers employing active Q-switching) such as Pockel's cell or an acousto-optical device,[56] which are based on the interaction between the electromagnetic radiation and an electrical or acoustic wave, respectively, propagating in a crystalline medium.

In passive Q-switching, a material acting as a saturable absorber is placed between the active medium and the output mirror. As its name indicates, this material has the property of absorbing the electromagnetic radiation in an amount that increases less and less while the radiation intensity increases, that is, the differential increase decreases until total saturation of the absorber.[55,57] In this way, it absorbs the initial laser emission, increasing the energy losses in the laser cavity, but without preventing the amplification of the laser radiation in the active medium, so that the radiation increases until reaching a threshold energy that promotes the total saturation of the absorber, decreasing the energy losses and allowing the production of a laser pulse. Passive Q-switching is much employed in Nd:YAG lasers or similar solid state lasers, using a solid state saturable absorber, such as Cr^{4+}:YAG, and by putting similar wafers of the gain medium and the absorber together in a single chip, giving origin to microchip lasers.[55,58] Alternative approaches are the use of a single material acting as active medium and saturable absorber,[59] the growth of one material on another,[60] and the use of semiconductor saturable absorbers.[61] These devices are pumped by a diode laser (excitation source) and the increase of the pumping power changes the pulse

repetition rate, leaving the other pulse parameters unchanged, such as the pulse energy and the pulse duration, which are extremely stable. Microchip lasers present lower pulse to pulse amplitude variation (by one order of magnitude), higher repetition rates (up to tens of kilohertz), and lower pulse durations (low to hundreds of picoseconds) than do solid state actively Q-switched lasers.[55,57,62] On the other hand, they produce pulses with lower energies (generally up to hundreds of microjoules for each pulse), which can be partially compensated by the high laser beam quality (described by the beam propagation ratio, M^2, discussed below), allowing focusing to a micrometer sized spot (compared to spots of tens of micrometers generally obtained with solid state actively Q-switched lasers),[57,63] which increase the energy and power delivered per surface area (called fluence and irradiance, respectively).

Recently, Noll[23] proposed that papers dealing with LIBS should report, in addition to such basic information about the laser source as the wavelength and pulse duration, at least the irradiance, the beam diameter at the sample surface, and the detection timing (discussed in the section called Detecting Systems). The beam diameter describes the extent of an energy density distribution in a cross section of the beam at an axial location. As the laser beam is commonly conducted to the sample surface using some kind of convergent lens, several papers also inform the beam diameter at the focus, called beam waist diameter, and the position of the beam waist in relation to the sample surface, called beam waist position. Another important parameter of a laser source is the beam propagation ratio, which is related to the quality of the laser beam produced. The beam propagation ratio of a laser attains the minimum value 1 for an ideal Gaussian distribution of the energy density at the cross section of the laser beam (highest beam quality). Lasers typically used in LIBS present beam propagation ratio values ranging from 2 to 10. In relation to the laser pulses, it is also important to report the number of warming-up pulses, used to stabilize the thermal state of the laser (blocked so as not to irradiate the sample), the number of pre-pulses, applied to the sample in order to remove surface contaminations or surface layers, and the number of measuring pulses, employed to generate plasmas whose emission is acquired and analyzed.

Historically, different kinds of laser have been used for LIBS applications. The initial LIBS experiments were carried out using a 694 nm ruby laser with 50 ns pulse duration by Brech and Cross in 1962.[18] The lack of control of pulse to pulse stability of these laser sources led to the development of gas lasers and, in 1980s, solid state lasers.[5] Nowadays, although several LIBS applications employing gas lasers can be cited,[64-68] and, in spite of the advantages of using ultra-short pulse lasers (discussed later), the more used laser source in LIBS is the Nd:YAG solid state laser, especially the actively Q-switched one. In addition, the use of diode pumped Nd:YAG laser sources instead flashlamp pumped ones is increasing, even with the higher costs of the diode pumped ones, due to their reduced dimensions, better pulse-to-pulse reproducibilities and lower beam propagation ratios (down to 1.3).[23] Illustrations of a flashlamp pumped actively Q-switched solid state laser and a diode pumped microchip laser are shown in Figure 4 and photographs of craters produced by one and one thousand consecutive laser pulses on a surface of a steel sample, by a flashlamp pumped actively Q-switched Nd:YAG laser (1064 nm, 5 ns pulse duration, 120 mJ pulse energy), are shown in Figure 5. For the microchip laser represented in Figure 4, the rear mirror must be transparent to the wavelength of the radiation emitted by the diode laser (different from the wavelength of the radiation produced by the microchip laser), so that the active medium can be excited.

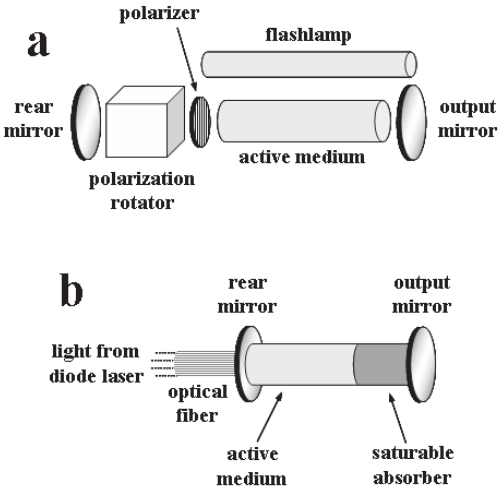

Figure 4. Illustrations of (a) a flashlamp-pumped actively Q-switched solid state laser and (b) a diode-pumped passively Q-switched microchip laser.

The laser wavelength depends on the transitions from higher to lower energy levels in the laser cavity, resulting in emission of radiation, which depends on the composition of the active medium. For instance, CO_2 lasers emit in the mid-infrared (MIR) spectral region,[64] excimer and N_2 lasers emit in the ultraviolet (UV) region,[65-68] and Nd:YAG lasers emit in the near-infrared (NIR) region. One paper illustrates the energy transitions in the Nd:YAG active medium showing the main transition that gives origin to the radiation at 1064 nm.[50] The laser wavelength

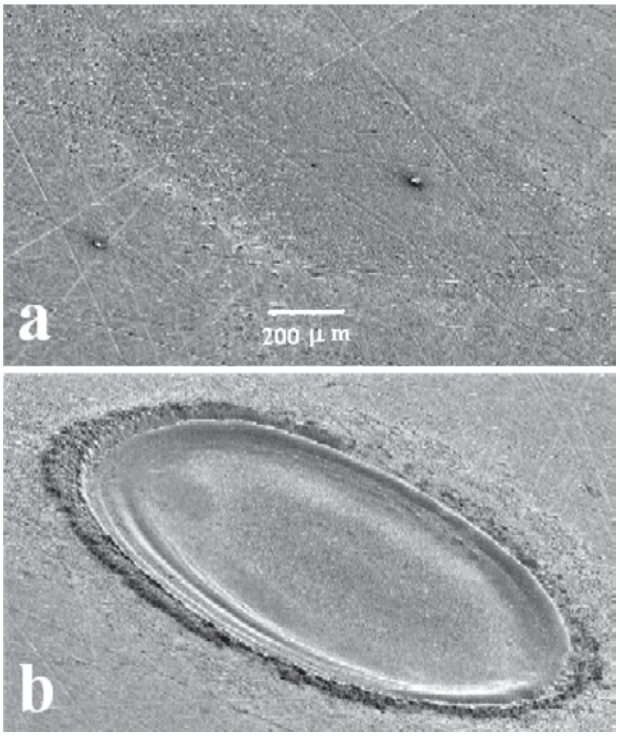

Figure 5. Photographs of aluminum samples showing the ablation craters produced by (a) one pulse and (b) one thousand consecutive laser pulses.

can also be changed to lower values by simply placing a wafer of an appropriate non-linear optical crystal, such as potassium titanium oxide phosphate (KTP) or beta barium borate (BBO), at the output mirror of the laser.[55,69] This is very useful with solid state lasers, such as the Nd:YAG laser, where the frequency of the laser radiation can be multiplied, enabling wavelength conversion from NIR down to the UV region, by placing one or more optical modules, each containing a piece of an appropriate non-linear optical crystal, at the laser output. Reviews about non-linear optical crystals used for laser wavelength conversion can be found in literature.[70,71] In LIBS, the laser wavelength, or the photon energy of the laser, affects the processes taking place in the formation of plasma, such as the creation of initial free electrons, and the laser-plasma interaction. It is recognized that the leading part of the laser pulse produces the plasma while the trailing part interacts with it by means of laser absorption. The formation and growth of free electrons and plasma initiation occur mainly by multiphoton ionization when using lasers emitting in the UV region whereas cascade ionization is the prevalent mechanism when using lasers emitting in the infrared (IR) region. After plasma formation, absorption of the laser radiation in the plasma occurs mainly by inverse *bremsstrahlung* absorption, which increases as the laser wavelength increases.[24,72-74] As a result, a UV laser pulse favors higher increasing rates of surface temperature and higher maximum surface temperatures (higher energy reaching the sample surface) and an IR laser pulse allows higher maximum plasma temperatures, higher maximum electron densities and higher plasma expansion (higher energy absorption by the plasma and greater laser-plasma interaction).[75,78] This leads, in general, to a higher ablation efficiency (amount of mass removed per unit energy delivered) and reproducibility, a lower fractionation and a lower background continuum emission when using UV lasers, as described by several papers,[27,76-79] and lower threshold fluences (minimum fluence to achieve ablation or a measurable emission signal) when using IR lasers, as described by Cabalín and Laserna[80] in the analysis of different metals and by Gómez *et al.*[81] in a study of removing graffitis from urban buildings. They also reported lower matrix effects due to different melting points of the metal samples and a higher removal efficiency of graffitis when using IR lasers in comparison with UV lasers. In addition, a UV laser beam generally can be focused to lower spot diameters on the sample surface.[80,82] That is why UV lasers are more used when a higher spatial resolution is required, as in microanalysis for surface mapping.[83] In spite of these differences, Cabalín *et al.*[82] reported similar analytical figures of merit (analytical curves, correlation coefficients, linear dynamic ranges, analytical precision and accuracy) when comparing the use of UV and visible laser radiation for the quantitative analysis of 4 minor elements in stainless steel samples when internal standardization (using a Fe line) was employed. In addition to several papers dealing with comparisons between laser wavelengths ranging from UV to NIR for LIBS applications, cited previously, Detalle *et al.*[84] published one of the few papers comparing a Nd:YAG laser at its fundamental emission (1064 nm) with a laser emitting at a higher wavelength, in this case a 2940 nm Er:YAG laser, using air and helium atmospheres. Although the pulse durations of the lasers were very different, which notably influenced their comparison, they reported a higher increase of emission lines and a higher increase of the maximum plasma temperature by changing from air to a helium atmosphere and a higher linearity when using the Er:YAG laser for the quantitative analysis of Mg and Si in aluminum alloy samples.

The laser pulse duration is given by the full width at half maximum (FWHM) of the pulse profile (laser energy versus time).[23] In LIBS, the pulse duration also affects plasma formation and properties and, therefore, the analytical results. Although most papers dealing with LIBS still employ lasers with pulse durations on the order of

nanoseconds, using gas lasers and, mainly, Nd:YAG lasers, lasers with pulse durations on the order of femtoseconds, called ultra-short pulse lasers, have became available in recent decades and their application in LIBS have increased over the last years. These lasers generally employ mode-locking techniques in order to extract the ultra-short laser pulses. Initially, active and passive mode-locking techniques were used, which are similar to those of active and passive Q-switching, but employing a periodic variation of the energy losses (loss modulation) above and below the constant cavity gain, with a shorter time below the gain (which defines the pulse duration) and a period depending on the cavity length and the propagation velocity of the laser pulse (cavity round-trip time).[52-54] The first mode-locked lasers were developed in the mid-1960s using ruby or a Nd:Glass (a Nd^{3+}-doped silicon oxide crystal), enabling the production of laser pulses with durations on the order of picoseconds for the first time.[85,86] The first femtosecond lasers were colliding-pulse mode-locked dye lasers, which also employ a dye-chain amplifier for energy amplification, developed in 1980s, and allowing pulse durations down to 30 fs.[87,88] However, self mode-locked (a kind of passive mode-locking using the called Kerr lens inside the laser cavity) Ti:sapphire lasers, which are easier to use and now allow application of laser pulses with pulse durations down to a few femtoseconds, are replacing dye lasers for ultra-short pulse applications ever since their development in the early 1990s.[89,90] In addition to the improvements in the laser cavity and in the mode-locking techniques, energy amplifiers based on the technique of chirped pulse amplification have replaced the dye-chain amplifiers used in the past. Chirped pulse amplification is based on stretching the laser pulse, which leads to a reduction in its maximum intensity, followed by its amplification and a subsequent recompression back to the femtosecond scale.[52,90,91] In recent years, most papers dealing with ultra-short pulse lasers applied to LIBS use the self mode-locked Ti:saphire lasers employing chirped pulse amplification.[75,92-96] In LIBS, when a laser pulse with a duration on the order of femtoseconds is applied to the sample, as this time is shorter than the thermal coupling time constant in matter (about 1 picosecond), the mechanisms leading to plasma formation are dominated by multiphoton ionization over thermal decomposition, with a subsequent plasma decrease without further interaction with the laser pulse.[97] This results, for LIBS applications, in comparison with nanosecond lasers, in higher ablation efficiencies, lower maxima and faster decreases in plasma temperatures.[98,99] In addition, as the pulse energy is delivered over a very short time duration, higher irradiances are achieved with lower ablation threshold energies.[92,100] The higher ablation efficiencies are due to a precise material removal by explosive ejection of matter practically without any thermal (such as melting) or mechanical damage to the sample surrounding the ablated region,[101,102] leading to higher repeatabilities on successive ablations and lower relative standard deviations (RSD) on emission measurements. The lower plasma temperatures lead to lower blackbody (fourth power temperature dependent) and background emissions,[94,95] allowing the detection to start earlier after the application of the laser pulse (sometimes without any time delay),[93,94] and practically negligible emission from the surrounding atmosphere.[92,95] As thermal decomposition does not take place in plasma formation and the melting and boiling points of several compounds are not achieved by the lower plasma temperatures, a differential thermal evaporation of the compounds present in a solid sample, for instance, is minimized, and lower matrix effects also might be expected. In addition, although Rohwetter *et al*.[92] have reported higher crater diameters and higher mass removal rates from ablation using femtosecond pulses, the lower ablation threshold energies in femtosecond laser pulses allow the use of lower pulse energies, decreasing the diameters of the ablation-produced craters and increasing the space resolution in microanalysis for surface mapping.[96] Another feature, reported by Baudelet *et al*.,[95] is the production of more molecular species by femtosecond pulses than by nanosecond ones, leading to the observation of more molecular bands in the emission spectra, which is very interesting for applications using biological samples. In spite of these advantages, Le Drogoff *et al*.,[94] in a comparison between 3 pulse durations ranging from femtosecond scale to hundreds of picoseconds, reported the occurrence of a higher self-absorption for some emission lines in copper and aluminum alloy samples when using the femtosecond pulse, similar limits of detection (LOD) for the different pulse durations when using gated detection in optimized conditions, and lower LOD for 2 ps pulse duration when using non-gated detection (no time delay between the laser pulse and start of detection; see section on Detecting Systems for a detailed description of gated detection). Rieger *et al*.[103] reported similar background emission and line intensities for pulse durations of 50 ps and 10 ns at energies significantly above the breakdown threshold in silicon and aluminum samples. In addition, Sirven *et al*.[93] reported similar background and line intensity-related temporal decays for a given fluence using pulse durations of 100 fs and 10 ns, in spite of the higher maximum background intensity when using the nanosecond laser pulse, in aluminum samples.

Although femtosecond lasers have overcome some of the limitations inherent in the LIBS technique, their high

costs, complexity, power demands and skill requirements still limit a wider use of them in LIBS. An alternative approach for improving some figures of merit of the LIBS technique is the use of double-pulse or multi-pulse excitation. In double-pulse LIBS, a second laser pulse is applied after a delay time from the first laser pulse, called interpulse separation,[23] re-exciting the region where the plasma generated by the first pulse was created and, sometimes, also the sample surface. There is some controversy in the literature about the maximum interpulse separation required for the effectiveness of double-pulse excitation. Although it was demonstrated that the long relaxation time of nitrogen oxides produced by the first laser pulse in air could prolong the existence of hot air in the region where the plasma was generated up to the millisecond scale,[104] Noll[23] proposed an interpulse separation up to 200 μs in order not to re-achieve a physical equilibrium in the region irradiated by the first pulse, whereas Scaffidi *et al*.[105] propose a time up to 100 μs, and Gautier *et al*.[106] suggest a time up to about 50 μs in order to produce emission enhancements in double-pulse LIBS. Double-pulse excitation can be applied by using two laser sources and some electronic device, such as a delay generator (see section on Detecting Systems for details), to trigger the application of the pulses and control the interpulse separation (used in the most papers), by using just one laser source emitting pulses at high frequency (to achieve the required low interpulse separations),[107] or by using just one laser source emitting just one pulse, which is divided by a beam splitter, with the application of one of the resulting two pulses optically delayed in relation to the other pulse.[108] Double-pulse LIBS also can be employed in different configurations, represented in Figure 6, concerning the direction of propagation of the laser pulses and their temporal sequence.[23,105] The orthogonal configurations differ from each other according to the sequential order of the pulses. In orthogonal re-heating, the first laser pulse is applied on the sample surface, perpendicular to it, and the second pulse, horizontal with respect to the surface, is focused slightly above it, in the region were the first plasma was created. In orthogonal pre-ablation, the first laser pulse is driven horizontally to the sample surface, being focused slightly above it, and the second pulse is applied on the surface, perpendicular to it, right below the region where the first plasma was created. Collinear is the configuration used in the most papers, because it enables an easier alignment of the laser beams, while the crossed beam configuration is the least used, though a recent paper effectively using this configuration can be cited.[109] Double-pulse excitation was first reported by Piepmeier and Malmstadt[110] in 1969 and

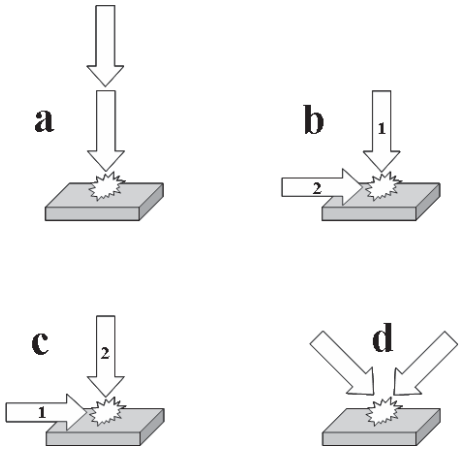

Figure 6. Schematic representations of different double-pulse configurations: (a) collinear, (b) orthogonal re-heating, (c) orthogonal pre-ablation and (d) crossed beam (the arrows represent the direction of propagation and the numbers represent the temporal sequence of the two laser pulses).

Scott and Strasheim[111] in 1970, but only in 1985 was a study demonstrating improvements in LOD using double-pulse LIBS made by Cremers *et al*.[112] All used the collinear configuration. Since then, several papers dealing with double-pulse LIBS have reported, mainly, higher intensities of emission lines, typically up to 2 orders of magnitude, and lower LOD, down to parts per billion (ppb) or sub-ppb, in comparison with single-pulse LIBS.[107,113-124] The first papers employing orthogonal configurations in re-heating and pre-ablation modes for double-pulse LIBS date from 1991 and 2000, respectively.[115,116] Although most papers dealing with multi-pulse excitation employ the double-pulse approach, a recent paper have demonstrated emission measurements after seven excitation pulses, using a microchip laser with 25 μs of interpulse separation, reporting up to 129 fold line emission enhancements in comparison with the single-pulse approach.[107] It is important to point out that the analytical advantages of double or multi-pulse excitation cannot be explained just in terms of a higher total delivered energy due to the application of more than one pulse instead of just one, because some papers have also reported these improvements even when the total energy of a double or multi-pulse was the same of that of a single-pulse.[117,118] Although the mechanisms leading to the analytical improvements of double-pulse excitation in LIBS are not yet completely understood, there is agreement in the literature about three possible main sources of these emission enhancements: (*i*) higher ablated mass; (*ii*) re-excitation of the material ablated in the first laser pulse by the second laser pulse with consequent higher plasma temperature and electron density in the second plasma;

and (*iii*) physical and energetic effects associated with the formation of the first plasma, such as lower atmospheric pressure and atmospheric number density in the region where the first plasma was created and a higher sample temperature with the application of the second pulse, leading to a lower ablation and/or plasma threshold energy, also improving the ablation and increasing the plasma temperature.[105,119] Besides, orthogonal re-heating and pre-ablation configurations appeared as attempts to study the second and third emission enhancement sources, respectively, separately, though there are indications that all of them coexist even in these configurations. Some papers also made use of laser pulses with different wavelengths or different pulse durations in double-pulse LIBS.[118,120-122] Gautier *et al*.[118] employed two Nd:YAG laser sources, emitting at 532 and 1064 nm, for a comparative study between the two orthogonal configurations for double-pulse LIBS, always using the visible laser pulse for ablation (first pulse in the re-heating mode and second pulse in the pre-ablation mode). They described, for the analysis of several metals in aluminum alloy samples, different optimal interpulse separations according to the configuration used, 200 ns for the re-heating mode and 15 μs for the pre-ablation mode, and observed a higher detectivity when using the re-heating mode. St-Onge *et al*.[120] employed two Nd:YAG laser sources for the study of Si and Mg lines (four atomic and ionic lines) in aluminum alloy samples by double-pulse LIBS in collinear configuration, varying the wavelength of the first and second pulses (UV + NIR, NIR + UV and NIR + NIR). Although they observed higher emission intensities using any of the double-pulse configurations in comparison with the single-pulse approach, they reported higher emission intensities for almost all lines studied and higher crater diameters when using the UV + NIR sequence, proving a higher ablation efficiency of the UV laser pulse and a higher re-excitation of the material ablated in the first pulse by the NIR pulse. Surprisingly, for one of the emission lines studied, they also applied the UV + NIR pulses simultaneously, without interpulse separation, obtaining emission enhancements similar to those of sequential double-pulse. Both papers cited here for double-pulse LIBS using different laser wavelengths also reported higher intensity enhancements as higher the energy of emission lines.[118,120] Scaffidi *et al*.[121,122] have employed a femtosecond laser pulse followed by a nanosecond pulse for the analysis of Fe and Cu in brass samples by double-pulse LIBS in orthogonal pre-ablation and collinear configurations. In the orthogonal pre-ablation configuration, they reported a decrease in the intensities of nitrogen and oxygen lines related to the presence of air associated with an increase of the atomic lines related to the ablated brass with an interpulse separation of up to 140 μs. In the collinear configuration, they studied two focusing positions, on the sample surface and slightly above it, reporting emission intensity enhancements correlated to the first plasma lifetime and correlated to nitrogen and oxygen atomic emission reductions, respectively. For underwater analysis, the analytical improvements of double-pulse LIBS are still more evident due to the strong confinement of plasma formation and to the much weaker emission signals in single-pulse mode.[123] In the double-pulse mode, the first laser pulse creates a gaseous cavity in the water above the sample surface, which is excited by the second pulse, increasing detectivity to a level comparable to that of single-pulse LIBS in air,[124] making the double-pulse LIBS also potentially useful for marine research.

2.2. Optical components and other parts

In addition to the laser source, to excite the samples, and the wavelength selector and detecting system, to analyze radiation emitted from the plasma in order to characterize the sample, a LIBS instrument requires optical components, used mainly to direct the laser radiation onto the sample surface and to collect the radiation emitted by the plasma and direct it into the wavelength selector.

One of the simplest optical configurations is to have the laser output directed perpendicularly to the sample surface, employing a lens to focus the laser radiation and another lens, tilted in relation to the axis of the laser beam, collecting the emitted radiation and focusing it onto the entrance of the wavelength selection device.[75] If the laser output is not directed to the sample surface, some kind of mirror, such as a dichroic mirror, or prism, such as a turning or folding prism, must be used to redirect the laser beam, initially traveling horizontal to the sample surface, for instance, to the focusing lens and sample surface.[83,125,126] The use of a microscope or just its objective lens to focus the laser beam is very common.[57,83,103,107] This allows a more precise focus and a lower focusing area, leading to a higher space resolution and, in the case of using the microscope, better observation of the sample surface, leading to a better control of the area to be ablated. Collection of the emitted radiation also can be made on the same axis as that propagating the laser beam by using a dichroic or pierced mirror. When using the pierced mirror, the laser beam passes through a hole at the center of the mirror, while the reflective face of the mirror collects the emitted radiation and redirects it to the collecting lens

and wavelength selector.[84,119,120] In the case of the dichroic mirror, the laser beam is reflected by it and redirected to the focusing lens and sample surface, while the collecting optics is disposed behind the mirror.[103,127] The inverse is also possible, with the laser beam passing through the dichroic mirror and emitted radiation being reflected by it and redirected to the collecting lens and wavelength selector.[128] The dichroic mirror must be highly reflective at the laser wavelength and highly transparent in the wavelength range of the selector, or vice-versa. The dichroic mirror also can be used to allow the perpendicular acquisition of plasma images by a camera (see section on Detecting Systems for details) and in the application of double-pulse excitation in the collinear configuration by using two laser sources.[83,103,107,122,124] In the latter case, one laser beam passes through the dichroic mirror while the other one is reflected by it and redirected to the sample surface. Another kind of beam splitter also can be used to collect a fraction of the laser radiation during the application of the laser pulse, which can be redirected to a photodiode for triggering the detection in relation to the laser pulse (see section on Detecting Systems for details),[81] for instance, or to divide the emitted radiation, one part being used for plasma imaging and the other part redirected to the collecting lens and wavelength selector.[103] Another kind of optics used in LIBS, for focusing the laser beam and for collecting the radiation emitted by the plasma, are those of telescopes, allowing the samples to be placed several meters away from the instrument, which is very useful for remote analysis.[92,129]

Several papers have employed optical fibers in LIBS applications, in conjunction with the previously cited optics, either for directing the laser or collecting the radiation emitted by the plasma, or for both. Their use for collection of the emitted light, associated with a collecting lens and coupled to the wavelength selector, is more frequent than for drive the laser radiation. When employed for both operations, either one or two optical fiber cables can be used. In the case of using just one optical fiber cable, a dichroic mirror (or another kind of beam splitter) must be used so that the laser radiation can be focused on the optical fiber, and the emitted radiation, traveling in the opposite direction, can be directed to the wavelength selector.[128,130] When using two optical fiber cables, the laser and the radiation emitted by the plasma travel through different fibers.[131,132] When the laser pulse is directed by optical fibers, two lenses are used at the output side (directed towards the sample surface) of the optical fiber cable, one collimating and the other focusing the laser radiation.[131,132] The collection of the radiation emitted by the plasma can also be made by using two lenses, one collimating and the other focusing the emitted radiation on the collecting optical fiber cable or directly onto the entrance of the wavelength selector.[75,119]

In addition to the optics, moveable sample stages (rotating or X-Y stages, sometimes under computer control), for changing the surface region under analysis and for surface mapping applications,[83,95,107,119] and sample chambers, for analysis under vacuum or gas insertion, simulating specific atmospheres or atmospheric pressures,[133,134,135] have been used.

2.3. Wavelength selectors

Spectrographs based on different set-ups of diffraction gratings, lenses and mirrors, such as the well known Czerny Turner and Paschen Runge designs, have been intensively employed in LIBS for many years and are still used.[94,132,136-138] However, due to the high complexity of LIBS spectra, with multiple emission lines (many sometimes at very close wavelengths) from the vacuum ultraviolet to the near infrared (according to the elements present in the sample), an ideal wavelength selector for LIBS should have the capability of covering large wavelength ranges simultaneously and with high resolution, which is not the case with conventional grating spectrographs. These wavelength selectors can either cover a short wavelength range with high resolution, decreasing the capability of multielement detection, or cover a wide wavelength range with lower resolution, sometimes resulting in problems of detection of specific emission lines due to their overlapping with other lines. In order to overcome these limitations and to avoid more expensive instrumentation, Body and Chadwick[136] employed up to four grating-based spectrographs, simultaneously covering different spectral regions with high resolution, to analyze the radiation emitted by the plasma. In spite of the limitations, grating spectrographs are still important in designing low cost instruments, such as that described by Neuhauser *et al*.[137] using a Paschen Runge design in a Rowland circle type spectrograph. Another important feature is the capability to be compacted in miniaturized devices coupled to detecting systems composed of a linear array of sensors (discussed later). These kinds of spectrometers, available commercially, have been used in many works.[57,138]

In the last years, a kind of spectrograph already used in other atomic emission spectroscopic techniques since the 1990s,[139,140] called echelle spectrograph, which comprises a special kind of grating in a specific design, is being increasingly used in LIBS. It is also compact and, associated with appropriate detectors, constitutes a

spectrometer covering a wide range of wavelengths (commonly from 200 up to 1000 nm) with a high resolving power ($\lambda/\Delta\lambda$ up to above 10000). The echelle technology has been developed since about the early 1950s,[141,142] and the first applications of echelle spectrographs in LIBS date from the late 1990s.[143,144]

The echelle spectrograph employs a grating containing grooves having a step like profile with one highly reflecting facet for each groove. The angle between the facet perpendicular and the grating perpendicular is called the blaze angle and the largest efficiency for diffraction by an echelle grating is obtained at wavelengths satisfying the condition for reflection from the groove facets. In a simplified way, when an incident beam of radiation is diffracted by an echelle grating, a linear dispersion of high resolution is produced in the focal plane, which is constituted by several continuous wavelength ranges (called spectral orders) superimposed on each other. Therefore, in each direction containing emerging beams from the diffraction grating, there could be radiation of several wavelengths, each from a different spectral order. This means that the spectral images of several wavelengths coincide in the focal plane. In this way, an echelle spectrograph also employs a cross dispersing element (also called the order sorter), either a second grating or a prism placed at 90° in relation to the echelle grating, in order to separate the different orders by shifting them orthogonally to the dispersion of the echelle grating, generating a high resolution bi-dimensional dispersion of wavelengths versus spectral orders (Figure 7a). Therefore, the echelle spectrographs must be used with detecting devices composed of a bi-dimensional array of sensors (discussed later), placed at the focal plane of the bi-dimensional dispersion. The emission signals are acquired, compiled and the rows of the different orders are linked together in a linear spectrum. Lindblom[145] provided a good explanation of the basic principles related to echelle spectrographs. Modern echelle spectrographs are capable of generating a dispersion with a high diffraction efficiency in all orders and with a practically constant spectral resolution over the whole wavelength range.

Florek *et al.*[146] described the development of a stand-alone echelle spectrometer. By changing the echelle grating (specific groove density and blaze angle) and the cross-dispersing prism, their echelle spectrograph can generate a bi-dimensional dispersion of any rectangular shape to match bi-dimensional detecting systems of different areas, placed outside the spectrograph housing. Sabsabi *et al.*[147] described a comparison between two commercial echelle spectrometers (ESA 3000 from LLA Instruments and Mechelle 7500 from Multichannel

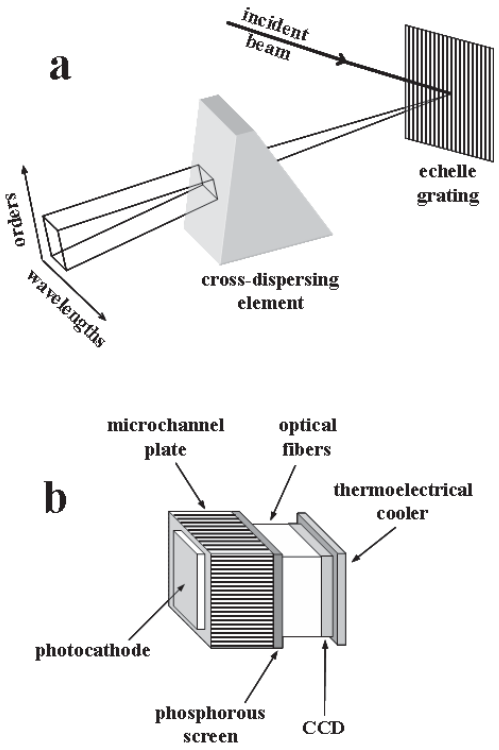

Figure 7. Illustrations of (a) an echelle spectrograph and its generated bi-dimensional dispersion and (b) a bi-dimensional ICCD.

Instruments) in terms of detectivity and precision for determination of Be, Mg, Si, Mn, Fe and Cu in Al alloy samples, concluding that both presented similar performances.

Unlike the dispersive spectrographs, optical filters are less employed as wavelength selectors in LIBS mainly because of their lower resolution and the selection of virtually only one wavelength at their exit, limiting the number of emission lines that can be simultaneously detected to one line per filter and, therefore, reducing the capability of multielement detection. However, due to the higher throughput of optical filters (there is no slit) in relation to dispersive spectrographs, modern tunable filters, such as acousto-optical tunable filters (AOTF), have been used in LIBS for plasma imaging, at a particular line emission, using bi-dimensional detecting systems.[45,148-150] An AOTF is an optical band pass filter based on a diffraction of the radiation by an acoustic wave, whose frequency determines the selected wavelength, propagating through an isotropic or anisotropic crystal medium (depending on the wavelength range of the AOTF).[151] Plasma imaging using AOTF has been used for investigating the spatial and temporal distribution of atomic and ionic lines,[45] the effect of the focusing lens, the lens to sample distance, the angle of incidence of the laser pulse onto the sample,[45,148] and the effect of

atmospheric pressure on the size and shape of the resulting plasma.[149]

Another type of tunable filter, called liquid crystal tunable filter (LCTF), has also been employed for plasma imaging.[150] The LCTF is a birefringent filter based on the constructive interference of theoretically just one wavelength, which is transmitted through the device, and destructive interferences of all others by different phase retardation between the ordinary and the extraordinary radiation rays passing through a liquid crystal.[152] Stratis *et al*.[150] made a comparison between an AOTF and a LCTF for plasma imaging. Both filters are capable of rapid wavelength selection with microsecond to millisecond tuning speeds while preserving imaging integrity. They observed a higher background interference in the images generated using the LCTF and a higher interference of strong atomic emission lines out of the tuning range using the AOTF. They also acquired multiple images at different wavelengths (for different laser pulses) around certain atomic emission lines using both filters, which were integrated in order to generate rough emission spectra, demonstrating higher resolution for the LCTF.

2.4. Detecting systems

A great variety of detector types have been used in LIBS. Among them, the less frequently employed are those having only one sensor per device, such as photomultiplier tubes (PMT). The lack of papers using this kind of detector is obvious since their use restricts the number of emission lines that can be simultaneously detected to the number of photomultiplier tubes employed in the instrument. However, photomultiplier tubes present the advantage of high detectivity in the visible spectral region and, therefore, they have been employed for specific applications with good results.[137,153-155]

The advent of high-quality solid state detectors is revolutionizing the field of atomic spectroscopy. In LIBS, those made up of a combination of several sensors (also called pixels) in one device, allowing the simultaneous acquisition of emission lines along a wide range of wavelengths, have been intensively employed, such as photodiode arrays (PDA) and charge coupled devices (CCD). The PDA are constituted by a linear array of up to 4096 photodiodes with a common n-type silicon as substrate while the CCD are constituted by a great variety of linear or bi-dimensional configurations of several sensors, each made up of three electrodes over a common substrate of p-type silicon. In a bi-dimensional configuration, they are also called CCD cameras.[46-48]

The linear configurations (PDA or CCD) are very used in conjunction with conventional grating spectrographs while bi-dimensional CCD are especially employed with echelle spectrographs, due to the characteristic bi-dimensional dispersion generated by this kind of wavelength selector (see previous section). In one special exception, Yaroshchyk *et al*.[156] used the bi-dimensional capability of a CCD camera in conjunction with a conventional grating spectrograph for the simultaneous detection of two plasma generated from liquid jets, one of them containing the analyte, by means of the partition of the detector into two linear detection regions. Their dual beam spectrometer for LIBS allows a substantial spectral simplification, by rationing the analyte and reference spectra, and lower LOD for liquid samples.

The resolution of an emission spectrum is not only limited by the resolution of the wavelength selector. It seems obvious that the higher the number of sensors present in a PDA or CCD, the higher the resolution of the acquired emission spectrum for the same wavelength range. In one of the first uses of a CCD camera in conjunction with an echelle spectrograph, the CCD area (due to its limited number of pixels) was sufficiently lower than the area of the focal plane of the echelle spectrograph, so that only one third of the total spectrum could be measured at one time to achieve a good resolution.[143]

Both PDA and CCD, in linear or bi-dimensional configurations, can employ an ultraviolet (UV) sensitisizer or an intensifier for signal enhancement, the later giving origin to intensified PDA and CCD (IPAD and ICCD). The UV sensitizer is a scintillating coating applied directly onto their sensitive surfaces in order to convert UV radiation into visible radiation, making them more sensitive in the UV spectral region, where both are originally less sensitive.[145] The intensifier used is generally based on a microchannel plate (MCP), which also employs a photocathode and a phosphorous screen. Briefly, the incoming photons are converted to electrons by means of the photocathode, which are accelerated and multiplied in the MCP by application of a voltage, and then back-converted to photons when reaching the phosphorous screen. These photons are guided by a fiber optic taper or by a lens to the sensitive surface of the detecting device.[147,157] The acceleration voltage applied on the MCP is variable, defining the gain of the intensifier, and its ability for fast switching allows gating of the optical detection on a nanosecond time scale (down to few nanoseconds). An illustration of a bi-dimensional ICCD is shown in Figure 7b.

Modern CCDs also include gating capabilities even without employing any intensifier, called gated CCD, but with higher gating times (generally down to hundreds of

nanoseconds).[138,145,158] The very fast gating capability is quite important since it allows a delay in starting detection in relation to application of the laser pulse, called delay time, removing from the detector signal the high intensity background continuum emission present in the early moments of plasma formation. In addition, it is used to optimize the detection for different decay rates between the plasma background continuum and the atomic emission for a given element.[159] The use of gating detection in LIBS led to the appearance of the term TRELIBS.[21] However, nowadays, its use has decreased since gating detection has became more common in LIBS. Gating detection, using IPAD, ICCD or gated CCD, provides control of not only the delay time, but also the time for signal integration after the detection begins, called integration time gate, improving the analytical signal. It also permits averaging of multiple spectra for a series of laser pulses, one spectrum for each laser pulse, to compensate pulse-to-pulse variations, frequently seen in LIBS.[160] The delay time is controlled by the electronics already present in the detecting devices or by a separate delay generator.[107,137,156] In both cases, counting of the delay time is initiated by a trigger pulse generated either by the laser source or by an additional detector, such as a fast photodiode, disposed to detect the laser radiation,[81,92] or the initial plasma formation.[107] Yamasaki *et al*. described the development of a gated integrator suitable for gating control in LIBS, allowing the control of the delay time and the integration time gate down to 200 ns and 25 ns, respectively.[161]

In addition of providing the acquisition of emission spectra, CCD cameras have also been used in LIBS applications for plasma imaging or sample imaging, in order to monitor plasma formation,[150,162,163] or to adjust the sample position and the optical alignment in space resolved applications,[66,83,107] respectively. Studies of the temporal evolution of the plasma and the laser pulse are also carried out using fast photodiodes and PMT connected to oscilloscopes,[57,134] while the acoustic emission associated to the laser ablation process can be measured using microphones connected to an oscilloscope or,[81] in a lower cost system, a standard microcomputer sound card.[125] The variation of acoustic emission as a function of the laser energy can be used to calculate the ablation threshold energy, or the minimum energy needed to start the ablation process, for a given sample. Photodiodes have also been used to detect the laser radiation in order to determine the laser pulse energy,[66] although this is done more frequently by means of energy sensors, such as pyroelectric joulemeters.[81,107,120]

In comparison to PDA, CCD present a higher detectivity at lower radiation levels (such as those related to laser induced plasmas), the possibility of being used with echelle spectrographs (when using CCD cameras) and the possibility of gating detection even when a signal intensifier is not employed. That is why CCD have been more frequently used in LIBS in recent years, in spite of their higher costs, although some examples of recent uses of PDA in LIBS can be cited.[84,120,128,164,165] Recent papers dealing with comparisons between detecting systems employing ICCD and a non-intensified CCD for LIBS reported better performances for the ICCD in terms of temporal resolution, dynamic range and detectivity, even with the intensifier gains adjusted to their minimum values.[138,158] Carranza *et al*.[158] observed an increase in the signal to noise ratio (SNR) of the ICCD in relation to the CCD system from 2.8 to 25-fold for the 393.37 nm calcium emission line measured in calcium-based aerosols. Sabsabi *et al*.[138] observed an increase in the LOD of the ICCD in relation to the CCD system from 1 to 2 orders of magnitude from analytical curves for Cu, Mn, Mg and Be in aluminum alloy samples and Ni, Fe and Ag in copper alloy samples. On the other hand, although the use of ICCD is becoming almost compulsory in LIBS (especially for quantitative applications), they present some drawbacks in relation to modern non-intensified CCD: much higher cost, lower resolution due to slight overlapping between the electrons of adjacent microchannels in the MCP, and a restriction of the upper wavelength range to about 850 nm depending on the photocathode.[145] In addition, non-intensified CCDs can be more easily integrated into portable instruments due to their smaller dimensions.

Recent advances in PDA and CCD technologies have introduced new devices with great potential for been employed in detecting systems for LIBS, such as the geiger PDA (GPDA), the electron bombardment CCD (EBCCD) and the electron multiplication CCD.[138,157,166] The geiger photodiode is a photodiode operated under reverse polarization using a voltage above the breakdown voltage of the p-n junction (which is much lower than the voltage needed for the operation of a PMT), resulting in a high internal signal gain by impact ionization without any additional external amplification or detection cooling (as for ICCD).[166] In relation to ICCD, the GPDA can also detect single photon events; present a lower dark signal, but also a lower dynamic range (due to the high detectivity); and also present gating capabilities with a simpler gating control, but with higher delay times (down to hundreds of nanoseconds). The EBCCD is a kind of ICCD, whose intensifier also employs a photocathode, but does not use a MCP.[157] The incoming photons are converted to electrons by the photocathode, which are

accelerated by a voltage up to 8000 V (applied between the photocathode and the CCD), reaching the CCD with enough energy for each electron to excite up to 1200 further electrons on the sensitive surface of the device (amplification of up to 1200). EBCCD cameras present a high detectivity, without the loss of resolution related to the use of the MCP, but very reduced gating capabilities, since fast switching of the high voltage is not possible synchronously over the whole area of the CCD surface in less than 10 μs.

2.5. Mobile instruments

The operating principles and the fundamentals of LIBS make this technique especially attractive for field analysis, since practically no sample pre-treatment is necessary and just optical access to the sample is required (for laser pulse application and collection of the radiation emitted by the plasma), avoiding the costs of sample collection and pre-treatment, commonly required for laboratory analyses with other analytical techniques. However, field application requires the development of portable or mobile instruments, integrating components of reduced dimensions and, eventually, supplied by batteries. In this way, recent advances in instrumentation related to LIBS also have contributed to an increasing interest in field applications using this technique. To cite some, the implementation of optical fibers, collecting the radiation emitted by the plasma and sometimes also driving the laser pulse, integrated into a sampling probe, or a measuring head or arm connected to the analysis or main unit of the instrument; and the development of diode-pumped solid state lasers, especially microchip lasers, and modern non-intensified gateable CCD, due to their reduced dimensions. The first portable LIBS instrument was reported in 1996 and, since then, several papers have reported portable or mobile LIBS instruments for field applications. Some of them are described in detail here.

The first portable LIBS instrument was developed at Los Alamos National Laboratory and reported by Yamamoto *et al.*[167] The instrument had a weight of 14.6 kg, and fitted completely into a small carrying case of 46×33×24 cm^3. It was composed of a sampling probe containing a flashlamp-pumped passively Q-switched Nd:YAG laser source (1064 nm, 4 to 8 ns pulse duration, 15 to 20 mJ pulse energy and 1 Hz pulse repetition rate), a focusing lens and an optical fiber cable to collect the emitted radiation, and an analysis unit containing the laser power supply (optionally a 12 V battery), a grating spectrograph, a 1024×256 pixel non-gateable CCD, and a laptop computer. The spectrograph and detector were adjusted to cover a spectral range of about 100 nm in the UV. The instrument was evaluated for the analysis of metals in the environment: Ba, Be, Pb and Sr in soils; Pb in paint; and Be and Pb in particles collected in filters. In 2001, Wainner *et al.*[168] reported a similar portable LIBS instrument, but employing a gateable 250×12 pixel CCD covering a spectral range of 20 nm with a resolution of 0.35 nm.

In 1997 Singh *et al.*[169] reported a mobile instrument used for the analysis of toxic metals in gaseous emissions. The instrument had a measuring probe, containing a frequency-doubled actively Q-switched Nd:YAG laser source (532 nm), an optical fiber cable to collect the emitted radiation and associated focusing and collecting optics, and an analysis unit containing the laser controller, timing electronics (such as a delay generator), a grating spectrograph, a 1024 pixel IPDA and a laptop computer. The spectral coverage was 19 nm wide with a resolution of 0.16 nm. The gated detection used a delay time between 5 and 10 μs and an integration time gate between 10 and 20 μs.

In 1998, Castle *et al.*[170] reported the first all battery powered portable LIBS instrument. The instrument had a weight of 13.8 kg and a design very similar to the first portable instrument, fitting completely into a small carrying case of 48.3×33×17.8 cm^3, but including an additional battery in the analysis unit for detector and electronics supply. It employed a Nd:YAG microchip laser source (1064 nm, 3.6 ns pulse duration, 21 mJ pulse energy, 1/3 Hz pulse repetition rate), a miniature spectrometer containing a grating spectrograph and a 2046 pixel non-gateable CCD, covering a spectral range of 123 nm with a resolution of 0.4 nm. The instrument was evaluated for the analysis of Pb in paint, Mn in steel and iron ores and Ca in organic samples.

In 1999, Neuhauser *et al.*[171] reported a mobile LIBS instrument for monitoring heavy metals in aerosols. As that reported by Singh *et al.*,[169] their instrument presented higher dimensions than those portable cited previously because it employed, in addition to a frequency doubled actively Q-switched Nd:YAG laser source (532 nm, 6 ns pulse duration, 70 mJ pulse energy and 10 Hz pulse repetition rate) instead of a microchip laser, also a conventional computer instead of a laptop. Another difference is the integration of the laser source into the analysis unit, a 19 inch rack, also containing the laser controller, the computer, timing electronics, a grating spectrograph and an IPDA, covering a spectral range of 22 nm with a resolution of 0.2 nm. In this case, the measuring head contained only two optical fiber cables, separately driving the laser pulse and collecting the emitted radiation, and the associated focusing and

collecting optics. The gated detection employed a delay time of 500 ns and an integration time gate between 700 and 4500 ns. In 2002, Panne *et al*.[172] reported an improved version of this instrument, employing an echelle spectrograph and a bi-dimensional ICCD covering the spectral range between 200 and 780 nm. In addition, the measuring probe was substituted by a 4 m long aluminum rail containing the laser source and the collecting optical fiber cable and associated optics, allowing the analysis of Ti, Fe, Mn, Mg, Ca, Si, Na and Al directly in mineral melt in an industrial environment.

In 2003, Palanco *et al*.[173] reported a portable LIBS instrument employing a more robust measuring probe and an automated analytical procedure for quantitative determination controlled by home-made software, allowing, for instance, to check whether the sample surface is prepared for the analysis and to detect possible interferents before the quantitative measurements. The instrument design is similar to those of previously described portable instruments, but employing a mount attached to the output of the Nd:YAG laser source (1064 nm, 50 mJ pulse energy) at the measuring probe to support the focusing lens and collecting optics (lens and optical fiber cable), enabling their ready adjustment and providing sampling stability and ease of handling. The main unit contained the laser power supply, timing electronics, a compact grating spectrograph and a 1024×128 pixel ICCD. A spectral coverage of 19 nm width was chosen for the analysis of Cr, Ni, Mn, Mo and Ti in steel samples. The gated detection used a delay time of 0.7 μs and an integration time gate of 10 μs. Recently, Cuñat *et al*.[174] reported a new version of this instrument, employing a miniature grating spectrometer containing a 2048 pixels non-gateable CCD, widening the spectral coverage to 100 nm.

In 2005, DeLucia and co-authors[126,175] reported the use of a portable LIBS instrument, developed by the U.S. Army Research Laboratory in association with Ocean Optics, having the aim of enabling field identification of potentially hazardous materials. The especial feature of this prototype is that, in addition to all the battery supply, its main unit, containing a small board computer, a lithium ion battery, laser control electronics and a 7-channel spectrometer (7 grating spectrographs associated with 7 3648 pixel gateable CCD), was within a backpack. That is why this prototype was called a man-portable LIBS. The measuring probe contained a very compact actively Q-switched Nd:YAG laser source (1064 nm, < 10 ns pulse duration, 50 mJ laser pulse, 0.5 Hz pulse repetition rate), an optical fiber cable to collect the emitted radiation and associated focusing and collecting optics. The battery allows continuous system operation for 2 h and the 7-channel spectrometer covers the spectral range from 200 to 980 nm with a resolution of 0.1 nm. In addition, the detecting system can be gated with a delay time resolution of 64 ns and an integration time gate down to 10 μs.

In addition to their portable instrument, described previously,[173] Palanco *et al*.[176] recently reported a new mobile LIBS instrument with larger dimensions, but having the capability of making measurements up to hundreds of meters away from the sample. For that, the instrument employs optical components similar to those used in telescopes in order to send the laser beam and gather the emitted radiation. These components were placed together with a Q-switched Nd:YAG laser source (1064 nm, 4.6 ns pulse duration, 350 mJ pulse energy and 20 Hz pulse repetition rate) and an optical fiber cable, driving the collected emitted radiation to the wavelength selector and detecting system, in an optical module placed on top of a rack. The bottom part of the rack integrated the laser power supply and controller, a delay generator, a computer, and an echelle spectrograph associated with a 1024×1024 pixel ICCD, allowing spectral coverage from 200 to 975 nm, or a conventional grating spectrograph associated with a 1024×128 pixel ICCD, reducing the spectral coverage to a 40 nm width within the range from 200 to 405 nm. The instrument was optimized for measurements at 120 m away from the samples and it has been employed, for instance, for the stand-off detection of explosive residues on solid surfaces.[177]

Recently, Bertolini *et al*.[178] have reported the development of the first mobile instrument for double-pulse LIBS analysis, named Modì (Mobile Double-pulse Instrument for LIBS analysis). The instrument employed a double-pulse Nd:YAG laser source capable of emitting two collinear laser pulses (1064 nm, 50 to 120 mJ pulse energy, 0 to 60 μs interpulse separation and 10 Hz double-pulse repetition rate), a focusing lens and collecting optics (lens and optical fiber cable), a sample chamber containing a motorized X-Y stage and an optical microscope for precise sample positioning and microanalysis, a computer, and an echelle spectrograph associated with a bi-dimensional ICCD. In addition, it also integrated an articulated five-joint measuring arm containing optical fiber cables and associated focusing and collecting optics for alternative direct measurements on large objects. The instrument has been used, for instance, for the standardless analysis of polluted soils by means of a calibration-free method.[179]

2.6. Commercial instruments

Due to recent advances in the technology related to LIBS instrumentation, the relatively recent increasing interest in

LIBS applications, and the definition of some of the limitations of the LIBS technique, in comparison with other well established atomic spectroscopic techniques, especially in terms of detectivity and repeatability, only recently have modern and complete LIBS instruments, integrating all needed instrumental components, become commercially available. Even nowadays, most LIBS applications still employ lab-made instruments, developed with components acquired separately. Here, we will present some options of commercial LIBS instruments, from several manufacturers, found on the Internet, discussing and comparing their specifications. The following information about the instrumentation is in accordance with that reported by the manufacturers.

Ocean Optics (Dunedin, USA) provides the LIBS-ELITE spectrometer.[180] It is composed of a laser source, which is a 1064 nm Nd:YAG laser with a pulse duration of 4 ns and a pulse energy of either 90 or 200 mJ (chosen at purchase), with a focusing controller to adjust the ablation spot diameter from 20 to 1200 μm; a sample chamber containing a high resolution camera and a X-Y stage, providing precise sample positioning and space resolved microanalysis, and a rear port for gas purging controlled by a rotometer; and a 7-channel spectrometer, each channel containing a grating spectrograph associated with a linear gateable CCD with 2048 pixels, covering the spectral range from 200 to 980 nm with a resolution of 0.1 nm. The detection system can be gated with delay times from -121 to 135 μs in relation to the laser pulse, with a resolution of 500 ns.

LLA Instruments (Berlin, Germany) produces the LIPAN 3001 Laser Plasma Analyzer spectrometer.[181] It employs a 1064 nm Nd:YAG laser source, with a pulse duration of 6 ns and a pulse repetition rate of 10 Hz; and a spectrometer with an echelle spectrograph, covering the spectral range from 200 to 780 nm with a linear dispersion from 5 to 19 pm, and an ICCD camera with 1024×1024 pixels. The delay time of the ICCD camera can be defined with a resolution of 20 ns. The manufacturer also provides the models LIPAN 3002, a mobile instrument which employs, instead of the conventional sample chamber of the LIPAN 3001 model, a measuring head to drive the laser radiation and collect the plasma emission, facilitating integration with industrial processes; and LIPAN 3010, which contains a microscope and a X-Y stage integrated into the sample chamber, providing precise sample positioning and microanalysis. The LIPAN 3010 also employs a frequency doubled or quadrupled Nd:YAG laser source for conversion of the fundamental laser wavelength down to 266 nm, allowing more efficient laser ablation and higher space resolution (down to 10 μm).

XRF Scientific (Osborne Park, Australia) makes the Spectrolaser 1000HR spectrometer.[182] It contains a 1064 nm Nd:YAG laser source with pulse energies of 90, 200 or 300 mJ (user controlled); a sample chamber with a stepper motor controlled linear stage for sample scanning and an inlet for gas purging; and a 4-channel spectrometer, each channel with a Czerny Turner grating spectrograph and a linear gateable CCD, covering the spectral range from 190 to 950 nm with a resolution of 0.09 nm (at 300 nm). Detection can be gated with delay times from -2 to 15 μs in relation to the laser pulse, with a resolution of 80 ns. The manufacturer also provides a low cost model, called Spectrolaser 1000S, which employs only a single channel spectrometer covering a limited wavelength range (chosen at purchase), with a typical width from 50 to 100 nm and resolution up to 0.1 nm; and the Spectrolaser Target, which employs a high resolution camera and a stepper motor controlled X-Y-Z stage in the sample chamber, allowing precise sample positioning and microanalysis, in addition to a frequency tripled Nd:YAG laser source for laser emission at 355 nm for more efficient laser ablation and a smaller ablated area.

The companies StellarNet (Oldsmar, USA) and Kigre (Hilton Head, USA) provide the Porta-LIBS-2000 spectrometer.[183,184] It has a 1064 nm Nd:YAG microchip laser as excitation source, with a pulse duration of 4 ns, a pulse energy of 25 mJ and a pulse repetition rate of 1 Hz; and a modular spectrometer containing up to 8 channels (chosen at purchase and later expandable), each channel with a grating spectrograph and a linear CCD with 2048 pixels, covering a spectral range of 100 nm for each channel (starting from 200 nm and going up to 1000 nm for 8 channels) with a resolution of 0.1 nm. The web sites of the manufacturers do not provide the timing information of the gated detection. For a low cost configuration, there are spectrometer channels covering a spectral range of 200 nm each with half resolution.

Avantes (Eerbeek, Netherlands) produces the AvaLIBS spectrometer.[185] It contains a 1064 nm Nd:YAG laser source, with a pulse energy of up to 50 mJ and a pulse repetition rate of up to 30 Hz, with a focusing controller to adjust the ablation spot diameter; and a spectrometer containing up to 7 channels (chosen at purchase), each channel with a grating spectrograph and a linear CCD with 2048 pixels, covering a spectral range of 100 nm for each channel (starting from 200 nm and going up to 900 nm for 7 channels) with a resolution of 0.1 nm. The gated detection is performed with a resolution of 42 ns in the delay time.

In 2002, Song *et al.*[6] cited additional commercial instruments, such as the MΔ5095 from MelΔok and the Tracer 2100 from Advanced Power Technologies. However, an evaluation of the present configurations of

these instruments was not possible because their websites are no longer accessible.

Among the commercial instruments described here, the LIPAN is the only one that makes use of an echelle spectrograph and a bi-dimensional ICCD. That is why it presents the highest resolution, the lowest delay time resolution and, probably, the highest detectivity. On the other hand, it presents the lowest spectral coverage, which may be due to the limited range of spectral response of the photocathode of the intensifier. All the other instruments employ multiple conventional grating spectrographs coupled to linear CCD in order to decrease the costs of the spectrometer while maintaining reasonable spectral resolution. Among them, although they present similar resolutions, the Porta-LIBS presents the highest spectral coverage, but when using the spectrometer with the highest number of channels, the Spectrolaser should employ a CCD with the highest number of pixels, since it presents a large spectral coverage with same resolution using a spectrometer with only 4 channels, and the AvaLIBS presents the lowest delay time resolution. In order to provide surface scanning and microanalysis, the LIBS-ELITE, the LIPAN and the Spectrolaser have sample stages with high precision computer controlled positioning, and the LIPAN and the Spectrolaser can use the third harmonic of laser radiation, for UV ablation, leading to a better spatial resolution. In addition, the LIPAN can be more easily integrated into industrial processes by making use of a measuring head while the Porta-LIBS is the only one that is really portable, taking advantage of using a microchip laser, being able to be run on a 12 V battery.

3. Applications

Due to its potential to handle samples in the solid, liquid and gaseous (including aerosols) form, which may or may not be conductive, LIBS has been applied both for qualitative and quantitative purposes in a multitude of matrices of interest to many areas. Some of these applications are unique to LIBS and make use of the intrinsic attributes of the technique, such as its microanalyses capability, possibility of remote analyses and quasi-non-destructive nature. The following section does not intend to be an extensive overview, but provides the most significant, representative and recent analytical applications of LIBS, as reported in the literature.

3.1. Alloys and metallurgic samples

LIBS is an attractive tool for the analysis of alloys because the technique can be employed directly on a solid sample without the necessity of sample pre-treatment, saving time and operating costs. The alloy of highest interest is steel, probably due to its wide industrial applications. Brass, gold and aluminum alloys have also been analyzed by the LIBS technique. Some implementations, such as LIBS scanning microanalyses (detection of defects and elemental surface analyses),[66,96,186,187] molten alloy analyses (including probes that resist high temperatures and fully automated systems with automatic samplers)[188,189] and applications in alloying processes (industrial routine), [132, 190-193] deserve mention. Applications like the analyses of alloys under water[194,195] have increased awareness of the technique. These applications have become possible due to the versatility of the technique that allows the utilization of probes and microscopic focusing.

Sturm *et al.*[196,197] and Vrenegor *et al.*[198] investigated the use of the multi-pulse excitation LIBS in steel alloys. Triple laser pulses were generated by one laser source (modified to produce three separate lasers pulses)[196] or by two lasers sources (one producing double-pulses and other producing a single-pulse).[197] Double-pulses were produced using only one laser head.[198] The main components of the LIBS systems were one[196,197] or two Q-switched Nd:YAG lasers[198] operating at 1064 nm with a pulse duration on the order of nanoseconds. The sample chamber was flushed with argon gas. The main difference between the LIBS systems in these three papers is basically related to the laser parameters (total energy, pulse duration and configuration). The first paper focused on the analyses of light elements in the vacuum ultraviolet spectral region: C, P, S, Mn, Ni, Cr and Si. Analytical curves with good correlations ($r > 0.9$, with the exception of sulfur) were obtained and detection limits in the range of 7 to 11 μg g^{-1} were found. In the second paper,[197] the elements quantified were C, P, S, Al, Cr, Cu, Mn and Mo. The performance of the triple-pulse configuration was compared with single-pulse and double-pulse configurations and an increase of detectivity was observed probably due to an enhancement of material ablation. Good LOD, around 7 to 10 μg g^{-1} for Al, C, Cu, Mn and Mo and LOD two or three times greater for Cr, Ni, P and S, were achieved. The third paper[198] investigated the use of interelemental correction to reduce matrix effects. Quantitative analyses of Ni, Cr, Cu, Mo, Si, Ti, Mn, Al and C was done in high alloy steel. Investigations were made with single and double-pulse configurations with the same total energy and two different laser burst energies. Single-pulse mode was better for Cr, Ni, Cu and Mo and double-pulse mode was better for Si, Ti, Mn and C. The use of interelemental corrections improved the detection limits up to two or three times.

Lopez-Moreno *et al.*[199] employed a portable prototype LIBS system for real-time analyses of steel production processes. The elements analyzed were Cr, Mo, Ni, Mn and Si in low-alloy steel. A miniature spectrometer was evaluated in this paper. The analytical curves were obtained using Fe emission lines as reference lines and compared with the curves obtained using an echelle spectrograph coupled to an ICCD camera, operated in a non-triggered and non-gated mode. The detection limits and RSD obtained with the miniature spectrometer were similar with those obtained with the ICCD, with the exception of Ni and Si, which were not possible to be analyzed with the prototype due to limitations of the spectrometer. The noise contributions to the measurements and the effect of sample temperature on spectral line intensities (important for on-line applications) were studied. It was observed that the use of some prior laser shots reduce the noise contribution and a high sample temperature contributes to increase the intensities of the spectral lines, probably due to the increase of the ablated mass.

Loebe *et al.*[186] investigated glass and tool steel defects by means of local resolved chemical analyses by using a microscopic laser induced plasma analyzer. This system allowed lower detection limits and a spatial resolution of 5 mm. Non-homogeneities of the tool steel and glass samples were characterized, it being possible to identify defects and contamination in steel and glass matrices. This paper demonstrates the potential of LIBS for quality control of industrial processes.

Hemmerlin *et al.*[200] utilized an industrial prototype that combined, in the same system, the ability to use a laser source or an electrical spark. The performance of spark optical emission spectrometry and laser induced breakdown spectroscopy was compared for quantitative steel analyses of, mainly, C, N and S, but also of Mn, Cr, Ni and Mo. VUV optics and a Paschen Runge spectrometer were utilized. Optimization of laser source parameters (energy and wavelength), integration time gate and delay time were carried out. A study of the correlation between ablation rate and LIBS signal was also done. Analytical curves obtained by LIBS and spark-OES presented great similarity. The background equivalent concentration (BEC) obtained for S and N were similar. The detection limits obtained with the LIBS instrument were comparable with the detection limits obtained with spark-OES, but in general spark-OES presented the better results. This demonstrated that more studies are necessary to improve LIBS performance so that it can be comparable to a consolidated analytical technique such spark emission spectroscopy.

Bassiotis *et al.*[201] determined Mn, Ni, and Cr in steel using a low energy pulsed Nd:YAG (5-30 mJ) operating in the fundamental wavelength and of 355 nm (15 mJ). Good analytical curves for the elements (correlation coefficients near 1) and detection limits equal to 113 and 235 μg g^{-1} for Mn were attained when the laser was operated in 1064 nm (30 mJ) and 355 nm (15 mJ), respectively.

Khater *et al.*[202,203] quantified carbon in steel alloys in the vacuum ultraviolet spectral region. The first paper contains a study about the selection of the most appropriate spectral lines for carbon analyses.[202] In the second paper, the spectral lines identified to present the best performance were employed to carry out the experimental LIBS studies.[203] The analytical performances of four ionic spectral lines (45.96 nm C^{2+}, 68.73 nm C^{+}, 97.70 nm C^{2+} and 117.57 nm C^{2+}) were studied. All lines presented good results, but the 97.70 nm line allows for the lowest detection limit and the best linear analytical curve. Lens type (cylindrical and spherical), power density of the laser, laser wavelength (1064 nm, 532 nm, 355 nm and 266 nm), pressure (range of 4.93×10^{-6} atm to 4.93×10^{-3} atm) and ambient atmospheres (air, helium and argon) were the most important experimental parameters investigated to optimize the system for quantitative analyses. A Q-switched Nd:YAG laser and its harmonics were used to study the influence of laser wavelength. The highest signal-background ratio was provided by the 1064 nm wavelength pulse (400 mJ of energy) in an air atmosphere at 2.96×10^{-4} atm using plano-convex cylindrical lenses with a focal length of 150 mm. However, the highest spectral line intensity was obtained in an argon atmosphere at approximately 4.93×10^{-4} atm with 800 mJ $pulse^{-1}$. With the optimization of these parameters, the detection limit that in the first paper was (87 ± 10) μg g^{-1} was improved to (1.2 ± 0.2) μg g^{-1} with a RSD of 15% for the 97.70 nm spectral line.

Balzer *et al.*[190,191] showed two interesting applications of LIBS for on-line monitoring of the steel process: measurements of coating thickness of galvanized sheet steel and monitoring of the Al depth profile of hot-dip galvanized sheet steel. In the first paper,[190] the instrument used an echelle spectrograph coupled to an ICCD camera (with a broadband photocathode). In the second paper,[191] the system was a Paschen Runge spectrometer with 16 photomultipliers on the Rowland Circle. Both LIBS systens used a flashlamp-pumped Nd: YAG laser that operated at 1064 nm. The laser was modified to emit up to six pulses at 10 Hz with interpulse separation higher than or equal to 2 μs with the same optical assembly. Also, a double-pulse separation mode, with interpulse separation

of 4 ms and burst energies varying from 0.5 to 2.6 mJ[190] and from 0.1-2.1 mJ[191] was employed. In addition, a triple-pulse arrangement with an interpulse separation fixed at 4 μs and burst energies varying in the range 0.165-1.65 mJ were employed.[190] In the two papers the conditions of an industrial plant were simulated. For measurements of coating thickness in galvanized sheet steel[190] the samples were moved on a x-y plane and two different atmospheres were tested, argon and nitrogen. To evaluate the aluminum depth profile,[191] the samples were moved under the focusing objective with different velocities. These two papers show that is possible to use LIBS for these industrial applications instead of X-ray fluorescence with an additional advantage of also analyzing light elements (e.g. aluminum).

Noll *et al.*[192] placed a LIBS system in an industrial plant to identify the quality of the mixture of high-alloy steel grades used to produce pipe fittings and tubes. This is important because the use of the wrong high-alloy steel grades can cause corrosion of pipes and tubes and consequent damages and losses in industrial plants. The system was development at Fraunhofer Institute for Laser Technology and was called Laser Identification of Fittings and Tubes (LIFT). The LIFT was installed in an industrial plant in 1998 and its performance was evaluated for 5 years in routine use. Basically, the LIFT consisted of a Nd:YAG laser (50 Hz and 100 mJ pulse^{-1}), a photodiode to monitor the laser pulse energy, a triangular sensor to check the sample location, an emission collecting optical part and a Paschen Runge spectrometer coupled with 12 photomultipliers. The performance was satisfactory; the LIFT correctly classified all the fittings with incorrect steel grades and the fittings with right steel grade with errors of only less than 0.1%. The system presented an improvement of about 5 times in the analytical throughput (samples analyzed per hour) in comparison with spark-OES. This is a good example to demonstrate the strong potential of LIBS for on-line process monitoring.

Palanco and Laserna[132] developed a fully automated system with the objective of identifying mistakes in mixtures of stainless-steel. The system consisted of a robotic arm used for sample handling, a LIBS instrument and a personal computer with software to control the laser pulses, to command the robotic arm and to acquire and process the emission spectral data. The laser pulse was transmitted through an optical fiber coupled with a focusing system and the plasma emission was collected by another optical fiber. The system compared the correct and expected sample composition with the heated sample composition to verify the possible occurrence of mistakes in the mixture. Multivariate calibration was used to determine Fe, Cr, Ni, Cu, Mo, Ti and Mn. The precision was better than 6%, with the exception of titanium and manganese (10-15%) and good analytical curves were obtained for most of the elements ($r > 0.98$). All the samples analyzed were identified appropriately (correct degree of mixture or not).

Bulajic *et al.*[193] studied the feasibility of the LIBS technique to detect the deterioration/corrosion of steel pipes in industrial plants. The steel pipes undergo chemical and mechanical degradation and thermal stress due to their high temperatures environment. Therefore, a scan-head to work along with LIBS analyses was created. It had a pulsed laser (10 Hz), a small laser diode to control the focal point position, a CCD camera to measure position and correct for vibration and scanning mirrors to indicate the focal point. A linear LIBS scan to check compositional non-homogeneities was proposed. The linear scan was demonstrated to generate confident estimates of the plant condition about every 15 min.

Ismail *et al.*[204,205] compared the detection limits and plasma parameters of aluminum alloys and steel alloys with LIBS analyses. The emphasis of their first paper was to correlate the matrix effects and plasma parameters with different detection limits presented for the same elements in two different matrices, using single-pulse LIBS.[204] The emphasis in the second paper was to correlate the matrix effects and plasma parameters with the enhancements of detection limits when the double-pulse technique was employed for the same elements in the two matrices.[205] Effects of the plasma temperature and electron density were investigated. The elements analyzed in both papers were Mg, Si, Mn and Cu while the second paper Al, Ti, Cr, Fe and Ni were also analyzed. The LOD's obtained for Mn, Cu and Si in steel alloys were lower than in aluminum alloy, the opposite effect was obtained for the LOD for Mg.[204] A small improvement in detection limits (in comparison with single-pulse) was obtained when the double-pulse technique was employed in the aluminum alloy matrix.[205] These two papers show how the major elements of a given sample matrix can affect the detection of the other elements in both single and double-pulse modes, as a function of the plasma parameters and element properties.

Cravetchi *et al.*[96,187] evaluated potential of the LIBS for microanalyses of aluminum alloys. In their LIBS configuration the laser beam was focused on the sample using a microscope objective (10·, N.A. = 0.25 and focal length 20 mm[187] and 15 mm[96]) which also collected the plasma emission. The scanning LIBS microanalyses of aluminum alloys was used in an attempt to distinguish the precipitates formed on the sample surface from the

normal surface and to quantify the precipitates. In addition, the system could study a sample surface with the help of scanning electron microscopy (SEM). The precipitates formed on the surface of the aluminum alloy are $(Cu,Fe,Mn)Al_6$ and $CuMgAl_2$ and they were distinguished by means of the emission spectra obtained after scanning of the surface with a spot size on the order of a few μm. It was demonstrated, in the two papers, that both systems can differentiate the precipitates, but only in the first paper was it possible to make a quantitative analyses of the precipitates (the results were compared with those obtained by a electron microprobe X-ray analyzer), resulting in a more complete definition of the contour map of the sample surface.

Gomba *et al.*[153] determined lithium in aluminum-lithium alloys under a controlled xenon atmosphere at low pressure (0.39 atm). The xenon lines were used to calculate the temperature and the electron density of plasma. An algorithm was used to calculate the lithium concentration value by using the plasma parameters. This brought an innovation to LIBS analyses, allowing determination of even the lowest concentration constituents when the plasma conditions are not favorable (the conditions did not support the Local Thermal Equilibrium, LTE). The values encountered showed good agreement with those obtained by ICPOES. The discussion about plasma parameters, behavior of the intensities of the emission lines and other theoretical aspects involved in LIBS were carefully and precisely treated. This paper is a good reference to provide information about the plasma parameters and lists a number of references on the subject.

De Giacomo *et al.*[194] used a double-pulse configuration to analyze bronze samples submerged in water, simulating an analyses under seawater. The analyses of submerged samples had been described before showed lack of sensitivity. With the use of the double-pulse LIBS, the lack of sensitivity was mostly overcome.[195, 206] The second laser pulse was delayed 8 ns in relation to the first one. Both laser pulses had 8 ns of duration and 100 mJ of energy and were produced by a Q-switched Nd:YAG laser operated at 1064 nm. The sample was immersed in a column of synthetic seawater that was about 2 cm above the focal point and was periodically changed. A telescope was used to collect plasma emission and to deliver it to the spectrograph. The results obtained in water had better agreement with the real values than the results obtained in air. The plasma temperature was higher in water than in air for most of the spectral windows. This fact suggests a more efficient thermalization.

In a later paper, De Giacomo *et al.*[207] used a double-pulse configuration to analyze bronze samples. The laser used to produce the two pulses in the earlier paper was replaced by two lasers, both operating at 532 nm with energies of 400 mJ (FWHM 7 ns). The paper presents a good discussion about experimental parameters involved in the implementation of LIBS. These parameters also presented more favorable values in water than in air. These two papers show the feasibility of an interesting implementation of LIBS systems that demonstrates the potential to analyze of alloys samples under the sea. This could be of interest for ship maintenance and/or in-situ archaeological analyses of objects found submerged.

Yaroshchyk *et al.*[208] developed a software to model the emission spectra of LIBS and to predict the sample concentration by means of a calibration-free algorithm. The estimated concentrations obtained using the software were compared with the results from a commercial LIBS instrument and with the results obtained by two alternative analytical techniques: ICPOES and XRF. The samples analyzed were bauxites, some minerals (andesites, dacites and skarns) and brass; the two first samples were analyzed in a helium atmosphere and the last, in air. The laser energies were 150, 90 or 120 mJ $pulse^{-1}$ for bauxite, brass and minerals, respectively. The elements quantified in the samples were Al, Fe, Ti, Cu, Zn, Si, Na and K. Good results using calibration-free LIBS were obtained for Al and Si in bauxite and minerals and Cu and Zn in brass sample, the others elements showed overestimated concentration values when compared with the values obtained with ICPOES and XRF.

Goode *et al.*[209] utilized LIBS to differentiate metal alloys. Brass, nickel, zirconium, and copper alloys and diverse kinds of steel were analyzed. Due to the complexity of the alloy spectra, chemometrics methods were employed to identify the metal alloys. It was possible to correctly identify 97.4% of the spectra obtained, demonstrating the potential of the LIBS to classify these different samples.

Galbács *et al.*[210] proposed a new calibration method to determine the concentration of elements in binary alloys using LIBS spectra. The method was based on the dependence of elemental concentration on to the linear correlation coefficient. With the objective to demonstrate the feasibility of the method, it was applied to quantify Cu in brass. To verify if this method could also be applied to non-binary alloys, Al, Si and Cu were quantified in an aluminum alloy. The results were compared with those obtained using a microscopic laser-induced breakdown described in an earlier paper[211] and with the certified values of reference materials. The calibration method developed presented good results for both binary and non-binary

alloys, despite the fact the method had been conceived considering only binary alloys analyses. The analytical curves showed good correlations ($r > 0.99$) and were highly repetitive due to the elimination of the effects of signal fluctuations. The RSD were, in general, lower (in the range of 0.2-3.2%) than those obtained by the conventional method (12-28%).

Corsi *et al.*[212] used LIBS to analyze gold jewellery. The elements of interest in precious alloys are Au, Ag, Cu and Pd. The calibration-free method was used for spectra analyses.[40] The use of this method allowed the quantification of the concentrations of all alloy elements (major and trace elements), even when present in concentrations below the usual LIBS detection limits. Values near to the nominal concentrations were encountered with errors lower than 1% and RSD about 0.1%. The accuracy and the RSD's found using the method proposed in this paper are better than the values found by the conventional calibration methods used in LIBS. A strong reason for this is that the proposed method minimizes the effects of the sample matrix.

Rai *et al.*[130,213,214] designed a fiber-optic LIBS system (FO-LIBS) aiming at on-line analyses of molten aluminum. A prototype was developed and its performance compared with the performance of a conventional LIBS system (without the utilization of fiber optics to deliver the laser beam). The FO-LIBS presented comparable detection limits for Mg, Cr, Fe and Mn (same order of magnitude), a better detection limit for Cu, but a detection limit about hundred times higher for Zn in analyses of solid samples. Some parameters of the system (e.g. influence of gain of the detector, effect of integration time gate), parameters related to the laser/FO-LIBS system construction (e.g. influence of laser power on fiber damage, effect of laser power variation with time), and effects of the surrounding atmosphere and focal lengths, among other, were studied.[213] The instrument was then employed to acquire spectra of solid samples and molten alloy.[130,214] The probe, containing the collimating and focusing optics was introduced into the melt which reached a final temperature of 800 ºC in atmosphere of argon. The results demonstrated that the emission lines of elements in the molten phase are different than the emission lines in the solid phases, producing different analytical curves. Thus, it was impracticable to apply an analytical calibration curve produced using solid alloys to analyze molten alloys, it being necessary to obtain analytical curves with melted samples.

Panne *et al.*[172] monitored the differences in composition of molten mineral samples. The emission lines of Ti, Fe, Mn, Mg, Ca, Si, Na and Al were identified and used for qualitative analyses. The molten samples reached temperatures between 1400 and 1600 ºC and were also analyzed by X-ray fluorescence (XRF). The results demonstrated a superior performance of LIBS in relation to XRF analyses concerning the identification of changes of concentration. Changes in concentrations in the range 0.1-0.2% were not resolved by XRF and some problems came up due to the high temperatures employed. On the other hand, with LIBS, emission lines appeared noisier and the detection limits in XRF were better than in LIBS.

Peter *et al.*[215] obtained analytical curves for C, P, S, Ni and Cr in molten steel using multi-pulse excitation in LIBS (triple laser pulses). The LIBS components described in a previous paper,[186] were installed in a thermally stabilized housing on a platform that could be lifted vertically. A moveable lance to sampling was constructed to facilitate the analyses and protect the optical components that were cooled by a water flow, keeping the temperature below 150 ºC. The laser beam was focused on the surface of the melted sample inside the tip of the sampling lance (around 20 cm of immersion). An argon flow was employed to maintain an inert atmosphere and allow for UV emission. The analytical curves presented good correlation coefficients and a wide linear range, and the method could reach low detection limits in the range 5-21 $\mu g\ g^{-1}$ with RSD's of approximately 2%. The results found show the feasibility of the LIBS technique not only to directly analyze molten steel, but also to indicate the presence of light elements in the melt.

Gruber *et al.*[128,216] constructed a LIBS system and tested it in the analyses of molten steel in the laboratory[128] and later in on-line analyses under reduced pressure.[216] Detection limits encountered in laboratory were 0.053, 0.054, 0.104 and 0.207% for Cr, Cu, Mn and Ni, respectively. Analytical curves were obtained for consecutive additions of material to the melt (Mn-granulate, Cr-granulate, Cu-rods, Ni-wire). Losses attributed to the volatilization of elements or oxide formation and saturation effects were detected. In the on-line measurements, variations in concentration were also detected, demonstrating the efficiency of the system for monitoring and controlling the steel manufacturing process. An inert atmosphere was employed in both cases.

Hubmer *et al.*[189] also employed LIBS to monitor the steel manufacturing process. The laser beam produced by a Q-switched Nd:YAG laser was guided to a AOD (argon-oxygen-decarburization of liquid hot metal) converter. The plasma emission was collected by an optical fiber and sent to an echelle spectrograph. The emission measurements were made together with temperature measurements. For each sample, 20 measurements, each

one produced by 230 laser shots, totaling 4600 laser shots per sample, were performed. In an analysis carried out in the laboratory, the molten samples reached a temperature of about 1600 ºC. Analytical curves for the elements Cr, Ni, Mo, Cu and Co were constructed and the results obtained were similar to the results obtained for samples at room temperature, reported in the literature.

3. 2. Environmental applications

The interest in using LIBS for environmental analyses is attributed mainly to its potential for *in-situ* field analyses. The main problem faced by those who want to employ this technique for environmental analyses is in the interference caused by matrix effects. However, the utilization of an internal standard and other alternative calibration methods has ameliorated this matter. Water[217-222] and soil[223-233] analyses have produced most of the papers found in the literature.

Niu *et al*.[234] determined strontium in marine algae using the method of standard additions. Usually, the methods used to analyze this type of sample require sample digestion and they show the strong interference of calcium. Small volumes of standard solutions were added to the ground sample that was further mixed with cellulose and pressed to form pellets. LIBS allowed the analyses of marine algae without interference of calcium (by choosing of an emission peak without spectral interference) producing results in good agreement with certified values. The RSD's were about 5% and the analytical curves presented good linearity with correlation coefficients higher than 0.99.

Barbini *et al*.[235] constructed a LIBS instrument to carry out elemental analyses of marine sediments during the XVI Italian campaign in Antarctica. The LIBS apparatus, including the optical part, was mounted on an anti-vibration support to reduce the effect of the ship's movement. Samples were collected on different dates and at different times from different positions and depths. Qualitative measurements were carried out to identify the emitting elements. The elements Si, Al, Fe, Mg, Mn, Na, Ti, Ba, Sr and Ca were found in all samples. Semi-quantitative scannings of depth distributions were performed and a normalization method was employed to reduce the influence of surface roughness, laser instability and sample properties. Barium presented the highest decrease of concentration with increasing depth. This type of analyses is important to supply information on elemental stratifications presenting biological and geographic importance. Quantitative analyses showed goods results for some elements (e.g. Cr and Si), but for elements with emission lines that undergo self-absorption the results were under-estimated. The quantitative measurements were made by a method previously described by Lazic *et al*.,[223] called self-absorption model.

Gondal *et al*.[236] employed LIBS to obtain elemental analyses in crude oil residues. Eight trace elements had their concentrations estimated: Ca, Fe, Mg, Cu, Zn, Na, Ni and Mo by LIBS and ICPOES. Cylindrical discs of a solid paste of crude oil residue samples were used while calibration standards employed pellets made of differing amounts of powders of the pure metals and KBr. The detection limits were low, from 2-14 μg g^{-1} and the estimated concentrations of the elements were, in general, similar to those obtained by ICPOES.

Gondal and Hussain[237] quantified toxic metals in wastewater collected from local paint manufacturing plant. The results showed the concentrations of different elements of environmental significance such as Pb, Cu, Cr, Ca, S, Mg, Zn, Ti, Sr, Ni, Si, Fe, Al, Ba, Na, K and Zr, in paint wastewater were in the 1 to 301 μg g^{-1} range.

Mateo *et al*.[238] utilized the LIBS technique to monitor the process of cleaning of coastal rocks contaminated with tanker oil spill using lasers. The results obtained by qualitative analyses employing LIBS were compared with qualitative measurements using scanning electron microscopy-energy dispersive X-ray spectroscopy (SEM-EDS) and presented good agreement. The cleaning of rocks contaminated with fuel was carried out employing a Q-switched Nd:YAG laser operating at two wavelengths (1064 nm-900 mJ $pulse^{-1}$ and 355 nm-200 mJ $pulse^{-1}$). The cleaning process was monitored by collecting the plasma emission. The different element peaks were identified. Some elements were detected only on contaminated rocks (C, Mg and Ca) and others only in non-contaminated rocks (Si and Al). Therefore, when the concentration of the first elements stops decreasing and the concentration of latter ones stops increasing, the cleaning process is complete.

Yamaguchi *et al*.[217,218] have determined particles of manganese and aluminium carbonate and oxide in water. Initially, only aluminum particulates (in form of white fused alumina and gibbsite) were analyzed.[217] Six different diameters of fused alumina particles (1.3, 2, 4, 8, 14, 30 and 57 μm) and particles of gibbsite of 3.8 μm diameter were analyzed. The results were influenced by particle size, the highest correlation coefficients for white-fused alumina solutions were obtained for 2 and 8 μm particles (R^2 = 0.98 for both) and similar correlation coefficient (R^2 = 0.95) obtained for white-fused alumina of 4, 14 and 30 μm diameter were observed for gibbsite solutions. In fused alumina solutions with a particle size of 57 μm it

was not possible to perform quantitative analyses due the instability of the atomic emission spectra. A saturation effect was observed with the increase of particulate concentration (for particle diameters of 2 μm this happened above 4 mmol L^{-1}). Afterwards, quantitative analyses of suspensions of Al_2O_3, $CaCO_3$ and MgO were carried out and calcium colloids of a real sample of underground water were analyzed.[218] The concentration ranges analyzed using LIBS were similar to ICPOES and in the range of concentrations of the aquatic environment. Aluminum and calcium could be quantified simultaneously by LIBS.

Bundschuh *et al.*[219] applied LIBS to quantitative analyses of Ba^{2+}, Pb^{2+}, Ca^{2+} and Eu^{3+} in aqueous solutions and Eu_2O_3 in the form of colloidal suspension. The LIBS system was capable of differentiating Eu_2O_3 in the form of a colloidal suspension from Eu^{3+} in an aqueous solution. This fact was utilized to study the formation of europium hydroxide colloids in aqueous solution, varying the pH until reaching the solubility limit. The detection limits were 0.09, 4.9, 13.1 and 5.0 mg L^{-1} for the metal ions Ca^{2+}, Ba^{2+}, Pb^{2+}, Eu^{3+}, respectively and 0.03 mg L^{-1} for Eu_2O_3 in colloidal suspension. The paper also presented the utilization of the LIBD (laser-induced breakdown detection) technique for its study of colloidal solutions. The combination of both techniques provided qualitative and quantitative information about colloidal systems.

Samek *et al.*[220] have determined trace elements in water samples. Line broadening, electron density, plasma temperatures, local thermal equilibrium, optical thickness and self-absorption were studied and evaluated. Firstly, analytical curves for Al, Ca, Cr, Cu, Li, K, Mg, Mn, Na, Pb and U were made. The hydrogen emission lines (H_α, H_β and H_γ) and the emission lines of Li, Ca and Cu were employed as references. At this stage the analytes were added to water in the form of hydroxides or nitrites. The performance of these lines as internal standards was evaluated for some elements. Detection limits vary widely from 0.009 to 450 mg L^{-1}. The plasma emission was focused directly onto the slit of the spectrograph. Later, the performance of the system was checked by analyzing real samples using a fiber-optic system to collect the plasma emission. Water samples from two rivers and seawater were also analyzed for toxic heavy metals, demonstrating the potential of LIBS to analyze real samples. In the last stage, a telescopic system, developed for remote analyses, was evaluated for analyses of Tc in solution.

Koch *et al.*[221] and Fichet *et al.*[222] employed LIBS instruments in the analyses of Cr in liquids. The first paper analyzed Cr in aqueous solutions[221] and the second in water and oil samples.[222] A linear range of 20-100 μg g^{-1} and a detection limit down to 40 μg g^{-1} were obtained by Koch *et al.*[221] Detection limits of same order of magnitude were attained by Fichet *et al.*,[222] 20 μg g^{-1} in water and 30 μg g^{-1} in oil samples with RSD of about 3%. These values do not fulfill the requirements for routine determination of Cr in liquids, being necessary extension of the linear range and improvement of the detection limit.

López-Moreno *et al.*[239] aimed at qualitative and quantitative analyses of contaminants, mainly Cr and Fe, in coastal samples (bark, leaves, soil, dock rock, stone and fragments of wall) of an area with high industrial activity. An instrument for long distance analyses (12 m) was used. A commercial Newton telescope collected and sent the plasma emission to the slit of the spectrograph. The presence of Cr and Fe was confirmed by comparison with the sample matrix free of contaminants. The influence of moisture and salinity was evaluated and showed that these factors contributed for reduction of the ablation rate in samples when compared with dry samples. Another factor studied was the difference between depth profiles for horizontal and vertical sides of the samples. A higher contamination was detected on the surface of the horizontal face of the sample when compared to the vertical face which could have part of its contamination removed by the continuous splashing with sea water. Quantitative analyses were carried out by normalizing the analyte peak emission using Mn peak emission. Detection limits of 0.21 and 0.19% and dynamic range of 1.1-6.7 and 0.6-1.7% were obtained for Cr and Fe, respectively. Depth profiles for Cr were also obtained. Furthermore, three-dimensional depth analyses of Cr, Fe, Ca and Mg were obtained. Similar behaviors pointed out a decrease of Cr and Fe concentrations with depth. As demonstrated in this paper, the LIBS technique shows a high potential to supply information (qualitative or quantitative) about contaminants in environmental samples, adding the advantage of accessing the spatial distribution of the species along the sample.

Bublitz *et al.*[224] evaluated the performance of LIBS for qualitative and quantitative analyses of metal ions in soil samples. A 6 mm height layer (around 10 g) of sample was put inside a sample chamber rotated by an electric motor while its surface was revolved by a metal sheet. Iron, Si, Mg and Ca could be detected in dry soil samples from two different sites. Barium was chosen as internal standard in quantitative determinations with known amounts of barium salt added in calibration and measured samples. The influence of the water content in soil samples and the differences presented by dry and water-saturated samples were studied. The maximum intensity for the Ba peak emission was observed at around 6% water content

for the two soil samples and a numerical simulation was proposed for this behavior. A detection limit of 0.1% was reached for barium determination.

Hilbk-Kortenbruck *et al*.[225] analyzed heavy metals in soils by the LIBS and LIBS-LIF techniques. With the LIBS technique, satisfactory detection limits (evaluated following the recommendations of the German regulatory agency) were obtained for As, Cr, Cu, Ni, Pb and Zn (simultaneous detection) being equal to 3.3, 2.5, 3.3, 6.8, 17 and 98 μg g^{-1}, respectively. The LOD's for Cd, Hg and Tl were not satisfactory when LIBS was employed. However, the LIBS-LIF approach was used to try to improve the detection limits for Cd (0.3 μg g^{-1}) and Tl (0.5 μg g^{-1}) to levels in agreement with German regulations, but with reduction of the linear dynamic range. Satisfactory detection limits for Hg were not reached either with LIBS or by LIBS-LIF. ICPOES and FAAS measurements were made for comparison and reference.

Capitelli *et al*.[226] employed the same LIBS instrument described by Lazic *et al*.[223] for the determination of heavy metals in soils. The performance of the LIBS technique was compared with the ICPOES technique for Cr, Cu, Fe, Mn, Ni, Pb and Zn in 20 standard soil samples (four different series) and 3 sewage sludge samples. The detection limits for these elements were higher (30 mg kg^{-1} for Cr, Cu, Ni and Zn; 50 mg kg^{-1} for Pb; 500 mg kg^{-1} for Fe and 100 mg kg^{-1} for Mn) than reported in other papers, but below the limits stipulated for European Union. The RSD's obtained with LIBS were higher that those obtained with ICPOES, with the exception of values for Cr that were practically equal.

Bustamante *et al*.[227] determined calcium concentrations in depth profiles of soils. The samples were obtained from different depths (0-18 m) in the south of Patagonia, Argentina. The calibration samples were made of pellets of $CaCO_3$ and $BaCl_2$ in different proportions. The sample pellets (soil samples) were prepared using a $BaCl_2$ matrix and analyzed in a vacuum chamber at 6.58×10^{-4} atm. The ratio of intensities of Ca/Ba was used to construct the analytical curves. For the purpose of comparison, the soil samples were also analyzed by volumetric titration. The depth profile of calcium concentration obtained by both techniques (LIBS and volumetric titration) presented a very similar behavior.

Martin *et al*.[228,229] applied the LIBS technique for determination of total carbon and nitrogen in soils. The soil samples were analyzed by LIBS and by the combustion method (LECO CN-2000 elemental analyzer, LECO Corporation). An unsatisfactory correlation between the two methods (elemental analyses and LIBS) was obtained at low nitrogen concentrations, but at nitrogen concentrations higher than 0.1% high correlation (correlation coefficient higher than 0.9) was observed.[229] Pellets of 15 different soil samples with total carbon concentrations varying from 0.16 to 4.3% were analyzed. Some pellets were prepared with soil samples washed with acid (a procedure used to remove inorganic carbon). LIBS demonstrated to be a good tool to distinguish inorganic and organic soil carbon because a decrease in carbon concentration was verified after the acid wash. Analytical curves were obtained normalizing the carbon emission peak intensity with the silicon emission peak intensity. The standard deviations obtained by the LIBS technique were higher when compared with the conventional combustion method. Despite this fact, LIBS presents the potential for *in situ* analyses which, in many cases can justify its use despite its failure when comparing figures of merit. In addition, LIBS was employed to determine metal contaminants in freshwater invertebrates.[229]

Cremers *et al*.[230,231] measured total soil carbon by LIBS. The sample was placed in a small quartz tube (25 mm diameter, 75 mm long) and the laser beam was focused onto the center of the tube. The LIBS measurements were compared with the measurements obtained using the conventional dry combustion method (Dohrmann DC-180 analyzer, Tekmar-Dohrmann). First, the emission line of carbon at 247.8 nm was used for the analyses. With this emission line the detection limit was estimated as 300 mg C kg^{-1}, with a precision of 4-5% and accuracy in the range of 3-14%. Later,[231] the performance of carbon emission line at 193 nm was evaluated. This spectral line has the advantage of being free of spectral interferences caused by Fe (247.8 nm) affecting the line at 247.8 nm. By employing the emission line at 193 nm it was also possible to measure total carbon in soil samples. The calibration curve obtained with the 193 nm line showed a better correlation coefficient than with the 247.8 nm line (0.99 against 0.96, respectively). However, the verification curve (correlation with a conventional method) presented a poorer correlation coefficient (0.95 against 1).

Harris *et al*.[232] determined nitrogen in sand. Sand was employed as a substitute for soil to minimize spectral interferences and in order to compare the results with those previously obtained for soil analyses. The spectral range around 498-504 nm, employed in other papers,[228,229] was not used in this paper, because the emission peaks present in this region could be attributed to titanium emission (an element present in sand and also in soil). Therefore, the spectral range 741-749 nm was chosen. Analyses in an ambient atmosphere were not possible due to the interference of nitrogen, present even if low laser energy (18 mJ $pulse^{-1}$) was used. The RSD's for samples with

nitrogen concentrations below of 1% were very high, but in nitrogen concentrations above 1% the RSD's were low, about 2.11%. The detection limit for N was 0.8% with a correlation coefficient of 0.989.

Mosier-Boss *et al*.[233,240] built a FO-LIBS sensor and its performance was tested for the analyses of contaminated soil. The first paper[233] presented the results of analyses of three sites (two contaminated with Cr and one with Pb) while the second paper[240] showed the results for a site contaminated with automotive scrap residue. EPA Method 6010 based in ICPOES was used as comparative method. Uncontaminated soil, coming from the site under study, was used to prepare the calibration samples by additions of the contaminant metals. Lead was the metal employed to indicate soil contamination by automotive scrap, but it was observed that the presence of strontium and titanium also could be used to indicate the presence of automotive scrap residue contamination. The depth profile of distribution of elements (Pb and Cr) was determined by ICPOES and *in situ* by the FO-LIBS prototype at 6 different locations. The profile encountered employing the LIBS system presented good agreement with the profile obtained by the ICPOES technique. The detection limits were 130 and 120 μg g^{-1} (two different sites in the first paper) for Cr and 250 μg g^{-1} and 100 μg g^{-1} for Pb in the first and second paper (different sites in each paper), respectively.

Corsi *et al*.[179] demonstrated the feasibility of double-pulse LIBS to perform the analyses of polluted soils. A mobile prototype, called Modì, developed by Applied Laser Spectroscopy Laboratory of Pisa, Italy, was used. About 5 to 10 times enhancements of the intensities of the spectral lines were observed with the double-pulse system. However, no significant increase of temperature between single and double-pulse plasmas was observed. Employing the calibration-free method,[40] it was possible to detected elements that could not be detected by the single-pulse configuration at the same laser pulse energy (e.g. Cr, Ni and Pb). The intensity enhancements obtained in soil samples were compared with the intensity enhancements for sediment samples and showed a clear influence of particle size on the enhancement of the signal (small particles give higher signals). The soil samples showed lower signal intensity than sediment samples. On the other hand, more compact samples presented higher enhancements in LIBS signals than did granulated samples.

Buckley *et al*.[241,242] reported the implementation of LIBS as a continuous emissions monitor for toxic metals. This paper discusses performance improved by nearly two orders of magnitude with *in situ* monitoring following implementation of conditional data analysis, where only the spectra having information about targeted elements are averaged for a series of 600 to 1200 laser pulses. The results showed detection limits of between 2 and 100 μg/dscm (dscm is defined as dry standard cubic meter) for the toxic metals Be, Cd, Cr, Hg and Pb.

3.3. Archaeological materials and art objects

The field of conservation and restoration of Cultural Inheritances is characterized by increasing requests for non-destructive analytical techniques. Great importance is attributed to the determination of the composition of painted surfaces, with the identification of pigments and binding additives necessary to date and restore them (e.g. oil paintings, ceramics, *afrescos*). Similarly, the correct identification of the technological type of ancient alloys, together with the knowledge of alteration induced by the environment, is important for both curatorial documentation and conservation purposes. The advantages of LIBS over other quantitative techniques for elemental analyses applied on historical findings are mainly due to its low invasiveness, the possibility to perform *in-situ* measurements, high spatial discrimination, rapidity and capability for direct analysis without any sample treatment. It is also worth mentioning that the LIBS technique can be used together with cleaning process, often made using lasers, in order to monitor the process by simultaneous acquisition of information of the composition of the ablated during cleaning and avoiding over-cleaning of objects. The use of LIBS in art and archeology has been recently reviewed.[243] However, the number of papers on this subject has increased remarkably during the last few years.

Borgia *et al*.[244] applied LIBS for a fast and precise elemental analysis in the field of cultural heritage conservation, called calibration-free laser induced breakdown spectroscopy (CF-LIBS). They analyzed some ancient Roman *afrescos* (II century AD). The results showed that the application of this calibration-free procedure frees the LIBS technique from the need of reference samples or an internal standard. The authors concluded that CF-LIBS is a viable technique for *in situ* quantitative analysis of artworks, due to its intrinsic speed and precision.

Melessanaki *et al*.[245] reported the examination of pottery, jewelry and metal artifacts found in archaeological excavations in central and eastern Crete by LIBS. The study showed that the spectral data indicates the qualitative and often the semi-quantitative elemental composition of the examined materials and this study demonstrated the advantages of LIBS analysis in obtaining elemental

analysis information about the materials used for making and decorating ancient pottery or metal artifacts.

Colao *et al*.[246] presented a paper that quantitates LIBS analysis on copper based alloys, including ancient bronzes. The analytical results obtained with calibration curves and a calibration free model were compared on a set of ancient Roman coins. In this study, the double-pulse technique showed that LIBS analytical results could benefit from synchronization between the UV laser sources used, respectively, for cleaning (266 nm) and for LIBS analysis (355 nm).

Fornarini *et al*.[78] discussed the influence of laser wavelength upon the analytical results obtained with ancient bronzes. A Nd:YAG laser with irradiation at 1064 nm was more effective than the wavelengths of 355 nm. They modeled the laser process ablation with a set of reference samples of quaternary Cu/Sn/Pb/Zn alloys and the difference between laser plume composition and alloy composition was estimated for both of the wavelengths.

LIBS has been demonstrated for depth profiling measurements along the thickness of different types of thin organic films used as protective coatings on historical and archaeological metal objects by Pouli *et al*.[247]. In this study, the materials examined were acrylic varnish and microcrystalline wax. The output from a nanosecond ArF excimer laser at 193 nm was found appropriate for performing a reliable profiling of the coating and for the ablation etch rate of the corresponding coating material under the same irradiation condition. Finally, this work demonstrated that femtosecond irradiation at 248 nm was better than nanosecond irradiation at 248 nm, yielding well-resolved profiles as a result of efficient ablation achieved by means of the increased non-linear absorption induced by the high power density of the ultrashort pulses.

Fortes *et al*.[248] discussed the capability of LIBS for characterization and cataloging of metallic objects belonging to the Bronze and Iron Ages. A set of 37 metallic objects from different locations of the Southeastern Iberian Peninsula were sorted according to their metal content. They were able to detect Cu, As, Sn, Pb and Fe in the metallic samples.

Lazic *et al*.[249] studied the detection of different archaeological materials immersed in seawater by means of LIBS. The materials found in undersea archaeological parks, such as iron, copper-based alloys, precious alloys, marble and wood was examined.

Acquaviva *et al*.[250] discussed elemental analyses carried out by LIBS as a restoration test on a piece of ordnance. The technique was used to investigate the composition of a gun found on the Adriatic seabed and kept in the S. Castromediano Provincial Museum in Lecce (Italy). LIBS investigation was performed before and after its restoration. The results showed that the gun is made of bronze. While the presence of copper and tin was confirmed by energy dispersion X-ray spectroscopy.

Anglos *et al*.[251] and Golovlev *et al*.[252,253] used the LIBS technique to characterize the elemental composition of the surface and interior of 19th century, metal-based photographs called daguerreotypes. Major components of the daguerreotype surface include Ag, Cu, and Au. Minor components such as Si, Al, Ca and Mg reflect contaminant particles arising primarily from the cover glass. The LIBS technique is useful to understanding the composition of daguerreotypes and for identifying the specific pigments used by the photographer.

3.3.1. LIBS for determination of pigments and inks

Burgio *et al*.[165] reported the use of LIBS in combination with Raman microscopy for the identification of pigments in different types of painted works of art. The elemental analysis information obtained from the LIBS measurements was confirmed by the Raman measurements, which led to the identification of most pigments. They found Hg, Mg, Pb, Ca, Fe, Al and Si in most of the works of art analyzed.

Melessanaki *et al*.[254] investigated by LIBS the *in situ* identification of pigments in an illuminated manuscript dated from the 12th-13th century. In parallel to LIBS, hyper-spectral imaging analysis was performed. They detected Al, Ag, Au, Ca, Cu, Hg, Mg, Na, Pb, Si, Sn and Ti in the illuminated manuscript by LIBS.

Castillejo *et al*.[255] used two laser-based analytical techniques, LIBS and Raman microscopy, for the identification of pigments on a polychrome in a fragment of a gilded altarpiece of the Spanish Rococo period. The results were obtained with the fundamental (1064 nm) and the third harmonic (355 nm) of a Q-switched Nd:YAG laser (laser pulse of energy in the range 2-10 mJ). This work demonstrated the potential of laser-based analytical methods as an alternative to traditional techniques for the characterization of successive layers of pigments in painted structures such as polychromes.

Martin *et al*.[256] reported the analysis of two real samples of polychromes from the Spanish Baroque period and from the 15th century, by time-integrated LIBS. The time-integrated spectra showed negligible contributions of continuum background emission. In this work, the samples were irradiated with a XeCl laser (308 nm, 17 mJ, 10 ns) and the results compared to the third harmonic of a Nd:YAG laser (355 nm, 10 mJ, 10 ns). The results showed Ca, Al, Mg, Na, and Pb emission lines in the spectra of the 15th century samples.

Oujja *et al.*[257] discussed the structural characterization and identification of inks of contemporary artistic prints by LIBS. In this work, they compared the LIBS results with SEM, and indicated that LIBS is more sensitive for the detection of elements that are present in minor concentrations. The analysis showed Ca, Ca_2, Al, Na and CN in an Arches Paper sample. This study showed the potential of LIBS for the chemical and structural characterization of artistic prints.

Bicchieri *et al.*[258] related the characterization of azurite and lazurite based pigments (blue pigments in medieval manuscripts) by LIBS and micro-Raman spectroscopy. They showed that Raman spectroscopy and LIBS are perfectly complementary concerning the information that can be obtained (molecular structure and quantitative elemental composition). Moreover, the LIBS capability of performing stratigraphic measurement could be interesting for the analysis of paintings and illuminated manuscripts.

Castillejo *et al.*[259] related the use of two laser-based analytical techniques, LIBS and Raman microscopy, to analyze a polychrome from the Rococo period. They found that combining LIBS (1064 nm, pulse energy = 10 mJ) with Raman microscopy provides reliable and complete information on the pigment composition of the successive layers of a polychrome.

Clark *et al.*[260] related the combination of application of Raman spectroscopy and LIBS for the identification of pigments at different depths below the surfaces of painted artworks such as icons and polychromes. The results revealed the identities of the pigments found in the upper layers (white lead, zinc oxide used for repair purposes, vermilion, red earth) above a silver foil. They emphasized the power of the combined application of the two techniques for stratigraphic analyses of the pigmentation on artworks.

Castillejo *et al.*[261] used four spectroscopic techniques, Fourier transform Raman (FTR), FTIR, LIBS, and LIF to characterize the pigment and binder composition of polychromes from Spain (13th century). For the LIBS technique, a KrF excimer laser (13 mJ) was used. The authors concluded that LIBS is better than Raman spectra, because some Hg, Pb, and Fe containing pigments cannot be clearly assigned in the Raman spectra.

Brysbaert *et al.*[262] reported pigment analysis in Bronze Age Aegean and Eastern Mediterranean painted plaster by LIBS. In this study, the third harmonic (355 nm, 10 ns, 2-5 mJ pulse^{-1}) of a nanosecond Q-switched Nd:YAG laser was used. This study showed that the LIBS technique cannot completely replace other, more sophisticated and destructive techniques but, as shown in this work, in combination with micro-Raman analysis it can provide complete identification for several organic and inorganic pigments, provided that the necessary reference libraries are available. They proposed that this combination may replace, at least partly, the traditional combination of XRD and SEM-EDS.

3.3.2. Use in pottery and ceramic analysis

Terra Sigillata archaeological ceramics manufactured in different production centers were studied by LIBS by López *et al.*[263]. They established a procedure for the rapid classification of these ceramics as a function of their provenance by means of a combination of LIBS and statistical methods. The use of linear correlations allows for clustering the samples by quantitative comparison of LIBS spectra.

López *et al.*[264] applied the LIBS technique for the analysis of *Hispanic Terra Sigillata* (Roman) pottery dating back to the 1st-5th century A.C. from two important ceramic production centers in Spain. Complementary analyses were carried out with scanning electron microscopy linked with energy dispersive X-ray microanalysis (SEM/EDX). In this study they distinguished differences between slip and body and characterized the transition between both parts of the sample. In all the cases investigated, Ca and Fe are the elements which better defined the transition. Other elements such as Si or Al showed the differences existing between slip and body in these ancient ceramics in relation with their region and period of production. The LIBS technique detected, in all the samples analyzed, elements such as Mg and Ti that were not detected by EDX. They proved that the LIBS technique, in combination with the other analytical techniques, can provide useful scientific information in archaeological studies.

Colao *et al.*[265] investigated different types of artworks, such as medieval glazed Umbrian pottery and copper based alloys from Roman and modern periods, using the LIBS technique. Semi-quantitative analyses on the multi-layered ceramics regarding glaze, luster and pigment decorations present on the surface. The results showed that on the ancient pottery, LIBS measurements allowed semi-quantitative determinations of both the glaze and the decorative layer composition and consequently to classify the materials used. When compared to the other analytical techniques and literature data, LIBS demonstrated to be a promising technique for fast, non-destructive analyses of ceramic samples.

Yoon *et al.*[266] applied the LIBS technique to analyze ancient pottery glaze. The major glaze elements such as Fe, Ca, Mg, Al and Si were found. The authors compared

the results with X-ray fluorescence. Elemental analysis showed that the glaze color differences were due to Fe content variations.

Lazic *et al*.[267] reported the analyses of glaze and decorations present on the surface of Renaissance Umbrian pottery, performed by means of different spectroscopic and optical techniques, such as laser induced fluorescence (LIF) and LIBS. In this study, two types of ancient lustre were considered: red and gold. The time resolved LIF signatures of the red and gold lustres were identified by applying a laser excitation at 355 nm, with a delay of at least 450 ns from the laser pulse. The LIBS technique was applied on all the ceramic layers to determine semi-quantitatively their elemental composition. The results showed that the LIBS measurements, compared to other analytical and literature data, can be considered satisfactory for non-destructive semiquantitative analyses of ceramic samples.

Anzano *et al*.[268] described the use of LIBS to identify pottery groups manufactured in early Roman settlements. The LIBS spectra from ceramics in a 200-800 nm spectral window were compared with reference spectral libraries. The LIBS spectra of 8 archaeological samples were studied. Linear and non-parametric correlations were applied for classification of spectral data with approximately the same results. The robustness of the technique was demonstrated by the 90-99% reliability of the identification of almost all analyzed ceramics.

3.3.3. Determination of marble and marble incrustations

Compositional characterization of incrustations on marble with LIBS was proposed by Maravelaki-Kalaitzaki *et al*.[269] The elemental LIBS profiles of black incrustations based on relative spectral line intensity values showed that the Fe, Si, Al and Ti contents relative to Ca content decrease significantly with depth. Thus, the contamination is decreasing within the altered layers, since these elements originate from atmospheric pollution and deposition. In the case of soil-dust incrustation and patina samples Si(I) and Al(I) emissions, identified throughout the analyzed crust, indicate deposition of soils-dust and remnants of previous treatments, respectively. They emphasized that LIBS is a micro-destructive technique and can be used as an autonomous *in-situ* diagnostic technique to obtain in-depth elemental profiling of incrustation even in cases of highly non-homogeneous layered crusts.

Lazic *et al*.[270] analyzed white marble samples from ancient quarries by LIBS, both on the bulk material and on surface incrustations. In order to compare such different spectra, a method for data analysis was developed. The results allowed the identification of the impurities characteristic of marble and their incrustations. In this work, the accuracy of the analytical procedure was checked by comparative SEM-EDX and ICPOES measurements and the quantification of metal contents in the incrustations supported the occurrence of sulfates in the outer layers exposed to environmental agents.

Maravelaki-Kalaitzaki *et al*.[271] discussed the use and control of excimer lasers (KrF, λ = 248 nm and XeCl, λ = 308 nm) for the removal of incrustations (black crust, soil-dust and biological deposits) from Pentelic marble. To detect chemical composition and crust morphology, as well as to monitor the effects induced by the laser treatment, the authors used a number of surface analytical techniques, such as Fourier transform infrared spectroscopy (FTIR), SEM-EDX, X-ray diffraction (XRD), LIBS and optical microscopy. They concluded that the relative concentrations of the elements Si, Al, Fe, Cl, Na and K decrease significantly with depth using the LIBS technique.

3.3.4. LIBS for monitoring cleaning processes of art artifacts

Klein *et al*.[272,273] used the LIBS technique to control the cleaning process of polluted sandstone and medieval stained glass. They combined a KrF excimer (248 nm, pulses of 30 ns, 240 mJ) and LIBS to clean areas of the artwork. They concluded that the monitoring of the relative intensities of relevant emission peaks of several elements (Si, Mg, Ca e Al) can be used as a control parameter for the cleaning process as their relative intensity changes as the laser ablation removes the superficial incrustation. Later, Klein *et al*.[274] studied the feasibility and the comparison of different laser wavelengths in removing various types of incrustations from marble and stone. The fundamental wavelengths of a Q-switched Nd:YAG laser (1064 nm) and the second and third harmonic wavelength of the Nd:YAG laser (λ = 532 and 355 nm, respectively) were used in this work. The second harmonic wavelength was not able to remove the artificial black incrustation without leaving remnants of the incrustation. Irradiation by the fundamental mode caused a dramatic color-change. The third harmonic showed the best result. They used the LIBS technique to evaluate the results of removal.

Colao *et al*.[275] used LIBS as a diagnostic tool during the laser cleaning of ancient marble from Mediterranean areas. In this work, the effectiveness of the cleaning process was monitored by following the disappearance from the LIBS spectra of the incrustation elements during successive laser shots. The process was also accompanied by SEM imagining and EDX analyses, and the potential of the LIBS method was demonstrated.

Castillejo *et al.*[276] studied the effect of wavelength on laser cleaning of polychromes on wood (fragments of a 14th century) using the four harmonics of a Q-swiched Nd:YAG laser (1064, 532, 355 and 266 nm, 5 ns). To verify the best wavelength irradiation conditions to clean red, green, yellow and black painted areas. In this work, the modifications induced on the surface of the samples by the irradiation of the laser were studied using optical and vibrational spectroscopies, such as LIF, LIBS, FT-Raman and FT-IR. They observed that soiled red, green and yellow painted areas are efficiently cleaned using the 266 nm Nd:YAG laser wavelength. The third harmonic of the Nd:YAG laser at 355 nm was also adequate for cleaning the yellow areas. Laser treatment of the surface with the fundamental and second harmonics (1064 and 532 nm, respectively) induces various degrees of discoloration. The results showed that the pigments have been identified as vermilion (red), verdigris (green), orpiment (yellow) and amorphous carbon (black). In this work, only the LIBS technique gave indication of a copper based composition, in agreement with the identification by restorers of the pigment verdigris.

Castillejo *et al.*[277] reported a study on the chemical and physical changes induced by a KrF excimer laser at 248 nm on tempera paint dosimeter systems. The changes were evaluated by using a range of analytical techniques. These include profilometry, colorimetry, optical and vibrational spectroscopies, such as LIF, LIBS, FTR, and FT-IR. For LIBS measurements, the output of the KrF laser was focused on the surface of the samples by a quartz lens to reach the high-energy fluence needed for the formation of a plasma plume (0.5-1 J cm^{-2}). This work indicates that LIBS, in addition to its use as an on-line monitoring technique, also serves as an analytical tool for the evaluation of changes on the surface of laser-treated paints immediately after treatment.

Tornari *et al.*[278] discussed a laser-based methodology for the cleaning of artworks, with emphasis on the preservation of their structural integrity and identity. In this work, the control of material removal during laser cleaning was achieved by using LIBS. A Q-switched Nd:YAG laser operating at 1064 nm (fluence of 1.4 J cm^{-2}) was used. The authors combined the LIBS technique with structural analysis by holographic interferometry.

Scholten *et al.*[279] developed an innovative laser restoration tool for non-contact cleaning of painted artworks. They used several monitoring techniques during laser ablation and showed that LIBS is a suitable diagnostic technique for on-line control when there is a gradient in the concentration of various elements or in the degree of oxidation.

3.4. LIBS for analysis in space

Sallé *et al.*[280] reported a study of the *in situ* LIBS method at reduced pressure (9.21×10^{-3} atm CO_2 to simulate the Martian atmosphere) and at near vacuum (6.58×10^{-5} atm in air to simulate moon or asteroids pressure) as well as at atmospheric pressure in air (for Earth conditions and comparison). They showed the influence of the ambient pressure on the analytical curves prepared from certified soil and clay pellets. The results showed that useful analytical curves could be obtained at reduced pressure without temporal resolution of the emission signal. In this paper, the best linear regression coefficient and the best repeatability were obtained at 9.21×10^{-3} atm of CO_2 (Martian conditions).

Radziemski *et al.*[281] studied emissions from the LIBS plasma in the 100-200 nm region using a sample chamber filled with 9.18×10^{-3} atm of CO_2 to simulate the Martian atmosphere. The effects of delay time and laser energy on LIBS detection at reduced pressure were examined. The effect of ambient CO_2 on the detection of C in soil was also examined. Useful lines for the spectrochemical analysis of As, Br, S, Cl, P and C were determined.

In another study, Sallé *et al.*[134] tested the capabilities of two different experimental setups for *in situ* geochemical analysis of Mars soils and rocks at stand-off distances up to several meters using the LIBS technique. They established analytical curves for elements presents in Al alloys and in Martian atmospheric conditions. For Cr, Mg, and Si, the detection limits obtained were very close to those reported in the literature for more standard LIBS setups.

Knight *et al.*[149] presented the results of the characterization of LIBS for the stand-off analysis of soils at reduced air pressures and in a simulated Martian atmosphere (6.58×10^{-3}-9.21×10^{-3} atm pressure of CO_2). In this work, under Martian conditions, the analyte signals appear to be somewhat enhanced over those recorded at atmospheric pressure due to increased ablation. For other space applications in which the ambient pressure was below 1.32×10^{-3} atm, there was a significant decrease in the analyte signals, resulting in higher detection limits.

3.5. Application to pharmaceutical products

St-Onge *et al.*[282] reported on the capabilities of LIBS for rapid analysis of multi-component pharmaceutical tablets. They showed that changing the plasma environment (e.g., with a He flow over the tablet surface) or using internal standardization (with carbon line or the plasma continuum emission) can bring significant

improvements to the analytical performance of LIBS, namely of sensitivity, linearity, precision and reduction of matrix effects.

Mowery *et al*.[283] have utilized the LIBS technique as a rapid means of simultaneously determining the thickness and uniformity of an enteric coating on compressed tablets. The emission spectra of all 4 elements (Ti, Si, Mg and Ca) were simultaneously monitored as a function of the number of laser pulses in the same spatial location. They calibrated the depth of penetration of individual laser pulses using profilometry. The results indicate that a change in coating application of less than 2 m/m% on a 100 mg tablet can be easily detected.

More recently, St-Onge *et al*.[284] demonstrated the possibilities offered by LIBS for the direct and rapid analysis of liquid pharmaceutical formulations. They chose sodium chloride in solution as a model compound. A pulsed Nd:YAG laser (1064 nm, 10 ns) was used to produce a gaseous plasma from the liquid sample. The results showed that using surface analysis of a flowing solution, the RSD of a measurement lasting 50 s (average of 50 laser shots at 1 shot s^{-1}) was approximately 0.5% for isotonic solutions.

3.6. Medical and biological applications

Samek *et al*.[285-287] reported on quantitative LIBS analysis to study the presence of trace minerals in teeth. In these papers, selections of teeth from different age groups were investigated. The samples showed a series of elements normally present in trace amounts in biological specimens. The authors concluded that the concentrations of aluminium found in the teeth under investigation could most likely be attributed to the use of toothpaste with whitening additives as well as the presence of fillings.

Samek *et al*.[164] reported on the application of LIBS to the analysis of important minerals and the accumulation of potentially toxic elements in calcified tissue to trace the influence of environmental exposure and other medical or biological factors. This paper exemplified quantitative detection and mapping of Al, Pb, and Sr in representative samples, including teeth and bones. They studied this approach in detail for traces of Al, Pb, and Sr in over 50 specimens.

Sun *et al*.[288] investigated the feasibility of using LIBS as a quick and simple technique to analyze trace elemental concentrations in the stratum corneum of human skin. A 60 mJ $pulse^{-1}$ Nd:YAG laser operating at 1064 nm (pulse duration of 5 ns) was used to form the laser-induced plasma. An analytical curve with a linear correlation coefficient of 0.998 and a detection limit of 0.3 ng cm^{-2} were obtained for Zn. The results indicate that Zn was absorbed through the skin and the concentration decreased exponentially with depth into the skin.

Corsi *et al*.[289] analyzed the concentration of the main minerals present in human hair by calibration-free laser-induced breakdown spectroscopy (CF-LIBS). The results showed that CF-LIBS can be considered as a very promising technique for hair tissue mineral analysis. This technique allows for the determination of relative concentrations of the most interesting elements in hair, at levels of a few mg per 100 g of materials.

Fang *et al*.[290] used the LIBS technique to analyze and identify elemental constituents of urinary calculi. The results showed that the elements detected with this study were: Ca, Mg, Na, Sr, K and Pb. In this study they concluded that the technique offers the possibility of accurate measurements of trace elements in such stones without the need for any elaborate sample preparation, but for quantitative measurements the system needs to be calibrated for each elemental species.

Kumar *et al*.[291] discussed the characterization of malignant tissue cells by LIBS. The authors applied the LIBS technique to distinguish normal and malignant tumor cells from histological sections for the first time. The results showed that the concentration ratios of elements in normal and tumor cells (mainly Ca/K and Cu/K) were significantly different and instigate new studies in order to develop a new diagnose tool with potential use *in vivo*.

Martin *et al*.[292] applied the LIBS technique for the identification of metals such as palladium and silver dispersed in bacterial cellulose membranes. In this study, the experiments were conducted by use of wet and dry metal-doped membranes. To the authors, the advantage of this laser-based technique is that minimal sample handling and sample preparation are needed and measurements are completed in real time.

3.7. Aerosol measurements by LIBS

The use of LIBS for aerosol measurement has been reviewed by Martin *et al*.[3] Since their survey, many efforts have been made to improve the quality of the results and to extend the use of LIBS to analysis of aerosols.

Neuhauser *et al*.[171,293,294] reported the development of a mobile system for a direct analysis of automatically acquired aerosol filter samples. The authors concluded that LIBS have a considerable potential for characterization of heavy metal aerosols. The detection limits for heavy metals presented a range from about 10 to 500 ng cm^{-2}.

Boyain-Goitia *et al*.[295] showed an application of LIBS for the analysis of single biological microparticles

(bioaerosols), such as the pollens of a variety of flowers. The spectra were recorded by exposure of the pollens to a single laser pulse from a Nd:YAG laser (λ = 1064 nm, 30 mJ). They detected C, Mg, CN, Ca, Al, Cr, C_2, and Na. The overall conclusions that can be drawn from this work are that single-pulse, single bioaerosol analysis is indeed feasible but that substantial technical development work still needs to be done and that many more species need to be measured to generate a suitable reference library before detection and identification can be made reliably in real time.

Mukherjee *et al.*[296] described a method for the quantitative use of LIBS for the compositional characterization of nanoaerosols, using an internal standard. This work establishes LIBS as an effective analytical tool for quantitative estimation of the extent of oxidation in Al nanoparticles from time-resolved atomic emission spectra. The approach involves finding the optimal laser delay time to collect spectra for each of the elemental species of interest and measuring the plasma temperature and argon density under the same conditions.

Martin and Chang[297] used time-resolved LIBS as a tool for the detection of chromium in aerosols. In this article, LIBS was used to obtain the lowest limits of detection for chromium (400 ng $dscm^{-1}$) in droplets. A comparison with other LIBS instruments and with ICPOES showed that the limits of detection for chromium metal in aerosols range from 12 to 60 μg $dscm^{-1}$ and 200 ng $dscm^{-1}$ for LIBS and ICPOES, respectively. They have studied the effects of laser wavelength, excitation energy and optimum spectrometer delay time to optimize these low limits of detection.

The plasma-analyte interactions in double-pulse LIBS analysis of gaseous and aerosol samples have been reported by Windom *et al.*[298]. The authors described a 2-fold increase in the peak-to-base ratio and 4-fold increase for the signal-to-noise ratio with an increase in single particle rate when the results of the double-pulse are compared with the single-pulse system.

3.8. Military and homeland-security applications

DeLucia Jr. *et al.*[126] related a series of laboratory experiments using the LIBS technique for the potential detection of terrorist threats. The ability to discriminate between several chemical agent simulants presents on soil under laboratory conditions was demonstrated. They analyzed LIBS spectra of explosives and explosive devices such as landmines, chemical agent simulants, and biological agent simulants. The results showed that its versatility makes an especially attractive candidate sensor for a variety of security related applications. Harmon *et al.*[175] used the LIBS technique for landmine detection and discrimination. In this work the detection and discrimination were evaluated using both a laboratory LIBS and a prototype man-portable LIBS systems. Using a linear correlation approach, 'mine/no mine' determinations were correctly made for more than 90% of the samples in both tests. The results illustrate the potential that LIBS has to be developed into a confirmatory sensor system for landmine detection. Schade *et al.*[299] applied LIBS in combination with a conventional mine prodder for remote detection of explosives and mine housing material. In this work high powered subnanosecond laser pulses (1064 nm, pulse energy of 0.6 mJ and pulse duration of 650 ps) from a passively Q-switched Nd:YAG laser were used. The ratios of LIBS intensities for cyanide (CN) plasma emission at 388 nm and for the C-emission at 248 nm were used and this allowed the classification of different explosives and mine casing materials under real time conditions. DeLucia Jr *et al.*[300] discussed the analysis of a number of energetic materials and explosives by LIBS. They include black powder, neat explosives such as TNT, PETN, HMX, and RDX, propellants such as M43 and JA2, and military explosives such as C4 and LX-14. The authors related that the laser beam did not detonate any of the energetic materials studied. They observed that these nitrogen and oxygen rich materials yield LIBS spectra in air that have correspondingly different O:N peak ratios compared with air and this difference can help in the detection and identification of such energetic materials.

Morel *et al.*[301] used the LIBS technique for analyzing biological matter for the detection of biological hazards. Eight species were considered in this experiment, 6 bacteria and 2 pollens in pellet form. A 1064 nm Nd:YAG laser (100 mJ pulses during 6 ns) was used. Time-resolved LIBS exhibits good ability in differentiating among the 8 species.

Baudelet *et al.*[302] studied a sample of *Escherichia coli* by LIBS using femtosecond pulses. In this work, the spectrum showed strong CN molecular bands due to the direct ablation of native CN molecular bonds from the bacteria in contrast with weak atomic lines from carbon. To the authors, the association of significant and relevant molecular spectral information with atomic spectral information makes femtosecond LIBS a powerful analytical tool to address organic or biological samples.

3.9. Forensic analysis

Dockery and Goode[303] reported on the use of LIBS to determine whether the hands of a suspected gun user contain traces of gunshot residue (mainly Ba and Pb).

The samples were obtained by pressing adhesive tape against the skin of the suspect and analyzing the tape directly. Barium and Pb emissions predominate in the samples collected from a person who has recently shot a gun. The error rates associated with the LIBS identification of a subject who fired one shot from a clean gun were evaluated by Monte Carlo simulation techniques. The results showed that the use of the maximum signal, rather than the average, allows LIBS to detect the presence of particulate matter on the hands of a suspected shooter.

Almirall *et al*.[304] evaluated the LIBS technique as a tool for the forensic elemental analysis of glass and compared in performance to other elemental techniques. A Nd:YAG 1064 nm, 60 mJ pulse^{-1} was used. They concluded that LIBS offers potential as a discriminating technique that is fast, easy to use, almost non-destructive and relatively inexpensive.

3.10. Miscellaneous applications

Gleason and Hahn[305] discussed the process associated with mercury atomic emission in a LIBS and the interactions of mercury with oxygen species. The authors demonstrated that LIBS-based analysis of the 253.7 nm mercury atomic transition is affected by the presence of oxygen. In this study, based on plasma temperature measurements, thermal effects are not responsible for the observed signal reduction and the authors suggested several solutions to real-time monitoring problems, such as the use of temporal gating to limit mercury emission detection to relatively early temporal regimes where the potential effects of molecular quenching is mitigated by the presence of atomic oxygen.

Chen *et al*.[306] used the LIBS technique to map the distribution of particulate matter inside the plume created by laser ablation of a brass target. They used two lasers in this work, one Nd:YAG laser was focused on the target by means of a 150 mm focal length. The second Nd:YAG laser was focused on the plume by means of a 50 mm focal length positive lens. Both lasers were operated at the fundamental harmonic (1064 nm) and the energies of the first and the second lasers were 600 and 300 mJ, respectively. This study proved that LIBS is a useful tool for mapping the distribution of the particulate matter inside the plume created by laser ablation.

Fink *et al*.[307] discussed the use of LIBS for elemental characterization of recycled thermoplasts from consumer electronics. The experimental parameters (wavelength, delay time, integration time gate and irradiance) and corresponding analytical figures of merit were determined. The results showed that employing an echelle spectrograph allowed fast multielement analysis (Ti, Sb, Zn, Sn, Al, Cd, Cr, Pb) due to superior spectral coverage and spectral resolution.

Gornushkin *et al*.[308] reliably identified several groups of iron-based particulate materials (iron ores and iron oxides) by correlation analysis using a microscopic laser induced breakdown spectrometer. The robustness of the technique was demonstrated by the nearly 100% reliable identification of NIST iron ores and natural iron ore samples. To the authors, this technique should have applications in the metallurgical, mining, and semiconductor industries, and in medical, environmental and forensic sciences.

Caneve *et al*.[309] applied the LIBS technique to test the possibility of detecting and identifying asbestos in different samples with the perspective of extending this to field analysis without sample preparation. In this work, ratios of intensities of characteristic elements were tested as indicators for asbestos recognition. The results indicated a good correlation for Mg/Si and Fe/Si (spectral region around 290 nm) and showed the capability of LIBS as a diagnostic tool for this category of materials. The results were compared with those obtained by analyzing the same asbestos samples with a scanning electron microscopic equipped with an energy dispersive X-ray spectroscopic.

Ferioli and Buckley[310] described the use of LIBS for direct measurement of atomic species over a wide range of mixture fractions of C_3H_8, CH_4, and CO_2 in air. Atomic emission from laser-induced plasmas was observed and ratios of elemental lines present in the spectra were used to infer composition in reactants and in flames. In this paper the authors demonstrated that LIBS could be used to obtain quantitative equivalence ratio measurements for propane and methane in air and the C/(N + O) atomic ratio was used to quantify mixture fraction of C_3H_8 in air, and data from individual breakdown events have a RSD of 3% of the mean for mixtures of 0, 1 and 2% propane in air.

Smith *et al*.[311] applied LIBS for the determination of plutonium isotope ratios by direct observation of atomic emissions from laser-induced plasmas at high resolution. The Pu-239/Pu-240 isotope shift of –0.355 cm^{-1} from the plutonium atomic line at 594.52202 nm was clearly resolved in this work. The observed plutonium linewidths were 0.19 cm^{-1} (6.7 pm) and these linewidths are within the experimental error of the ideal instrument-limited linewidths, which was calculated to be 0.15 cm^{-1} (5.2 pm) based upon the known modulation transfer function for the ICCD system. The LIBS may be applicable for isotopic ratio determinations across the light actinide series.

Anzano *et al*.[312,313] related the instant identification of

post-consumer plastic by LIBS. LIBS spectra from plastic in a 200-800 nm spectral window were compared with reference spectral libraries. They studied the plasma emission spectra of polyethylene terephthalate (PET), high density polypropylene (HDPE), polyvinyl chloride (PVC), low density polyethylene (LDPE), polypropylene (PP) and polystyrene (PS). The robustness of the technique was demonstrated by the 90-99% realiable identification of almost all analyzed plastic.

Sallé *et al.*[314] made a comparative study of different methodologies for the quantitative elemental analysis of natural rock samples by the LIBS technique. The three methods evaluated clearly demonstrated that the matrix effects could be corrected by merely taking into account the difference in the number of vaporized atoms.

Rosenwasser *et al.*[315] described the development of a method for real-time automated quantitative analysis of mineral ores using a LIBS instrument. The auto-sampler permits the execution of methods for performing calibrations and analyses of multiple elements on multiple samples. Methods were developed to automatically perform metallic element calibrations for phosphate ore samples containing known concentrations of the following minerals: P_2O_5, CaO, MgO, SiO_2 and Al_2O_3. The results showed linear regression coefficients better than 0.980 for all analytes.

D´Ulivo *et al.*[316] reported the application of LIBS to the determination of deuterium/hydrogen number ratio (β) in headspace gases. The results showed that the best performances were obtained for β close to unity, which makes LIBS perfectly suited for the detection of H-D exchange taking place during aqueous hydrolysis of $NaBD_4$ or $NaBH_4$.

Wilsch *et al.*[317] proposed the use of a LIBS technique for on-site application having the possibility to investigate a wide range of different measuring points. The LIBS set-up consists of a pulsed Nd:YAG laser (pulse duration of 10 ns, 300 mJ $pulse^{-1}$, repetition rate of 20 Hz, 1064 nm) that was focused on the surface of the sample. The results found for chloride in concrete structures were successfully validated by comparison with the results of standard chemical measurements.

Nasrazadani and Namduri[318] used LIBS to take the spectra of iron oxides samples. Complementary techniques to LIBS, such as FTIR spectroscopy and X-ray diffraction (XRD) analysis were also used to characterize iron oxides. This study demonstrates that LIBS can be successfully applied to characterize the oxidation states of multivalent oxides of elements like Fe, Cr, Pb and others.

Cáceres *et al.*[319] reported a simple quick-freeze method for the quantitative analysis of trace metal ions in liquids applying the LIBS technique. They reported that using this procedure with calibrated samples, well-characterized linear analytical curves were determined for Na and Al water solutions over the 0.01-1% concentration range. The results allowed detection limits of the order of mg kg^{-1}.

LIBS was applied to determine the carbon content of pulverized coal, char and fly ash by Noda *et al.*[320] The authors tested the applicability under several gas conditions. The results showed that the simultaneous detection of Si, Al, Fe, Ca and C requires a spectrograph having a wide wavelength range to detect the carbon signal with high resolution as well as the Si, Al, Fe and Ca signals. In this paper emission signals were detected using a two grating spectrograph (f = 250 mm, grating 1: 3600 lines mm^{-1}; grating 2: 600 lines mm^{-1}) and an ICCD camera (integration time gate of 200 ns) with a Nd:YAG laser at 1064 nm.

Lal *et al.*[321] investigated the application of LIBS for the determination of the elemental composition of the glass batch used as a surrogate for radioactive glass waste and that used to manufacture the most common type of flat glass. This study clearly demonstrated the potential of LIBS for *in situ* monitoring of glass batches in the glass industry. The accuracy and precision of the glass-batch measurements with both systems are better than 5% for the major elements and better than 10% for most of the minor elements. Lal *et al.*[322] also investigated the effect of various parameters on the accuracy of the LIBS data taken from pellet samples. The results showed that the RSD of the LIBS data obtained using pellets was approximately 10 times lower than that of the data acquired from powdered samples.

Molina *et al.*[323] studied the effect of temperature and CO_2 concentration on laser-induced breakdown spectroscopy measurements of alkali fume. They used a Q-switched, Nd:YAG laser with a 10 ns pulse duration, a typical output energy of 360 mJ, and a repetition rate of 5 Hz was operated at the fundamental frequency (1064 nm). The experiments showed that, for a delay time of 10 μs and an integration time gate of 50 μs, the presence of CO_2 and changes in gas temperature affect the intensity of both the continuum emission and the Na D lines. The intensity increased for the neutral Ca and Mg lines in the presence of 21% CO_2 when compared to 100% N_2, whereas the intensity of the ionic Mg and Ca lines decreased.

Häkkänen and Korppi-Tommola[324] used LIBS to study inorganic pigment and organic binder distributions in paper coatings. The plasma was generated by focusing a pulsed XeCl excimer laser beam (diameter 100 μm, irradiance 0.3 GW cm^{-2}, 15 ns) on the sample surface at atmospheric pressure. Emission line intensities from ionic

and neutral magnesium atoms were used to effect plasma temperature corrections in determining silicon and calcium in coatings. For the coatings containing calcium carbonate the self-absorption of the Ca(I) 423 nm line in air was observed. In an argon buffer, self-absorption was not present. Later, Häkkänen *et al*.[325] used LIBS to determine various properties of coated and uncoated papers. Depth profiles of double-coated papers were determined and microscopic variations of pigments in a double-coated paper were also analyzed. The results showed that the carbon-calcium intensity ratio increases with binder content and, in the samples analyzed, the binder concentration is higher in the top most layer than in the second layer.

Bicchieri *et al*.[326] discussed a study of foxing stains on paper by chemical methods, infrared spectroscopy, micro-X-ray fluorescence spectrometry and LIBS. They decided to focus on the influence of the different Fe valences in the formation of stains in the paper. They obtained precise elemental information from LIBS and structural information from vibrational spectroscopy.

3.11. Chemometrics applications

Statistical methods have been used to interpret spectroscopic data produced by a variety of techniques aimed at many applications. Nevertheless, relatively few papers have been published combining the attractive features of LIBS (no sample preparation, rapid data collection, rugged design and, mainly, its multivariate nature) with the analyzing power of chemometrics, such as partial least-squares regression (PLS),[327,328] pattern recognition (principal component analysis, PCA, and cluster analysis),[329-333] soft independent modeling of class analogy (SIMCA),[334] neural networks analysis (NNA),[335-338] among others.

Munson *et al*.[339] investigated the efficiency of sample identification using LIBS coupled with various statistical techniques, such as linear correlation, PCA and SIMCA. The influence of data selection, sample averaging, spectral weighting, LIBS laser power and the sample matrix on the ability of these statistical models to perform species differentiation was studied. Samples investigated include several biological warfare agent simulants, biological interferents (pollens and molds), and chemical nerve agent simulants. The results indicate that spectral averaging and weighting schemes may be used to significantly improve sample differentiation.

Amador-Hernández *et al*.[340] proposed the application of LIBS for quantitative determination of gold and silver in Au-Ag-Cu alloys. The study showed that the determination of gold and silver in jewelry samples could be satisfactorily developed by LIBS-PLS methods. In this work the influence of some spectral characteristics (e.g. emission line interferences, high-continuum background, line broadening effects, self-absorption and self-reversal phenomena) were tested in order to establish the capabilities of PLS to enhance analytical results obtained with simple, low cost instrumentation. Garcia-Ayuso *et al*.[341] discussed the suitability of LIBS for the characterization of jewelry products by the development of a method based on the use of an Nd-YAG laser. The method was developed by using both multivariate optimization and calibration procedures with application of the appropriate quality criteria. Chemometric analysis of the data and the use of PLS regression for calibration guaranteed the ruggedness of the proposed method. In spite of the interferences present in the samples, the results confirmed the good predictive ability of the PLS models for the analysis for Au and Ag in jewelry. Later, Jurado-López and Luque de Castro[342-344] reported on a new application of LIBS and multivariate data analysis, namely PLS regression, using jewelry as the example. The method was designed for the quantitative characterization of the interface of gold-filled jewelry by monitoring the emission lines of the elements present in the sample, while subjecting the piece to a number of separate laser pulses. The method also provided quantitative information about the composition of a given layer of special interest at the interface in order to know the existence of diffusion phenomena.

Jurado-López and Luque de Castro[345] studied the composition of the alloys used in the manufacture of jewelry pieces with the help of a spectral library. This work employed the LIBS spectra set of 32 alloys, with 25 of them chosen as library standards and seven used as prediction samples. The composition of the alloys was obtained by FAAS and a rank correlation method was applied for comparison between spectra. The composition of the samples was also predicted by PLS regression. The study showed the capacity of this technique for the rapid analysis of these types of material. They also made a comparison between a LIBS-PLS method and methods based on some well-known techniques, such as ICPOES, FAAS, and atomic scanning microscopy (ASM).[346] This study was presented in order to both validate the content of gold and silver in alloys to be used as solid standards and developed an alternative to the established methods for the hallmark of gold and silver in jewelry. Seventeen alloys with gold concentrations between 80 and 100% and variable concentration of other metals usually present in jewelry were used as solid standards for LIBS. The

results confirmed a good predictive ability of the PLS models based on LIBS data for the analysis of gold and silver in jewelry, in comparison with the other well-known instrumental methods for metal determination.

Luque-García *et al.*[347] applied the LIBS-PLS method for the analysis of solid samples (homogeneous and heterogeneous). Results of the LIBS-PLS method were statistically compared with those obtained by GFAAS (for Ag and Cu) and FAES (for Ca) and a good agreement between the results was found. Although the LIBS method is not as accurate as the conventional methods, its use has a series of advantages (rapidity, no sample destruction and spatial resolution).

Martin *et al.*[348] used multivariate statistical analysis techniques (PCA and PLS) coupled with LIBS to identify preservative compounds (chromated copper arsenate, ammoniacal copper zinc or alkaline copper quat) and predicted elemental content in preservative-treated wood. The results demonstrated that Cu, observed at 324.74, 327.38, 510.58, 515.30, 521.78 nm, and Zn, at 330.26, 334.50, 472.26, 481.06 nm, are the important elements in building a model. They also demonstrated that strong correlations were obtained between the measured and the LIBS-predicted values for Cu, As, Zn, and Cr concentrations.

Sirven *et al.*[349] discussed the used of LIBS for the analysis of 3 chromium-doped soils. In this work two chemometric methods, PCA and NNA, were used to discriminate soils on the basis of their LIBS spectra. Prediction accuracy and precision of 4-5% were obtained with a reasonably small neural network.

Amador-Hernández *et al.*[350,351] proposed a simple and rapid method based on LIBS-pattern recognition for the three-dimensional characterization of screen-printed electrodes. The identifications of the elements found in the electrodes were carried out by comparison of their plasma emission spectra with those obtained from standard materials and tabulated data. Neutral atomic line emissions observed in the visible region from 450 to 610 nm were selected for the determination of the major components during the three-dimensional study of the electrode, as such, C (I) at 513.3 nm, Ag (I) at 520.9 nm, Au (I) at 523.0 nm, Pd (I) at 529.6 nm, Pt (I) at 530.1 nm and Ti (I) at 498.2 nm. The application of principal component analysis-cluster analysis (PCA-CA) was an excellent aid for classification of the available spectroscopic information, in order to establish patterns of the lateral and in-depth distribution of all elements.

Corsi *et al.*[352] discussed the use of LIBS to analyze archaeological copper objects from the burial site of "Fontino" cave. In this work, the samples were classified using PCA and a quantitative analysis of the elemental composition of 11 different elements ranging from the major matrix element (Cu, more than 90%) to trace elements (Ag, Al, As, Fe, Pb, Sb) was made. The analyses were performed without the need for reference standards.

Samuels *et al.*[353] used LIBS to study bacterial spores, molds, pollens and proteins. In this work, each LIBS spectrum was analyzed by PCA and was found to contain adequate information to support discrimination among these biomaterials.

Sirven *et al.*[354] related the use of LIBS to measure chromium concentrations in soil samples. They made a comparison between direct use of the analytical curve and two chemometric techniques, PLS and NNA. The evaluation was made in terms of prediction accuracy, precision and limit of detection. The results showed that NNA clearly gave the best results, with accuracy and precision at least twice as good as the analytical curve while PLS showed an even worse performance.

Panne *et al.*[355] employed a PLS regression model based on LIBS data to explore the analysis of glass and glass melts during vitrification as well as bottom ashes. They used a total of 23 samples, 19 samples for the calibration set and 4 samples for the test set. This work presented the best results with a single component model (93% explained variance).

Hybl *et al.*[356] discussed LIBS as a potential method for detecting airbone biological agents. The authors used the PCA to illustrate that linear combinations of the detected atomic lines, which are present in different ratios in each of the samples tested, can be used to discriminate biological agent simulants from other biological matter. In this work, Ca, Mg, and Na, which are present in varying concentrations between 0.3 and 11% (by mass) in the *Bacillus anthracis* (Bg) particles, were evaluated.

Bohling *et al.*[357] used a miniaturized laser technology, fiber optics and time-resolved detection of LIBS intensities at 388 nm for real-time spectroscopic classification of different mine casing materials and explosives. They improved the accuracy in the identification of different materials with identical atomic composition by time-resolved LIBS and application of self-learning neural networks. In this investigation only one classification characteristic was used to train the neural network. The result could easily be improved by adding more classification characteristics and by increasing the number of data sets for training the neural network.

Sattmann *et al.*[358] applied the LIBS technique to investigate the possibility of using this method for the identification of different materials. They studied the plasma

emission of high-density polyethylene (HDPE), low-density polyethylene (LDPE), polyvinyl chloride (PVC), polyethylene terephthalate (PET), and polypropylene (PP). The results showed that the automatic evaluation of the spectral data measured on clean samples with neural networks enables identification accuracies in the range of 93 to 96% for PE and PP and of > 99% for PET and PVC.

Freedman *et al.*[359] built and tested a miniature LIBS instrument. It was built with a microchip laser (Litton Synoptics) that produced pulses of 500 ps at 14 μJ energy and 7.8 kHz, an optical system that allowed a 1.5 cm focal length which focused the plasma emission onto an optical fiber. Craters of 20 μm diameter were created by the laser. The analyses of 7 trace elements were evaluated by reference samples of aluminum alloy containing Cu, Fe, Mg, Mn, Ni, Si and Zn. Analytical curves were obtained by two protocols, using internal standardization of integrated peaks areas and PLS. The analytical curves obtained by the peak integration method showed exponential behavior and PLS analytical curves produced a linear fit, presenting a reduction of noise near the origin. In relation to the figures of merit, the PLS analyses presented better results regarding detection limits, but the RSD's were better only for Mg, Si and Zn. In general low detection limits, in the range of 0.11 to 1.87% for peak integration analyses and 0.05 to 0.36% in PLS analyses, were obtained. The RSD's in the range of 12 to 20% and 4 to 29% for peak integration analyses and PLS analyses, respectively, were achieved. The LIBS system proposed is attractive due to its simplicity (easily to build) and low price. More investigation is necessary to establish the representativeness of the small areas sampled by the low energy laser pulses employed.

4. Conclusions and Further Remarks

The LIBS technique is very rapidly finding its niche among the modern spectrometric techniques. The bibliographic references cited in this review allow observing the various field of application of the technique. Its use in non-conductive solid samples presents an advantage over the arc/spark spectrography and other well established techniques such as ICPOES and AAS. However, up to the moment, the detectivities (typical detection limits of $\mu g\ g^{-1}$) and precision of LIBS are not good as arc/spark spectrography and become even worse when compared with ICPOES and AAS. One can foresee hyphenating LIBS with concentration techniques in order to overcome the limitations imposed by these detection limits for liquid samples or even for solid samples after digestion. For instance, recently, a flow-injection technique has been coupled to LIBS (FI-LIBS) in order to concentrate aluminium in liquid samples.[360] This can be done by means of a liquid-solid extraction and concentration scheme and the multielemental characteristic of LIBS will facilitate the use of non-selective reagents. On the other hand, using such procedures will impose complexity to the analytical method and jeopardize one of the main characteristic of the technique: its direct use on a raw sample.

Comparison of the results obtained for the content of elements present in a sample as determined by LIBS and by a bulk technique such as ICPOES may sometimes be meaningless. The material ablated by one laser pulse is taken from a limited area of few micrometers of the sample surface and amounts to nanograms or few micrograms while bulk methods will determine the average concentration of the analyte in a quantity of the sample that is about 10^3 to 10^6 times greater and effectively represents the whole sample. Of course, averaging the emitted radiation after many laser pulses and using some pre-pulses to clean the sample surface can minimize this difference, but it is very difficult to reduce it to a negligible level.

The reproducibility of the LIBS signals obtained by common lasers producing pulses of about 5 ns duration is also not as good as with other spectrometric techniques. The typical standard deviations for a signal obtained after averaging many pulses from a smooth and homogeneous surface (free of variations of concentration) are in the range from 2 to 10%. Some improvement in this figure of merit is expected when faster lasers (operating in the femtosecond time scale) become common and the thermal stochastic nature of the ablation process produced by nanosecond laser pulses will be replaced by a purely photonic process. However, the cost of such devices must decrease and its robustness augmented before many laboratories can take part in this development and study LIBS with ultra-short pulse lasers.

The cause of the LIBS disadvantage regarding the aspect of representativeness of the bulk sample is converted to one of its great advantages when the aim is microanalysis. Surface lateral resolution of few micrometers and depth resolution also of this order of magnitude impart unique characteristics to LIBS and certainly defines one of its more promising applications. Up to the moment there is no counterpart for LIBS when microanalysis of metallic and non-metallic surfaces and depth profiles is the issue. Many efforts will certainly devoted to the development of microanalysis by LIBS in the near future. The quasi non-destructive (surely, causing no discernible damage to the naked eye) character of the

technique enables its use on art, archaeological objects and jewelry with more versatility than its counterpart X-ray fluorescence, that has similar detection limits. Improvements in calibration-free LIBS methods will make the technique even more powerful for use in the field as the requirements for standards (rarely available for such type of samples) are eliminated.

The portability of the LIBS systems indicates the technique for field analyses of environmental interest by screening and mapping critical areas which can be contaminated by organic or inorganic pollutants. In this area, the development of in-field low cost instrumentation will certainly play the most relevant role in the near future. The agricultural area might also make use of developments in portable instrumentation as, most certainly, would homeland security and military areas.

There are great expectations for more results from the application of LIBS in aerosol analysis. So far, the potentialities of the technique have been demonstrated in a number of papers. This issue is relevant for environmental and home security fields.

Remote analysis is another niche that will be occupied by LIBS without any rival technique. The ability of a LIBS system in generating, collecting and measuring a signal produced from a sample distant by more than 50 m is unique among the spectroscopic elemental analytical techniques. Military, home security, analysis of dangerous material or in dangerous places and environmental areas will provide many interesting applications for this technique. More unorthodoxy applications of the remote characteristics of LIBS are found in space analysis. Many possibilities can be foreseen. A NASA project to place a LIBS instrument on a vehicle for exploring Mars is programmed for the year 2009.[12]

The LIBS technique provides a great potential to be hyphenated with Raman vibrational spectroscopy because both techniques share most of the same equipment. In fact, a simple control of the laser pulse energy and some adaptations in the optics can easily convert a LIBS system into a Raman spectrometer. The techniques are complementary to a high degree and the hyphenated instrument would provide access to analytical information on inorganic and organic species present in a sample. Some advances are expected on the subject of joining LIBS and Raman spectroscopy in the near future, mainly concerning the instrumental aspects involved.

The near infrared (NIR) spectral region of the emission spectrum generated by LIBS is still to be exploited for analytical purposes. The best ICCD-based detectors available can extend the monitored spectral range up to wavelengths of about 925 nm (at cost of a lower quantum efficiency). This type of device has recently been employed for determination of sulfur in the first paper exploiting the NIR spectral region of LIBS.[361]

While research on LIBS will continue to grow in an exponential fashion in the next several years, the knowledge accumulated in academia will be transferred to commercial instrument companies that will, in last instance, be responsible to popularize the technique. Recent initiatives to standardize LIBS nomenclature and relevant instrumental parameters are actions pointing in the direction of a mature technique which will certainly play a relevant role in analytical chemistry in the foreseeable future.

Acknowledgments

The authors are grateful to Dr. Carol H. Collins for manuscript revision and many helpful suggestions. CP and FBG are grateful to FAPESP for a research grant and post-doctoral fellowship, respectively. JC and LMCS are grateful to CNPq for the MSc and PhD fellowships, respectively.

Celio Pasquini *graduated in chemistry at the Chemistry Institute of (Universidade Estadual de Campinas (UNICAMP) where he also concluded his MSc and PhD programs in instrumentation and automation in analytical chemistry. He was a post-doc of the King´s College-London for two years and is presently a full professor of the Chemistry Institute-UNICAMP where he served as the director of the institute for the years 1998-2002.*

Fabiano B. Gonzaga *got his BSc degree in chemistry at Universidade Federal de Viçosa (UFV) in 2000. He made his PhD studies at Universidade Estadual de Campinas (UNICAMP), from 2002 to 2006, working together Prof. Celio Pasquini in the development of a near infrared emission spectrometer. From 2006 now, he is a post-doctoral researcher at UNICAMP, under supervision of Prof. Celio, working in the development of alternative and low cost detection systems for LIBS.*

Juliana Cortez *graduated in chemistry at the Universidade Estadual de Maringá (UEM) in 2004. Her MSc in LIBS area was initiated in 2005 and finished in 2007 under the supervision of Prof. Dr. Celio Pasquini at UNICAMP. She is now a PhD student continuing her studies in LIBS area with the same supervisor.*

Lucas M. C. Silva *received his BSc in chemistry in 2003 and MSc in Analytical Chemistry in 2005 from Universidade Estadual de Londrina (UEL) under the supervision of Prof. Dr. Ieda S. Scarminio. He is currently a PhD student in the Group for Instrumentation and Automation in Analytical Chemistry at Chemistry Institute (UNICAMP), working with Laser Induced Breakdown Spectroscopy technique (LIBS) under the supervision of Prof. Dr. Celio Pasquini.*

References

1. Song, K.; Lee, Y.; Sneddon, J.; *Appl. Spectroc. Rev.* **1997**, *32*, 183.
2. Rusak, D.A.; Castle, B.C.; Smith, B.W.; Winefordner, J.D; *Trends Anal. Chem.* **1998**, *17*, 453.
3. Martin, Z.M.; Cheng, M.D.; Martin, R.C.; *Aerosp. Sci. Technol*. **1999**, *31*, 409.
4. Sneddon, J.; Lee, Y.; *Anal. Lett.* **1999**, *32*, 2143.
5. Radziemski, L.J.; *Spectrochim. Acta, Part B* **2002**, *57*,1109.
6. Song, K.; Lee, Y.; Sneddon, J.; *Appl. Spectrosc. Rev.* **2002**, *37*, 89.
7. Tognoni, E.; Palleschi, V.; Corsi, M.; Cristoforetti G.; *Spectrochim. Acta, Part B* **2002**, *57*, 1115.
8. Song, K.; Lee, Y.; Sneddon, J. In *Advances in Atomic Spectroscopy-Volume 7*; Sneddon, J., ed.; Elsevier Science: Amsterdam, **2002**, ch. 6.
9. Winefordner, J.D.; Gornushkin, I.B.; Correll, T.; Gibb, E.; Smith, B.W.; Omenetto, N.; *J. Anal. At. Spectrom.* **2004**, *19*, 1061.
10. Vadillo, J.M.; Laserna, J.J.; *Spectrochim. Acta, Part B* **2004**, *59*, 147.
11. Santos Jr., D.; Tarelho, L.V.G.; Krug, F.J.; Milor, D.M.B.; Martin Neto, L.; Vieira Jr. N.D.; *Rev. Analytica*, **2006**, *24*, 72.
12. Cremers, D.A.; Radziemski, L.J.; *Handbook of Laser-Induced Breakdown Spectroscopy*, Wiley: New York, **2006**.
13. Misiolek, A.W.; Palleschi, V.; Schechter, I. eds.; *Laser Induced Breakdown Spectroscopy*, Cambridge University Press: Cambridge, **2006**.
14. Singh, J.P.; Thakur, S.N. eds.; *Laser Induced Breakdown Spectroscopy*, Elsevier Science:Amsterdam, **2006**.
15. Einstein, A.; *Phys. Z.* **1917**, *18*, 121.
16. Shawlow, A.L.; Townes, C.H.; *Phys. Rev.* **1958**, *112*, 1940.
17. Maiman, T.H.; *Nature* **1960**, *187*, 493.
18. Brech, F.; Cross, L.; *Appl. Spectrosc.* **1962**, *16*, 59.
19. Runge, E.R.; Minck, R.W.; Bryan, F.R.; *Spectrochim. Acta, Part B* **1964**, *20*, 733.
20. Zel'dovich, Y.B.; Raizer, Y.P.; *Sov. Phys. JEPT* **1965**, *20*, 772.
21. Radziemski, L.J.; Loree, T.R.; Cremers, D.A.; Hoffman, N.M;. *Anal. Chem.* **1983**, *55*, 1246.
22. Cremers, D.A.; Radziemski, L.J.; *Anal. Chem*. **1983**, *55*, 1252.
23. Noll, R.; *Anal. Bioanal. Chem*. **2006**, *385*, 214.
24. Weyl, G. M. In *Laser-Induced Plasmas and Applications*; Radziemski, L. J.; Cremers, D. A., eds.; Marcel Dekker: New York, 1989, ch. 1.
25. Sacchi, C.A.; *J. Opt. Soc. Am. B* **1991**, *8*, 337.
26. Haglund, R.F. In *Laser Ablation and Desorption-Volume 30-Experimental Methods in Physical Sciences*; Miller, J.C.; Haglund, R.F., eds.; Academic Press: San Diego, **1998**, ch. 2.
27. Russo, R.E.; Mao, X.L.; Liu, H., Gonzalez, J.; Mao, S.S.; *Talanta* **2002**, *57*, 425.
28. Russo, R.E.; Mao, X.L.; Liu, C.; Gonzalez, J.; *J. Anal. At. Spectrom.* **2004**, *19*, 1084.
29. Bleiner, D.; Chen, Z.; Autrique, D.; Bogaerts, A.; *J. Anal. At. Spectrom.* **2006**, *21*, 910.
30. Vadillo, J.M.; Romero, F.; Rodrigues, C.; Laserna, J.J.; *Surf. Interface Anal.* **1999**, *27*, 1009.
31. Mao, X.L.; Chan, W.T.; Shanon, M.A.; Russo, R.E.; *J. Appl. Phys*. **1993**, *74*, 4915.
32. Capitelli, M.; Casavola, A.; Colonna, G.; De Giacomo, A.; *Spectrochim. Acta, Part B* **2004**, *59*, 271.
33. Lunney, J.G.; Jordan, R.; *Appl. Surf. Sci*. **1988**, *127-129*, 941.
34. Callies, G.; Schittenhelm, H.; Berger, P.; Hügel, H.; *Appl. Phys. B* **1999**, *68*, 121.
35. Herman, J.; Boulmer-Leborgne, C.; Hong, D.; *J. Appl. Phys*. **1998**, *83*, 691.
36. Colonna, G.; Casanova, A.; Capitelli, M.; *Spectrochim. Acta, Part B* **2001**, *56*, 567.
37. Mazhukin, V.I.; Nossov, V.V.; Nickforov, M.G.; Smurov, I.; *J. Appl. Phys*. **2003**, *93*, 56.
38. Gornushkin, I.B.; Stevenson, C.L.; Smith, B.W.; Omenetto, N.; Winefordner, J.D.; *Spectrochim. Acta, Part B* **2001**, *56*, 1769.
39. Gornushkin, I.B.; Kazakov, A. Ya.; Omenetto, N.; Smith, B.W.; Winefordner, J.D.; *Spectrochim. Acta, Part B* **2004**, *59*, 401.

40. Ciucci, A.; Corsi, M.; Palleschi, V.; Rastelli, S.; Salvetti, A.; Tognoni, E.; *Appl. Spectrosc.* **1999**, *53*, 960.
41. Bulajic, D.; Corsi, M.; Cristoforetti, G.; Legnaioli, S.; Palleschi, V.; Salvetti, A.; Tognoni, E.; *Spectrochim. Acta, Part B* **2002**, *57*, 339.
42. Samek, O.; Margetic, V.; Hergenröder, R.; *Anal. Bioanal. Chem.* **2005**, *381*, 54.
43. Ciucci, A.; Palleschi, V.; Rastelli, S.; Barbini, R.; Fantoni, R.; Palucci, A.; Colao, F.; Ribezzo, S.; Van der Steen, H.J.L.; *Appl. Phys. B* **1995**, *63*, 185.
44. Castle, B.C.; Visser, K.; Smith, B.W.; Winefordner, J.D.; *Appl. Spectrosc.* **1998**, *52*, 649.
45. Multari, R.A.; Foster, L.E.; Cremers, D.A.; Ferris, M.J.; *Appl. Spectrosc.* **1996**, *50*, 1483.
46. Pennebaker, F. M.; Jones, D. A.; Greshan, C. A.; Williams, R. W.; Simon, R. E.; Schappert, M. F.; Denton, M. B.; *J. Anal. At. Spectrom.* **1998**, *13*, 821.
47. Harnly, J. M.; Fields, R. E.; *Appl. Spectrosc.* **1997**, *51*, 334A.
48. Janesick, J.; Putnam, G; *Annu. Rev. Nucl. Part. Sci.* **2003**, *53*, 263.
49. Byer, R. L.; *IEEE J. Sel. Top. Quant.* **2000**, *6*, 911.
50. Krupke, W. F.; *IEEE J. Sel. Top. Quant.* **2000**, *6*, 1287.
51. Tomiyasu, K.; *IEEE J. Quantum Elect.* **1965**, *1*, 144.
52. Reid, G. D.; Wynne, K. In *Encyclopedia of Analytical Chemistry*; Meyers, R. A., ed.; John Wiley: Chichester, 2000, p. 13644-13670.
53. Keller, U.; *Nature* **2003**, *424*, 831.
54. Kleinbauer, J.; Knappe, R.; Wallenstein, R.; *Top. Appl. Phys.* **2004**, *96*, 9.
55. Zayhowski, J. J.; *J. Alloy. Compd.* **2000**, *303*, 393.
56. Yamamoto, K. Y.; Cremers, D. A.; Foster, L. E.; Davies, M. P.; Harris, R. D.; *Appl. Spectrosc.* **2005**, *59*, 1082.
57. Gornushkin, I. B.; Amponsah-Manager, K.; Smith, B. W.; Omenetto, N.; Winefordner, J. D.; *Appl. Spectrosc.* **2004**, *58*, 762.
58. Zayhowski, J. J.; Dill III, C.; *Opt. Lett.* **1994**, *19*, 1427.
59. Wang P.; Zhou, S. H.; Lee, K. K.; Chen, Y. C.; *Opt. Commun.* **1995**, *114*, 439.
60. Fulbert, L.; Marty, J.; Ferrand, B., Molva, E.; *Conf. Lasers Electro-Optics Tech. Dig.* **1995**, *15*, 176.
61. Braun, B.; Kärtner, F. X.; Zhang, G.; Moser, M.; Keller, U.; *Opt. Lett.* **1997**, *22*, 381.
62. Zayhowski, J. J.; *Opt. Mater.* **1999**, *11*, 255.
63. Zayhowski, J. J.; *Lincoln Lab.* **1990**, *J.3*, 427.
64. Idris, N.; Terai, S.; Lie, T. J.; Kurniawan, H.; Kobayashi, T.; Maruyama, T.; Kagawa, K.; *Appl. Spectrosc.* **2005**, *59*, 115.
65. Romero, D.; Laserna, J. J.; *Spectrochim. Acta, Part B* **2000**, *55*, 1241.
66. Rieger, G. W.; Taschuk, M.; Tsui, Y. Y.; Fedosejevs, R.; *Appl. Spectrosc.* **2002**, *56*, 689.
67. Lo, K. M.; Cheung, N. H.; *Appl. Spectrosc.* **2002**, *56*, 682.
68. Garcia, C. C.; Corral, M.; Vadillo, J. M.; Laserna, J. J.; *Appl. Spectrosc.* **2000**, *54*, 1027.
69. Zayhowski, J. J.; *Conf. Lasers Electro-Optics Tech. Dig.* 1997, *11*, 463.
70. Bordui, P. F.; Fejer, M. M.; *Annu. Rev. Mater. Sci.* **1993**, *23*, 321.
71. Sasaki, T.; Mori, Y.; Yoshimura, M.; Yap, Y. K.; Kamimura, T.; *Mat. Sci. Eng. R* **2000**, *30*, 1.
72. Weyl, G. M. In *Laser-Induced Plasmas and Applications*; Radziemski, L. J.; Cremers, D. A., eds.; Marcel Dekker: New York, **1989**, ch. 1.
73. Fornarini, L.; Colao, F.; Fantoni, R.; Lazic, V.; Spizzichino, V.; *Spectrochim. Acta, Part B* **2005**, *60*, 1186.
74. Amoruso, S.; Bruzzese, R.; Spinelli, N.; Veletta, R.; *J. Phys. B* **1999**, *32*, R131.
75. Barthélemy, O.; Margot, J.; Chaker, M.; Sabsabi, M.; Vidal, F.; Johnston, T. W.; Laville, S.; Le Drogoff, B.; *Spectrochim. Acta, Part B* **2005**, *60*, 905.
76. Shuttelworth, S.; *Appl. Surf. Sci.* **1996**, *96*, 513.
77. Ducreux-Zappa, M.; Mermet, J. M.; *Spectrochim. Acta, Part B* **1996**, *51*, 333.
78. Fornarini, L.; Spizzichino, V.; Colao, F.; Fantoni, R.; Lazic, V.; *Anal. Bioanal. Chem.* **2006**, *385*, 272.
79. Durrant, S. F.; *J. Anal. At. Spectrom.* **1999**, *14*, 1385.
80. Cabalín, L. M.; Laserna, J. J.; *Spectrochim. Acta, Part B* **1998**, *53*, 723.
81. Gómez, C.; Costela, A.; García-Moreno, I.; Sastre, R.; *Appl. Surf. Sci.* **2006**, *252*, 2782.
82. Cabalín, L. M.; Romero, D.; García, C. C.; Baena, J. M.; Laserna, J. J.; *Anal. Bioanal. Chem.* **2002**, *372*, 352.
83. Menut, D.; Fichet, P.; Lacour, J.; Rivoallan, A.; Mauchien, P.; *Appl. Optics* **2003**, *42*, 6063.
84. Detalle, V.; Sabsabi, M.; St-Onge, L.; Hamel, A.; Héon, R.; *Appl. Optics* **2003**, *42*, 5971.
85. Mocker, H. W.; Collins, R. J.; *Phys. Lett.* **1965**, *7*, 174.
86. DeMaria, A. J.; Stetser, D. A.; Heynau, H.; *Appl. Phys. Lett.* **1966**, *8*, 174.
87. Valdmanis, J. A.; Fork, R. L.; *IEEE J. Quantum Elect.* **1986**, *22*, 112.
88. Fork, R. L.; Shank, C. V.; Yen, R. T.; *Appl. Phys. Lett.* **1982**, *41*, 223.
89. Spence, D. E.; Kean, P. N.; Sibbett, W.; *Opt. Lett.* **1991**, *16*, 42.
90. Yamakawa, K.; Barty, C. P. J.; *IEEE J. Sel. Top. Quant.* **2000**, *6*, 658.
91. Strickland, D.; Mourou, G.; *Opt. Commun.* **1985**, *55*, 447.
92. Rohwetter, P.; Yu, J.; Méjean, G.; Stelmaszczyk, K.; Salmon, E.; Kasparian, J.; Wolf, J. P.; Wöste, L.; *J. Anal. At. Spectrom.* **2004**, *19*, 437.
93. Sirven, J. B.; Bousquet, B.; Canioni, L.; Sarger, L.; *Spectrochim. Acta, Part B* **2004**, *59*, 1033.
94. Le Drogoff, B.; Chaker, M.; Margot, J.; Sabsabi, M.; Barthélemy, O.; Johnston, T. W.; Laville, S.; Vidal, F.; *Appl. Spectrosc.* **2004**, *58*, 122.

95. Baudelet, M.; Guyon, L.; Yu, J.; Wolf, J. P.; Amodeo, T.; Fréjafon, E.; Laloi, P.; *J. Appl. Phys.* **2006**, *99*, 084701-1.
96. Cravetchi, I. V.; Taschuk, M. T.; Tsui, Y. Y.; *Anal. Bioanal. Chem.* **2006**, *385*, 287.
97. von der Linde, D.; Sokolowsky-Tinten, K.; Bialkowski, J.; *Appl. Surf. Sci.* **1997**, *109-110*, 1.
98. Le Drogoff, B.; Margot, J.; Vidal, F.; Chaker, M.; Sabsabi, M.; Johnston, T. W.; Barthélemy, O.; *Plasma Sources Sci. Technol.* **2004**, *13*, 223.
99. Zeng, X.; Mao, X.; Greif, R.; Russo, R. E.; *Proc. SPIE* **2004**, *5448*, 1150.
100. Margetic, V.; Pakulev, A.; Stockhaus, A.; Bolshov, M.; Niemax, K.; Hergenröder, R.; *Spectrochim. Acta, Part B* **2000**, *55*, 1771.
101. Chichkov, B. N.; Momma, C.; Nolte, S.; von Alvensleben, F.; Tünnermann, A.; *Appl. Phys.* **1996**, *63*, 109.
102. Mao, S. S.; Mao, X.; Greif, R.; Russo, R. E.; *Appl. Phys. Lett.* **2000**, *77*, 2464.
103. Rieger, G. W.; Taschuk, M.; Tsui, Y. Y.; Fedosejevs, R.; *Spectrochim. Acta, Part B* **2003**, *58*, 497.
104. Sobral, H.; Villagran-Muniz, M.; *Appl. Phys. Lett.* **2000**, *77*, 3158.
105. Scaffidi, J.; Angel, S. M.; Cremers, D. A.; *Anal. Chem.* **2006**, *78*, 24.
106. Gautier, C.; Fichet, P.; Menut, D.; Lacour, J. L.; *Spectrochim. Acta, Part B* **2004**, *59*, 975.
107. Galbács, G.; Budavári, V.; Geretovszky, Z.; *J. Anal. At. Spectrom.* **2005**, *20*, 974.
108. Takaharu, K.; Hiroya, S.; Koichi, S.; Katsusuke, M.; *Japanese pat. JP62-85847* 1987.
109. Kuwako, A.; Uchida, Y.; Maeda, K.; *Appl. Optics* **2003**, *42*, 6052.
110. Piepmeier, E. H.; Malmstadt, H. V.; *Anal. Chem.* **1969**, *41*, 700.
111. Scott, R. H.; Strasheim, A.; *Spectrochim. Acta, Part B* **1970**, *25*, 311.
112. Cremers, D. A.; Radziemski, L. J.; Loree, T. R.; *Appl. Spectrosc.* **1984**, *38*, 721.
113. Pearman, W.; Scaffidi, J.; Angel, S. M.; *Appl. Optics* **2003**, *42*, 6085.
114. Pu, X. Y.; Cheung, N. H.; *Appl. Spectrosc.* **2003**, *57*, 588.
115. Uebbing, J.; Brust, J.; Sdorra, W.; Leis, F.; Niemax, K.; *Appl. Spectrosc.* **1991**, *45*, 1419.
116. Stratis, D. N.; Eland, K. L.; Angel, S. M.; *Appl. Spectrosc.* **2000**, *54*, 1270.
117. Sattman, R.; Sturm, V.; Noll, R.; *J. Phys. D Appl. Phys.* **1995**, *28*, 2181.
118. Gautier, C.; Fichet, P.; Menut, D.; Lacour, J. L.; L'Hermite, D.; Dubessy, J.; *Spectrochim. Acta, Part B* **2005**, *60*, 265.
119. Colao, F.; Lazic, V.; Fantoni, R.; Pershin, S.; *Spectrochim. Acta, Part B* **2002**, *57*, 1167.
120. St-Onge, L.; Detalle, V.; Sabsabi, M.; *Spectrochim. Acta, Part B* **2002**, *57*, 121.
121. Scaffidi, J.; Pearman, W.; Lawrence, M.; Carter, J. C.; Colston, B. W.; Angel, S. M.; *Appl. Optics* **2004**, *43*, 5243.
122. Scaffidi, J.; Pearman, W.; Carter, J. C.; Angel, S. M.; *Appl. Spectrosc.* **2006**, *60*, 65.
123. De Giacomo, A.; Dell'Aglio, M.; Colao, F.; Fantoni, R.; *Spectrochim. Acta, Part B* **2004**, *59*, 1431.
124. De Giacomo, A.; Dell'Aglio, M.; Casavola, A.; Colonna, G.; De Pascale, O.; Capitelli, M.; *Anal. Bioanal. Chem.* **2006**, *385*, 303.
125. Palanco, S.; Laserna, J.; *Appl. Optics* **2003**, *42*, 6078.
126. DeLucia, F. C.; Samuels, A. C.; Harmon, R. S.; Walters, R. A.; McNesby, K. L.; LaPointe, A.; Winkel, R. J.; Miziolek, A. W.; *IEEE Sens. J.* **2005**, *5*, 681.
127. Fichet, P.; Menut, D.; Brennetot, R.; Vors, E.; Rivoallan, A.; *Appl. Optics* **2003**, *42*, 6029.
128. Gruber, J.; Heitz, J.; Strasser, H.; Bauerle, D.; Ramaseder, N.; *Spectrochim. Acta, Part B* **2001**, *56*, 685.
129. Palanco, S.; Laserna, J.; *Rev. Sci. Instrum.* **2004**, *75*, 2068.
130. Rai, A. K.; Yueh, F. Y.; Singh, J. P.; Zhang, H.; *Rev. Sci. Instrum.* **2002**, *73*, 3589.
131. Masquardt, B. J.; Scott, S. R.; Michel, A. S.; *Anal. Chem.* **1996**, *68*, 977.
132. Palanco, S.; Laserna, J. J.; *J. Anal. At. Spectrom.* **2000**, *15*, 1321.
133. Radivojevic, I.; Haisch, C.; Niessner, R.; Florek, S.; Becker-Ross, H.; Panne, U.; *Anal. Chem.* **2004**, *76*, 1648.
134. Sallé, B.; Lacour, J.; Vors, E.; Fichet, P.; Maurice, S.; Cremers, D. A.; Wiens, R. C.; *Spectrochim. Acta, Part B* **2004**, *59*, 1413.
135. Arp, Z. A.; Cremers, D. A.; Harris, R. D.; Oschwald, D. M.; Parker, G. R.; Wayne, D. M.; *Spectrochim. Acta, Part B* **2004**, *59*, 987.
136. Body, D.; Chadwick, B. L.; *Rev. Sci. Instrum.* **2001**, *72*, 1625.
137. Neuhauser, R. E.; Ferstl, B.; Haisch, C.; Panne, U.; Niessner, R.; *Rev. Sci. Instrum.* **1999**, *70*, 3519.
138. Sabsabi, M.; Héon, R.; St-Onge, L.; *Spectrochim. Acta, Part B* **2005**, *60*, 1211.
139. Barnard, T. W.; Crockett, M. J.; Ivaldi, J. C.; Lundberg, P. L.; *Anal. Chem.* **1993**, *65*, 1225.
140. Hiddemann, L.; Uebbing, J.; Ciocan, A.; Dessenne, O.; Niemax, K.; *Anal. Chim. Acta.* **1994**, *283*, 152.
141. Harrison, G. R.; *J. Opt. Soc. Am.* **1949**, *39*, 522.
142. Harrison, G. R.; Archner, J. E.; Camus, J.; *J. Opt. Soc. Am.* **1952**, *42*, 706.
143. Bauer, H. E.; Leis, F.; Niemax, K.; *Spectrochim. Acta, Part B* **1998**, *53*, 1815.
144. Haisch, C.; Panne, U.; Niessner, R.; *Spectrochim. Acta, Part B* **1998**, *53*, 1657.
145. Lindblom, P.; *Anal. Chim. Acta.* **1999**, *380*, 353.
146. Florek, S.; Haisch, C.; Okruss, M.; Becker-Ross, H.; *Spectrochim. Acta, Part B* **2001**, *56*, 1027.
147. Sabsabi, M.; Detalle, V.; Harith, M. A.; Tawfik, W.; Imam, H.; *Appl. Optics* **2003**, *42*, 6094.
148. Multari, R. A.; Cremers, D. A.; *IEEE T. Plasma Sci.* **1996**, *24*, 39.

149. Knight, A. K.; Scherbarth, N. L.; Cremers, D. A.; Ferris, M. J.; *Appl. Spectrosc.* **2000**, *54*, 331.
150. Stratis, D. N.; Eland, K. L.; Carter, J. C.; Tomlinson, S. J.; Angel, S. M.; *Appl. Spectrosc.* **2001**, *55*, 999.
151. Tran, C. D.; *Anal. Chem.* **1992**, *64*, 971A.
152. Hoyt, C. C.; Benson, D. M.; *Photon. Spectra* **1992**, *26*, 92.
153. Gomba, J. M.; Ângelo, C. D.; Bertuccelli, D.; Bertuccelli, G.; *Spectrochim. Acta, Part B* **2001**, *56*, 695.
154. Parede, M.; Kurniawan, H.; Tjia, M. O.; Ikezawa, K.; Maruyama, T.; Kagawa, K.; *Appl. Spectrosc.* **2001**, *55*, 1229.
155. Huang, J. S.; Ke, C. B.; Huang, L. S.; Lin, K. C.; *Spectrochim. Acta, Part B* **2002**, *57*, 35.
156. Yaroshchyk, P.; Morrison, R. J. S.; Body, D.; Chadwick, B. L.; *Rev. Sci. Instrum.* **2004**, *75*, 5050.
157. Haisch, C.; Becker-Ross, H.; *Spectrochim. Acta, Part B* **2003**, *58*, 1351.
158. Carranza, J. E.; Gibb, E.; Smith, B. W.; Hahn, D. W.; Winefordner, J. D.; *Appl. Optics* **2003**, *42*, 6016.
159. Fisher, B. T.; Johnsen, H. A.; Buckley, S. G.; Hahn, D. W.; *Appl. Spectrosc.* **2001**, *55*, 1312.
160. Carranza, J. E.; Hahn, D. W.; *Spectrochim. Acta, Part B* **2002**, *57*, 779.
161. Yamasaki, K.; Tanaka, A.; Kimura, T.; Kajimoto, O.; *Rev. Sci. Instrum.* **1995**, *66*, 4395.
162. De Giacomo, A.; Dell'Aglio, M.; Santagata, A.; Teghil, R.; *Spectrochim. Acta, Part B* **2005**, *60*, 935.
163. Cabalín, L. M.; Laserna, J. J.; *J. Anal. At. Spectrom.* **2004**, *19*, 445.
164. Samek, O.; Beddows, D. C. S.; Telle, H. H.; Kaiser, J.; Liska, M.; Caceres, J. O.; Urena, A. G; *Spectrochim. Acta, Part B* **2001**, *56*, 865.
165. Burgio, L.; Melessanki, K.; Doulgeridis, M.; Clark, R. J. H.; Anglos, A.; *Spectrochim. Acta, Part B* **2001**, *56*, 905.
166. Myers, R. A.; Karger, A. M.; Hahn, D. W.; *Appl. Optics* **2003**, *42*, 6072.
167. Yamamoto, K. Y.; Cremers, D. A.; Ferris, M. J.; Foster, L. E.; *Appl. Spectrosc.* **1996**, *50*, 222.
168. Wainner, R. T.; Harmon, R. S.; Miziolek, A. W.; McNesby, K. L.; French, P. D.; *Spectrochim. Acta, Part B* **2001**, *56*, 777.
169. Singh, J. P.; Yueh, F. Y.; Zhang, H.; Cook, R. L.; *Process Contr. Qual.* **1997**, *10*, 247.
170. Castle, B. C.; Knight, A. K.; Visser, K.; Smith, B. W.; Winefordner, J. D.; *J. Anal. At. Spectrom.* **1998**, *13*, 589.
171. Neuhauser, R. E.; Panne, U.; Niessner, R.; *Anal. Chim. Acta.* **1999**, *392*, 47.
172. Panne, U.; Neuhauser, R. E.; Haisch, C.; Fink, H.; Niessner, R.; *Appl. Spectrosc.* **2002**, *56*, 375.
173. Palanco, S.; Alises, A.; Cuñat, J.; Baena, J.; Laserna, J. J.; *J. Anal. At. Spectrom.* **2003**, *18*, 933.
174. Cuñat, J.; Palanco, S.; Carrasco, F.; Simon, M. D.; Laserna, J. J.; *J. Anal. At. Spectrom.* **2005**, *20*, 295.
175. Harmon, R. S.; DeLucia, F. C.; LaPoite, A.; Winkel, R. J.; Miziolek, A. W.; *Anal. Bioanal. Chem*. **2006**, *385*, 1140.
176. Palanco, S.; López-Moreno, C.; Laserna, J. J.; *Spectrochim. Acta, Part B* **2006**, *61*, 88.
177. López-Moreno, C.; Palanco, S.; Laserna, J. J.; DeLucia, F.; Miziolek, A. W.; Rose, J.; Walters, R. A.; Whitehouse, A. I.; *J. Anal. At. Spectrom.* **2006**, *21*, 55.
178. Bertolini, A.; Carelli, G.; Francesconi, F.; Francesconi, M.; Marchesini, L.; Marsili, P.; Sorrentino, F.; Cristoforetti, G.; Legnaioli, S.; Palleschi, V.; Pardini, L.; Salvetti, A.; *Anal. Bioanal. Chem*. **2006**, *385*, 240.
179. Corsi, M.; Cristoforetti, G.; Hidalgo, M.; Legnaioli, S.; Palleschi, V.; Salvetti, A.; Tognoni, E.; Vallebona, C.; *Appl. Geochem.* **2006**, *21*, 748.
180. http://www.oceanoptics.com/products/libselite.asp, accessed in October 2006.
181. http://www.lla.de/en/index.php/content/view/14/34/, accessed in October 2006.
182. http://www.laseranalysis.com/pages/products/spectrolaser-1000hr.php, accessed in October 2006.
183. http://www.kigre.com/files/libsflyer.pdf, accessed in October 2006.
184. http://www.kigre.com/files/ndyag23.pdf, accessed in October 2006.
185. http://www.avantes.com/Applications/AvaLIBS.htm, accessed in October 2006.
186. Loebe, K.; Uhl, A.; Lucht, H.; *Appl. Opt.* **2003**, *42*, 6166.
187. Cravetchi, I.V.; Taschuk, M.; Tsui, Y.Y.; Fedosejevs, R.; *Spectrochim. Acta, Part B* **2004**, *59*, 1439.
188. Gruber, J.; Heitz, J.; Strasser, H.; Bäuerle, D.; Ramaseder, N.; *Spectrochim. Acta Part B* **2001**, *56*, 685.
189. Hubmer, G.; Kitzberger, R.; Mörwald, K.; *Anal. Bioanal. Chem.* **2006**, *385*,219.
190. Balzer, H.; Hölters, S.; Sturm, V.; Noll, R.; *Anal. Bioanal. Chem*. **2006**, *385*, 234.
191. Balzer, H.; Hoehne, M.; Noll, R.; Sturm, V.; *Anal. Bioanal. Chem*. **2006**, *385*, 225.
192. Noll, R.; Mönch, I.; Klein, O.; Lamott, A.; *Spectrochim. Acta, Part B* **2005**, *60*, 1070.
193. Bulajic, D.; Cristoforetti, G.; Corsi, M.; Hidalgo, M.; Legnaioli, S.; Palleschi, V.; Salvetti, A.; Tognoni, E.; Green, S.; Bates, D.; Steiger, A.; Fonseca, J.; Martins, J.; McKay, J.; Tozer, B.; Wells, D.; Wells, R.;Harith, M.A.; *Spectrochim. Acta, Part B* **2002**, *57*, 1181.
194. De Giacomo, A.; Dell'Aglio, M.; Colao, F.; Fantoni, R.; Lazic,V.; *Appl. Surf. Sci.* **2005**, *247*, 157.
195. Pichahchy, A.E.; Cremers, D.A.; Ferris, M.J.; *Spectrochim. Acta Part B* **1997**, *52*, 25.
196. Sturm, V.; Peter, L.; Noll, R.; *Appl. Spectrosc.* **2000**, *54*, 1275.
197. Sturm, V.; Vrenegor, J.; Noll, R.; Hemmerlin, M.; *J. Anal. At. Spectrom.* **2004**, *19*, 451.

198. Vrenegor, J.; Noll, R.; Sturm, V.; *Spectrochim. Acta, Part B* **2005**, *60*, 1083.
199. Lopez-Moreno, C.; Amponsah-Manager, K.; Smith, B.W.; Gornushkin, I.B.; Omenetto, N.; Palanco, S.; Laserna, J.J.;Winefordner, J.D.; *J. Anal. At. Spectrom*. **2005**, *20*, 552.
200. Hemmerlin, M.; Meiland, R.; Falk, H.; Wintjens, P.; Paulard, L.; *Spectrochim. Acta, Part B* **2001**, *56*, 661.
201. Bassiotis, I.; Diamantopoulou, A.; Giannoudakos, A.; Roubani-Kalantzopoulou F.; Kompsitas, M.; *J. Anal. At. Spectrom.* **2001**, *56*, 671.
202. Khater, M.A.; van Kampen, P.; Costello, J.T.; Mosnier, J-P; Kennedy, E.T.; *J. Phys. D: Appl. Phys*. **2000**, *33*, 2252.
203. Khater, M.A.; Costello, J.T.; Kennedy, E.T.; *Appl. Spectrosc.* **2002**, *56*, 970.
204. Ismail, M.A.; Imam, H.; Elhassan, A.; Youniss, W.T.; Harith, M.A.; *J. Anal. At. Spectrom*. **2004**, *19*, 489.
205. Ismail, M.A.; Cristoforetti, G.; Legnaioli, S.; Pardini, L.; Palleschi, V.; Salvetti, A.; Tognoni, E.; Harith, M.A.; *Anal. Bioanal. Chem.* **2006**, *385*, 316.
206. Rai, V.N.; Yueh, J.P.; Singh, J.P.; *Appl. Opt.* **2003**, *42*, 6047.
207. De Giacomo, A.; Dell'Aglio, M.; Casavola, A.; Colonna, G.; De Pascale, O.; Capitelli, M.; *Anal. Bional. Chem*. **2006**, *385*, 303.
208. Yaroshchyk, P.; Body, D.; Morrison, R.J.S., Chadwich, B.L.; *Spectrochim. Acta Part B* **2006**, *61*, 200.
209. Goode,S.R.; Morgan, S.L.; Hoskins,R.; Oxsher, A.; *J. Anal. At. Spectrom.* **2000**, *15*, 1133.
210. Galbács, G.; Gornushkin, I.B.; Smith, B.W.; Winefordner, J.D.; *Spectrochim. Acta Part B* **2001**, *56*, 1159.
211. Gornushkin, I.B.; Smith, B.W.; Nasajpour, H.; Winefordner, J.D.; *Anal. Chem.* **1999**, *71*, 5157.
212. Corsi, M.; Cristoforetti, G.; Palleschi, V.; Salvetti, A.; Tognoni. E.; *Eur. Phys. J. Part D* **2001**, *13*,373.
213. Rai, A.K.; Zhang, H.; Yueh, F.Y.; Singh, J.P.; Weisburg, A.; *Spectrochim. Acta Part B* **2001**, *56*, 2371.
214. Rai, A.K.; Zhang, H.; Yueh, F.Y.; Singh, J.P.; Weisburg, A.; *Appl. Opt.* **2003**, *42*, 2078.
215. Peter, L.; Sturm, V.; Noll, R.; *Appl. Opt.* **2003**, *30*, 6199.
216. Gruber, J.; Heitz, J.; Arnold, N.; Bäuerle, D.; Ramaseder, N.; Meyer, W.; Hochörtler, J.; Koch, F.; *Appl. Spectrosc.* **2004**, *58*, 457.
217. Yamaguchi, N.; Hotokezaka, H.; Nagasaki, S.; Tanaka, S.; *Soil Science Plant Nutrition* **2005**, *51*, 911.
218. Hotokezaka, H.; Aoyagi, N.; Kawahara, Y.; Yamaguchi, N.U.; Nagasaki, S.; Sasaki, K.; Tanaka, S.; *Microsyst. Technol.* **2005**, *11*, 974.
219. Bundschuh, T.; Yun, J.; Knopp, R.; *Fresenius J. Anal. Chem.* **2001**, *371*, 1063.
220. Samek, O.; Beddows, D.C.S.; Kaiser, J.; Kukhlevsky, S.V.; Liska, M.; Telle, H.H.; Young, J.; *Opt. Eng.* 2000, *39*, 2248.
221. Koch, S.; Garen, W.; Müller, M.; Neu, W.; *Appl. Phys. A: Mater. Sci. Process* **2004**, *79*, 1071.
222. Fichet, P.; Tousaint, A.; Wagner, J.-F.; *Appl. Phys. A: Mater. Sci. Process* **1999**, *69*, S591.
223. Lazic, V,; Barbini, R.; Colao, F.; Fantoni, R.; Palucci, A.; *Spectrochim. Acta Part B.* **2001**, *56*, 807.
224. Bublitz, J.; Dölle, C.; Schade, W.; Hartman, A.; Horn, R.; *Eur. J. Soil Sci.* **2001**, *52*, 305.
225. Hilbk-Kortenbruck, F.; Noll, R.; Wintjens, P.; Falk, H.; Becker, C.; *Spectrochim. Acta Part B* **2001**, *56*, 933.
226. Capitelli, F.; Colao, F.; Provenzano, M.R.; Fantoni, R.; Brunetti, G.; Senesi, N.; *Geoderma* **2002**, *106*, 45.
227. Bustamante, M.F.; Rinaldi, C.A.; Ferrero, J.C.; *Spectrochim. Acta Part B* **2002**, *57*, 303.
228. Martin, M.Z.; Wullschleger, S.T.; Garten Jr., C.T.; Palumbo, A.V.; *Appl. Opt.* **2003**, *42*, 2072.
229. Martin, M.Z.; Wullschleger, S.T.; Garten Jr., C.T.; Palumbo, A.V.; Smith, J.G.; *J. Dispersion Sci. Technol.* **2004**, *25*, 687.
230. Cremers, D.A.; Ebinger, M.H.; Breshears, D.D.; Unkefer, P.J.; Kammerdiener, S.A.; Ferris, M.J.; Catlett, K.M.; Brown, J.R.; *J. Environ. Qual.* **2001**, *30*, 2202.
231. Ebinger, M.H.; Norflect, M.L.; Breshears, D.D.; Cremers, D.A.; Ferris, M.J.; Unkefer, Lamb, M.S.; Goddard, K.L.; Meyer, C.W., *Soil Sci. Soc. Am. J.* **2003**, *67*, 1616.
232. Harris, R.D.; Cremers, D.A.; Ebinger, M.H.; Bluhm, B.K.; *Appl. Spec.* **2004**, *58*, 770.
233. Mosier-Boss, P.A.; Lieberman, S.H.; Theriault, G.A.; *Environ. Sci. Technol.* **2002**, *36*, 3968.
234. Niu, L.; Cho, H.; Song, K.; Cha, H.; Kim, Y.; Lee, Y.; *Appl. Spectrosc.* **2002**, *56*, 1511.
235. Barbini, R.; Colao, F.; Lazic, V.; Fantoni, R.; Palucci, A.; Angelone, M.; *Spectrochim. Acta Part B.* **2002**, *57*, 1203.
236. Gondal, M.A.; Hussain, T.; Yamani, Z.H.; Baig, M.A.; *Talanta* **2006**, *69*, 1072.
237. Gondal, M. A.; Hussain, T.; *Talanta*, in press.
238. Mateo, M.P.; Nicolas, G.; Piñon, V.; Alvarez, J.C.; Ramil, A.; Yañez, A.; *Anal. Chim. Acta* **2004**, *524*, 27.
239. López-Moreno, C.; Palanco, S.; Laserna, J.J.*; J. Anal. At. Spectrom.* **2004**, *19*, 1479.
240. Mosier-Boss, P.A.; Lieberman, S.H.; *Appl. Spec.* **2005**, *59*, 1445.
241. Buckley, S. G.; Johnsen, H. A.; Hencken, K. R.; Hahn, D. W.; *Waste Manage.* **2000**, *20*, 455.
242. Buckley, S. G.; *Environ. Eng. Sci.* **2005**, *22*, 195.
243. Anglos, D.; *Appl. Spectrosc*. **2001**, *55*, 186A.
244. Borgia, I.; Burgio, L. M. F.; Corsi, M.; Fantoni, R.; Palleschi, V.; Salvetti, A.; Squarcialupi, M. C.; Tognoni, E.; *J. Cult. Heritage* **2000**, *1*, S281.
245. Melessanaki, K.; Mateo, M.; Ferrence, S. C.; Betancourt, P. P.; Anglos, D.; *Appl. Surf. Sci.* **2002**, *197-198*, 156.
246. Colao, F.; Fantoni, R.; Lazic, V.; Caneve, L.; Giardini, A.; Spizzicchino, V.; *J. Anal. At. Spectrom.* **2004**, *19*, 502.
247. Pouli, P.; Melessanaki, K.; Giakoumaki, A.; Argyropoulos, V.; Anglos, D.; *Spectrochim. Acta, Part B* **2005**, *60*, 1163.

248. Fortes, F. J.; Cortés, M.; Simon, M. D.; Cabalín, L. M.; Laserna, J. J.; *Anal. Chim. Acta* **2005**, *554*, 136.
249. Lazic, V.; Colao, F.; Fantoni, R.; Spizzicchino, V.; *Spectrochim. Acta, Part B* **2005**, *60*, 1014.
250. Acquaviva, S.; De Giorgi, M. L.; Marini, C.; Poso, R.; *J. Cult. Heritage* **2004**, *5*, 365.
251. Anglos, D.; Melesanaki, K.; Zafiropulos, V.; Gresalfi, M. J.; Miller, J. C.; *Appl. Spectrosc.* **2002**, *56*, 423.
252. Golovlev, V. V.; Gresalfi, M. J.; Miller, J. C.; Romer, G.; Messier, P.; *J. Cult. Heritage* **2000**, *1*, S139.
253. Golovlev, V. V.; Gresalfi, M. J.; Miller, J. C.; Anglos, D.; Melesanaki, K.; Zafiropulos, V.; Romer, G.; Messier, P.; *J. Cult. Heritage* **2003**, *4*, S134.
254. Melessanaki, K.; Papadakis, V.; Balas, C.; Anglos, D.; *Spectrochim. Acta, Part B* **2001**, *56*, 2337.
255. Castillejo, M.; Martín, M.; Silva, D.; Stratoudaki, T.; Anglos, D.; Burgio, L.; Clark, R. J. H.; *J. Mol. Struct.* **2000**, *550*, 191.
256. Martin, M.; Castillejo, M.; Torres, R.; Silva, D.; Guerra-Librero, F.; *J. Cult. Heritage* **2000**, *1*, S293.
257. Oujja, M.; Vila, A.; Rebollar, E.; García, J. F.; Castillejo, M.; *Spectrochim. Acta, Part B* **2005**, *60*, 1140.
258. Bicchieri, M.; Nardone, M.; Russo, P. A.; Sodo, A.; Corsi, M.; Cristoforetti, G.; Palleschi, V.; Salvetti, A.; Tognoni, E.; *Spectrochim. Acta, Part B* **2001**, *56*, 915.
259. Castillejo, M.; Martín, M.; Silva, D.; Stratoudaki, T.; Anglos, D.; Burgio, L.; Clark, R. J. H.; *J. Cult. Heritage* **2000**, *1*, S297.
260. Clark, R. J. H.; *C. R. Chimie* **2002**, *5*, 7.
261. Castillejo, M.; Martín, M.; Oujja, M.; Silva, D.; Torres, R.; Domingo, C.; García-Ramos, J. V.; Sánchez-Cortés, S.; *Appl. Spectrosc.* **2001**, *55*, 992.
262. Brysbaert, A.; Melessanaki, K.; Anglos, D.; *J. Archaeolog. Sci.* **2006**, *33*, 1095.
263. López, A. J.; Nicolas, G.; Mateo, M. P.; Ramil, A.; Piñón, V.; Yáñez, A.; *Appl. Phys. A* **2006**, *83*, 695.
264. López, A. J.; Nicolás, G.; Mateo, M. P.; Piñón, V.; Tobar, M. J.; Ramil, A.; *Spectrochim. Acta, Part B* **2005**, *60*, 1149.
265. Colao, F.; Fantoni, R.; Lazic, V.; Spizzicchino, V.; *Spectrochim. Acta, Part B* **2002**, *57*, 1219.
266. Yoon. Y.; Kim, T.; Yang, M.; Lee, K.; Lee, G.; *Microchem. J.* **2001**, *68*, 251.
267. Lazic, V.; Colao, F.; Fantoni, R.; Palucci, A.; Spizzichino, V.; Borgia, I.; Brunetti, B. G.; Sgamellotti, A.; *J. Cult. Heritage* **2003**, *4*, 303.
268. Anzano, J. M.; Villoria, M. A.; Gornushkin, I. B.; Smith, B. W.; Winefordner, J. D.; *Can. J. Anal. Sci. Spectrosc.* **2002**, *47*, 134.
269. Maravelaki-Kalaitzali, P.; Anglos, D.; Kilikouglou, V.; Zafiropulos, V.; *Spectrochim. Acta, Part B* **2001**, *56*, 887.
270. Lazic, V.; Fantoni, R.; Colao, F.; Santagata, A.; Morone, A.; Spizzicchino, V.; *J. Anal. At. Spectrom.* **2004**, *19*, 429.
271. Maravelaki-Kalaitzaki, P.; Zafiropulos, V.; Fotakis, C.; *Appl. Surf. Sci.* **1999**, *148*, 92.
272. Klein, S.; Stratoudaki, T.; Zafiropulos, V.; Hildenhagen, J.; Dickmann, K.; Lehmkuhl, T.; *Appl. Phys. A* **1999**, *69*, 441.
273. Klein, S.; Hildenhagen, J.; Dickmann, K.; Stratoudaki, T.; Zafiropulos, V.; *J. Cult. Heritage* **2000**, *1*, S287.
274. Klein, S.; Fekrsanati, F.; Hildenhagen, J.; Dickmann, K.; Uphoff, H.; Marakis, Y.; Zafiropulos, V.; *Appl. Surf. Sci.* **2001**, *171*, 242.
275. Colao, F.; Fantoni, R.; Lazic, V.; Morone, A.; Santagata, A.; Giardini, A.; *Appl. Phys. A* **2004**, *79*, 213.
276. Castillejo, M.; Martín, M.; Oujja, M.; Rebollar, E.; Domingo, C.; García-Ramos, J. V.; Sánchez-Cortés, S.; *J. Cult. Heritage* **2003**, *4*, 243.
277. Castillejo, A.; Martín, M.; Oujja, M.; Silva, D.; Torres, R.; Manousaki, A.; Zafiropulos, V.; van den Brink, O. F.; Heeren, R. M. A.; Teule, R.; Silva, A.; Gouveia, H.; *Anal. Chem.* **2002**, *74*, 4662.
278. Tornari, V.; Zafiropulos, V.; Bonarou, A.; Vainos, N. A.; Fotakis, C.; *Opt. Lasers Eng.* **2000**, *34*, 309.
279. Scholten, J. H.; Teule, J. M.; Zafiropulos, V.; Heeren, R. M. A.; *J. Cult. Heritage* **2000**, *1*, S215.
280. Sallé, B.; Cremers, D. A.; Maurice, S.; Wiens, R. C.; *Spectrochim. Acta, Part B* **2005**, *60*, 479.
281. Radziemski, L.; Cremers, D. A.; Benelli, K.; Khoo, C.; Harris, R. D.; *Spectrochim. Acta, Part B* **2005**, *60*, 237.
282. St-Onge, L.; Kwong, E.; Sabsabi, M.; Vadas, E. B.; *Spectrochim. Acta, Part B* **2002**, *57*, 1131.
283. Mowery, M. D.; Sing, R.; Krisch, J.; Razaghi, A.; Béchard, S.; Reed, R. A.; *J. Pharm. Biomed. Anal.* **2002**, *28*, 935.
284. St-Onge, L.; Kwong, E.; Sabsabi, M.; Vadas, E. B.; *J. Pharm. Biomed. Anal.* **2004**, *36*, 277.
285. Samek, O.; Telle, H. H.; Beddows, D. C. S.; *BMC Oral Health* **2001**, *1*, 1.
286. Samek, O.; Beddows, D. C. S.;Telle, H. H.; Morris, G. W.; Liska, M.; Kaiser, J.; *Appl. Phys. A* **1999**, *69*, S179.
287. Samek, O.; Liska, M.; Kaiser, J.; Beddows, D. C. S.; Telle, H.; Kukhlevsky, S.; *J. Clin. Laser Med. Surg.* **2000**, *18*, 281.
288. Sun, Q.; Tran, M.; Smith, B. W.; Winefordner, J. D.; *Talanta* **2000**, *52*, 293.
289. Corsi, M.; Cristoforetti, G.; Hidalgo, M.; Legnaioli, S.; Palleschi, V.; Salvetti, A.; Tognoni, E.; Vallebona, C.; *Appl. Opt.* **2003**, *42*, 6133.
290. Fang, X.; Ahmad, S. R.; Mayo, M.; Iqbal, S.; *Laser Med. Sci.* **2005**, *20*, 132.
291. Kumar, A.; Yueh, F. Y.; Singh, J. P.; Burgess, S.; *Appl. Opt.* **2004**, *43*, 5399.
292. Martin, M.; Evans, B.; O'Neill, H.; Woodward, J.; *Appl. Opt.* **2003**, *42*, 6174.
293. Neuhauser, R. E.; Panne, U.; Niessner, R.; Steinicke, W. H.; Grimm, H. J.; *J. Aerosol Sci.* **1997**, *28*, S437.
294. Neuhauser, R. E.; Panne, U.; Niessner, R.; *J. Aerosol Sci.* **1998**, *29*, 109.

295. Boyain-Goitia, A. R.; Beddows, D. C. S.; Griffiths, B. C.; Telle, H. H.; *Appl. Opt.* **2003**, *42*, 6119.
296. Mukherjee, D.; Rai, A.; Zachariah, M. R.; *J. Aerosol Sci.* **2006**, *37*, 677.
297. Martin, M.; Cheng, M.D.; *Appl. Spectrosc.* **2000**, *54*, 1279.
298. Windom, B.C.; Diwakar, P.K.; Hahn, D.W. *Spectrochim. Acta, Part B* **2006**, *61*, 788.
299. Schade, W.; Bohling, C.; Hohmann, K.; Scheel, D.; *Laser Part. Beams* **2006**, *24*, 241.
300. DeLucia Jr, F. C.; Harmon, R. S.; McNesby, K. L.; Winkel Jr, R. J.; Miziolek, A. W.; *Appl. Opt.* **2003**, *42*, 6148.
301. Morel, S.; Leone, N.; Adam, P.; Amouroux, J.; *Appl. Opt.* **2003**, *42*, 6184.
302. Baudelet, M.; Guyon, L.; Yu, J.; Wolf, J. P.; Amodeo, T.; Fréjafon, E.; Laloi, P.; *Appl. Phys. Lett.* **2006**, *88*, 063901-1
303. Dockery, C. R.; Goode, S. R.; *Appl. Opt.* **2003**, *42*, 6153.
304. Almirall, J. R.; Umpierrez, S.; Castro, W.; Gornushkin, I.; Winefordner, J.; *Proceedings of SPIE-Volume 5778-Sensors, and Command, Control, Communications, and Intelligence (C3I) Technologies for Homeland Security and Homeland Defense IV*, Orlando, USA, 2005.
305. Gleason, R. L.; Hahn, D. W.; *Spectrochim. Acta, Part B* **2001**, *56*, 419.
306. Chen, Y.; Bulatov, V.; Singer, L.; Stricker, J.; Schechter, I.; *Anal. Bioanal. Chem.* **2005**, *383*, 1090.
307. Fink, H.; Panne, U.; Niessner, R.; *Anal. Chim. Acta* **2001**, *440*, 17.
308. Gornushkin, I. B.; Ruíz-Medina, A.; Anzano, J. M.; Smith, B. W.; Winefordner, J. D.; *J. Anal. At. Spectrom.* **2000**, *15*, 581.
309. Caneve, L.; Colao, F.; Fabbri, F.; Fantoni, R.; Spizzichino, V.; Striber, J.; *Spectrochim. Acta, Part B* **2005**, *60*, 1115.
310. Ferioli, F.; Buckley, S. G.; *Combust. Flame* **2006**, *144*, 435.
311. Smith, C. A.; Martinez, M. A.; Veirs, D. K.; Cremers, D. A.; *Spectrochim. Acta, Part B* **2002**, *57*, 929.
312. Anzano, J. M.; Gornushkin, I. B.; Smith, B. W.; Winefordner, J. D.; *Polym. Eng. Sci.* **2000**, *40*, 2423.
313. Anzano, J. Casanova, M. E.; Bermúdez, M. S.; Lasheras, R. J.; *Polym. Testing* **2006**, *25*, 623.
314. Sallé, B.; Lacour, J. L.; Mauchien, P.; Fichet, P.; Maurice, S.; Manhès, G.; *Spectrochim. Acta, Part B* **2006**, *61*, 301.
315. Rosenwasser, S.; Asimellis, G.; Bromley, B.; Hazlett, R.; Martin, J.; Pearce, T.; Zigler, A.; *Spectrochim. Acta, Part B* **2001**, *56*, 707.
316. D'Ulivo, A.; Onor, M.; Pitzalis, E.; Spiniello, R. Lampugnani, L.; Cristoforetti, G.; Legnaioli, S.; Palleschi, V.; Salvetti, A.; Tognoni.; *Spectrochim. Acta, Part B* **2006**, *61*, 797.
317. Wilsch, G.; Weritz, F.; Schaurich, D.; Wiggennhauser, H.; *Construct. Build. Mater.* **2005**, *19*, 724.
318. Nasrazadani, S.; Namduri, H.; *Spectrochim. Acta, Part B* **2006**, *61*, 565.
319. Cáceres, J. O.; López, J. T.; Telle, H. H.; Ureña, A. G.; *Spectrochim. Acta, Part B* **2001**, *56*, 831.
320. Noda, M.; Deguchi, Y.; Iwasaki, S.; Yoshikawa, N.; *Spectrochim. Acta, Part B* **2002**, *57*, 701.
321. Lal, B.; Yueh, F. Y.; Singh, J. P.; *Appl. Opt.* **2005**, *44*, 3668.
322. Lal, B.; Zheng, H.; Yueh, F. Y.; Singh, J. P.; *Appl. Opt.* **2004**, *43*, 2792.
323. Molina, A.; Shaddix, C. R.; Sickafoose, S. M.; Walsh, P. M.; Blevins, L. G.; *Spectrochim. Acta, Part B* **2005**, *60*, 1103.
324. Häkkänen, H. J.; Korppi-Tommola, J. E. I.; *Anal. Chem.* **1998**, *70*, 4724.
325. Häkkänen, H. J.; Houni, J.; Kaski, S.; Korppi-Tommola, J. E. I.; *Spectrochim. Acta, Part B* **2001**, *56*, 737.
326. Bicchieri, M.; Ronconi, S.; Romano, F. P.; Pappalardo, L.; Corsi, M.; Cristoforetti, G.; Legnaioli, S.; Palleschi, V.; Salvetti, A.; Tognoni, E.; *Spectrochim. Acta, Part B* **2000**, *57*, 1235.
327. Martens, H.; Naes, T.; *Multivariate Calibration*, Wiley: Chichester, 1989.
328. Brereton, R. G.; *Analyst* **2000**, *125*, 2125.
329. Brereton, R. G.; *Multivariate Pattern Recognition in Chemometrics, Illustrated by Case Studies*, Elsevier: Amsterdam, 1992.
330. Brereton, R. G.; Chemometrics: *Applications of Mathematics and Statistics to Laboratory Systems*, Ellis Horwood: Chichester, 1993.
331. Wold, S.; Esbensen, K.; Geladi, P.; *Chemom. Intell. Lab. Syst.* **1987**, *2*, 37.
332. Mardia, K. V.; Kent, J. T.; Bibby, J.; *Multivariate Analysis*, Academic Press: London, 1979.
333. Brereton, R. G.; *Analyst* **1995**, *120*, 2313.
334. Beebe, K. R.; Pell, R. J.; Seashottz, M. B.; *Chemometrics: A Practical Guide*, Wiley: New York, 1998.
335. Zupan, J.; Gasteiger, J.; *Anal. Chim. Acta* **1991**, *248*, 1.
336. MacCulloch, H. M.; Pitts, W.; *Bull. Math. Biophy.* **1943**, *5*, 115.
337. Cartwright, H. M.; *Applications of Artificial Intelligence in Chemistry*; Oxford: New York, 1995.
338. Zupan, J.; Gasteiger, J.; *Neural Networks for Chemists: An Introduction*; VCH: Weinheim, 1993.
339. Munson, C. A.; De Lucia Jr, F. C.; Piehler, T.; McNesby, K. L.; Miziolek, A. W.; *Spectrochim. Acta, Part B* **2005**, *60*, 1217.
340. Amador-Hernández, J.; García-Ayuso, L. E.; Fernández-Romero, J. M.; Luque de Castro, M. D.; *J. Anal. At. Spectrom.* **2000**, *15*, 587.
341. García-Ayuso, L. E.; Amador-Hernández, J.; Fernández-Romero, J. M.; Luque de Castro, M. D.; *Anal. Chim. Acta* **2002**, *457*, 247.
342. Jurado-López, A.; Luque de Castro, M. D.; *Talanta* **2003**, *59*, 409.
343. Jurado-López, A.; Luque de Castro, M.D.; *J. Anal. At. Spectrom.* **2002**, *17*, 544.
344. Jurado-López, A.; Luque de Castro, M. D.; *Appl. Spectrosc.* **2003**, *57*, 349.

345. Jurado-López, A.; Luque de Castro, M. D.; *Spectrochim. Acta, Part B* **2003**, *58*, 1291.
346. Jurado-López, A.; Luque de Castro, M. D.; *Anal. Bioanal. Chem.* **2002**, *372*, 109.
347. Luque-García, J. L.; Soto-Ayala, R.; Luque de Castro, M. D.; *Microchem. J.* **2002**, *73*, 355.
348. Martin, M. Z.; Labbé, N.; Rials, T. G.; Wullschleger, S. D. *Spectrochim. Acta, Part B* **2005**, *60*, 1179.
349. Sirven, J. B.; Bousquet, B.; Canioni, L.; Sarger, L.; Tellier, S.; Potin-Gautier, M.; Le Hecho, I.; *Anal. Bioanal. Chem.* **2006**, *385*, 256.
350. Amador-Hernández, J.; Fernández-Romero, J. M.; Luque de Castro, M. D.; *Anal. Chim. Acta* **2001**, *435*, 227.
351. Amador-Hernández, J.; Fernández-Romero, J. M.; Luque de Castro, M. D.; *Surf. Interface Anal.* **2001**, *31*, 313.
352. Corsi, M.; Cristoforetti, G.; Giuffrida, M.; Hidalgo, M.; Legnaioli, S.; Masotti, L.; Palleschi, V.; Salvetti, A.; Tognoni, E.; Vallebona, C.; Zanini, A.; *Microchim. Acta*. **2005**, *152*, 105.
353. Samuels, A. C.; DeLucia Jr, F. C.; McNesby, K. L.; Miziolek, A. W.; *Appl. Opt.* **2003**, *42*, 6205.
354. Sirven, J. B.; Bousquet; B.; Canioni, L.; Sarger, L.; *Anal. Chem.* **2006**, *78*, 1462.
355. Panne, U.; Clara, M.; Haisch, C.; Niessner, R.; *Spectrochim. Acta, Part B* **1998**, *53*, 1969.
356. Hybl, J. D.; Lithgow, G. A.; Buckley, S. G.; *Appl. Spectrosc.* **2003**, *57*, 1207.
357. Bohling, C.; Scheel, D.; Hohmann, K.; Schade, W.; Reuter, M.; Holl, G.; *Appl. Opt.* **2006**, *45*, 3817.
358. Sattmann, R.; Mönch, I.; Krause, H.; Noll, R.; Couris, S.; Hatziapostolou, A.; Mavromanolakis, A.; Fotakis, C.; Larrauri, E.; Miguel, R.; *Appl. Spectrosc.* **1998**, *52*, 456.
359. Freedman, A.; Iannarilli Jr., F.J.; Wormhoudt, J.C.; *Spectrochim. Acta Part B* **2005**, *60*, 1076.
360. Huang, J.S.; Liu, H.T.; Lin, K.C. *Anal. Chim. Acta* **2007**, *581*, 303.
361. Asimellis, G.; Giannoudakos, A.; Kompitsas, M. *Anal. Bioanal. Chem.* **2006**, *385*, 333.

Received: December 28, 2006
Web Release Date: May 15, 2007

FAPESP helped in meeting the publication costs of this article.